2000-06

El Nino and La Nina effects of tropical cyclones: the mechanisms

Ford, Bruce W.

Monterey, California. Naval Postgraduate School

NAVAL POSTGRADUATE SCHOOL
Monterey, California

THESIS

EL NINO AND LA NINA EFFECTS ON TROPICAL CYCLONES: THE MECHANISMS

by

Bruce W. Ford

June 2000

Thesis Advisor: Tom Murphree
Second Reader: Pat Harr

Approved for public release; distribution is unlimited.

REPORT DOCUMENTATION PAGE	Form Approved OMB No. 0704-0188

Public reporting burden for this collection of information is estimated to average 1 hour per response, including the time for reviewing instruction, searching existing data sources, gathering and maintaining the data needed, and completing and reviewing the collection of information. Send comments regarding this burden estimate or any other aspect of this collection of information, including suggestions for reducing this burden, to Washington headquarters Services, Directorate for Information Operations and Reports, 1215 Jefferson Davis Highway, Suite 1204, Arlington, VA 22202-4302, and to the Office of Management and Budget, Paperwork Reduction Project (0704-0188) Washington DC 20503.

1. AGENCY USE ONLY *(Leave blank)*	2. REPORT DATE June 2000	3. REPORT TYPE AND DATES COVERED Master's Thesis

TITLE AND SUBTITLE : EL NINO AND LA NINA EFFECTS ON TROPICAL CYCLONES: THE MECHANISMS	5. FUNDING NUMBERS
6. AUTHOR(S) Bruce W. Ford, LT, USN	
7. PERFORMING ORGANIZATION NAME(S) AND ADDRESS(ES) Naval Postgraduate School Monterey, CA 93943-5000	8. PERFORMING ORGANIZATION REPORT NUMBER
9. SPONSORING / MONITORING AGENCY NAME(S) AND ADDRESS(ES) N/A	10. SPONSORING / MONITORING AGENCY REPORT NUMBER

11. SUPPLEMENTARY NOTES The views expressed in this thesis are those of the author and do not reflect the official policy or position of the Department of Defense or the U.S. Government.

12a. DISTRIBUTION / AVAILABILITY STATEMENT	12b. DISTRIBUTION CODE
Approved for public release; distribution is unlimited.	

ABSTRACT *(maximum 200 words)* The effects that El Niño and La Niña events exert on western North Pacific tropical cyclones, and the physical mechanisms involved were examined using best track data from the Joint Typhoon Warning Center and NCEP reanalysis data. During El Niño and La Niña events, equatorial heating anomalies induce anomalous tropical and extratropical atmospheric wave trains which alter circulation, vertical shear, and steering flow.

The shear changes cause tropical cyclones to form farther south and east (north and west) than normal during El Niño (La Niña) events. These formation differences lead to longer (shorter) tracks and stronger (weaker) tropical cyclones during El Niño (La Niña) events. Late in the tropical cyclone season, the anomalous extratropical waves alter the subtropical ridge and steering flow to favor recurving (straight running) tropical cyclones during El Niño (La Niña). These track differences lead to a much higher number of landfalling tropical cyclones in southeast Asia during La Niña events.

A preliminary study of the North Atlantic shows that there are more, and stronger, tropical cyclones during La Niña than El Niño. This is the result of extratropical Rossby wave trains that originate in the east Asia and extend into the North Atlantic. There they alter the vertical shear, so that La Niña favor more formations in the tropical Atlantic, where other conditions are favorable for the development of strong tropical cyclones.

14. SUBJECT TERMS El Niño, La Niña, tropical cyclones, hurricanes, typhoons, climate, Pacific, Atlantic	15. NUMBER OF PAGES 190
	16. PRICE CODE

17. SECURITY CLASSIFICATION OF REPORT	18. SECURITY CLASSIFICATION OF THIS PAGE	19. SECURITY CLASSIFICATION OF ABSTRACT	20. LIMITATION OF ABSTRACT
Unclassified	Unclassified	Unclassified	UL

NSN 7540-01-280-5500

Standard Form 298 (Rev. 2-89)
Prescribed by ANSI Std. 239-18

THIS PAGE INTENTIONALLY LEFT BLANK

Approved for public release; distribution is unlimited

EL NINO AND LA NINA EFFECTS ON TROPICAL CYCLONES: THE MECHANISMS

Bruce W. Ford
Lieutenant, United States Navy
B.S., University of South Carolina, 1994

Submitted in partial fulfillment of the
requirements for the degree of

MASTER OF SCIENCE IN

METEOROLOGY AND PHYSICAL OCEANOGRAPHY

from the

NAVAL POSTGRADUATE SCHOOL
June 2000

THIS PAGE INTENTIONALLY LEFT BLANK

ABSTRACT

The effects that El Niño and La Niña events exert on western North Pacific tropical cyclones, and the physical mechanisms involved were examined using best track data from the Joint Typhoon Warning Center and NCEP reanalysis data. El Niño and La Niña events profoundly alter tropospheric circulation in the western North Pacific. This occurs when equatorial heating anomalies induce anomalous tropical Rossby-Kelvin waves and extratropical Rossby wave trains which alter circulation, vertical shear, and steering flow in the tropics and subtropics, especially late in the tropical cyclone season.

Alteration of vertical shear causes tropical cyclones to form farther south and east than normal during El Niño events, and further north and west than normal during La Niña events. These formation site differences lead to longer tracks and stronger tropical cyclones during El Niño, and shorter tracks and weaker tropical cyclones during La Niña events. The greater strength of tropical cyclones during El Niño events appears to be the result of the formation site difference that allow longer tracks over warm sea surface temperatures. The strength differences are not directly related to sea surface temperature anomalies, since these anomalies are negative (positive) in the areas through which the El Niño (La Niña) storms move. Late in the tropical cyclone season (September-November), the anomalous extratropical waves alter the subtropical ridge and steering flow in ways that favor recurving tropical cyclones during El Niño and straight running tropical cyclones during La Niña. These track

differences lead to a much higher number of landfalling tropical cyclones in southeast Asia during La Niña events.

A preliminary study of the North Atlantic shows that there are more tropical cyclones, especially strong tropical cyclones, during La Niña, and fewer during El Niño. This appears to be the result of the extratropical Rossby wave trains that originate in the east Asian - western North Pacific region and extend into the subtropical and tropical North Atlantic. There they alter the circulation and vertical shear, such that El Niño events decrease vertical shear in the subtropical Atlantic and increase shear in the tropical Atlantic, while La Niña events increase shear in the subtropical Atlantic and decrease shear in the tropical Atlantic. The shear changes during La Niña favor more formations in the tropical Atlantic, where other conditions are favorable for the development of strong tropical cyclones.

TABLE OF CONTENTS

LIST OF ACRONYMS

CDC	Climate Diagnostics Center
COADS	Comprehensive Ocean-Atmosphere Data Set
EN	El Niño
ENSO	El Niño Southern Oscillation
hPa	Hecta-Pascals
JTWC	Joint Typhoon Warning Center
LN	La Niña
MEI	Multivariate ENSO Index
NCEP	National Centers for Environmental Prediction
NHC	National Hurricane Center
NOI	Northern Oscillation Index
NPNANA	North Pacific – North American – North Atlantic
OLR	Outgoing Longwave Radiation
SCS	South China Sea
SLP	Sea Level Pressure
SO	Southern Oscillation
SOI	Southern Oscillation Index
SPLA	Sea Level Pressure Anomaly
SST	Sea Surface Temperature
SSTA	Sea Surface Temperature Anomaly
TC	Tropical Cyclone
TUTT	Tropical Upper-Tropospheric Trough
Z	Height

THIS PAGE INTENTIONALLY LEFT BLANK

LIST OF TABLES

THIS PAGE INTENTIONALLY LEFT BLANK

ACKNOWLEDGEMENT

Professor Murphree expended countless hours guiding this research, answering questions and providing the scientific leadership this work required and for that, I am deeply grateful. His contribution will not be forgotten. I would also thank Phaedra Green and Lynn DeWitt of the NOAA Pacific Fisheries Environmental Laboratory in Monterey for their assistance in avoiding code pitfalls. Finally, I'd like to thank my Life Partner, Jennifer, for her loving forebearance while I completed this project and Master's degree.

I. INTRODUCTION

A. BACKGROUND

People have struggled to understand and cope with their environment since the beginning of recorded time. These struggles have helped people to improve their understanding of the environment, so that many useful environmental predictions are now possible. These predictions depend heavily on knowing the typical patterns of environmental change. The physical environment varies over a broad range of space and time scales. Diurnal and seasonal variations are familiar examples of environmental changes that occur at very different time scales. Two familiar spatial variations are those between the tropics and the higher latitudes, and between oceanic and continental regions. Our ability to predict the environment suffers when the behavior of the environment is significantly different from its average behavior.

Such variations from the average occur during El Niño (EN) and La Niña (LN) events. EN and LN are interannual events that occur in the tropical Pacific and Indian ocean regions, last about a year, and occur every two to seven years. These events produce environmental changes that, on a human time scale, are second only to seasonal changes in their magnitude and scope. EN and LN induced perturbations are blamed for floods, droughts, fires, pestilence, diseases, and social disruptions around the world. It is still very difficult to predict the occurrence, intensity, and impacts of EN and LN events. This is in large part because the events usually occur only every few years, and because each event is relatively unique.

Tropical cyclones (TCs, for example typhoons in the western Pacific and hurricanes in the Atlantic) can have major environmental and social impacts, so it is important to be able to predict their formation, intensity, tracks, and duration. Several recent studies have implied that TCs are affected by EN and LN events (Chan 1985, Lander 1994). The purpose of this study is to clarify just what impacts EN and LN events have on TCs in the western tropical North Pacific, the most active TC region in the world, and to identify the mechanisms by which these impacts occur. In addition, this study includes a preliminary analysis of the mechanisms by which EN and LN events may impact TCs in the North Atlantic. It is our hope that by improving our understanding of the impacts of EN and LN events on TCs, we will arrive at a better understanding of EN and LN events, and TCs, which will lead to better use of forecasting resources, improved warnings, and a decreased loss of life and property to TCs.

B. EN AND LN EVENTS AND THEIR IMPACTS ON THE GLOBAL CIRCULATION

Walker (1924) and Walker and Bliss (1932) examined pressure, temperature, and precipitation anomalies in the Indian Ocean and the western Pacific. They found evidence of a transfer of atmospheric mass between the eastern Indian Ocean - maritime continent region and the southeastern tropical and subtropical Pacific region. This transfer occurred on an interannual scale and was named the Southern Oscillation. Walker and Bliss found significant correlations between the Southern Oscillation and atmospheric variations around the world (e.g., precipitation in Hawaii, temperature in western Canada, sea level

pressure in the southeastern United States). Walker (1924) and Walker and Bliss (1932) helped establish the existence of global environmental interactions, or teleconnections. However, they did not explain the mechanisms that produce teleconnections.

Bjerknes' (1966, 1969, 1971) studies of teleconnections found that anomalous air-sea interaction in the tropical Pacific could cause anomalous energy exchanges between the tropics and extratropics that, in turn, lead to global circulation anomalies. Bjerknes (1966, 1969) pioneered the use of the term El Niño to describe a set of interannual anomalies in the Pacific. These anomalies include unusually weak trade winds, warm sea surface temperatures (SSTs), strong atmospheric convective activity in the central and eastern equatorial Pacific, and unusually cool SSTs and weak convection in the western equatorial Pacific. Bjerknes also suggested that EN events were linked to the SO by way of the anomalous tropical sea level pressures and winds associated with the SO. Rasmusson and Carpenter (1982) concluded that EN events occur every two to seven years. Several studies (e.g., Bradley et al. 1987) noted that in some non-EN years, the anomalies associated with EN events were reversed (e.g., in the central and eastern equatorial Pacific, the trade winds were unusually strong and the SSTs were anomalously cool). This near-opposite situation was termed a La Niña event. Philander (1990) summarizes many of the major features of the SO and of EN and LN events.

The convective heating anomalies that occur throughout the tropical Pacific during EN and LN events have been shown in modeling studies to

produce tropical and extratropical atmospheric circulation anomalies. The tropical response to such anomalous tropical forcing was modeled by Matsuno (1966) and Gill (1980) who found that the forcing can produce an equatorial Rossby-Kelvin wave response, such as that shown in Figure 1. This forcing can be the result of anomalies in the equatorial heating, mass, and/or circulation fields. Modeling studies by Hoskins and Karoly (1981) and others have shown that the Rossby portion of this response may extend into the extratropics, thus potentially producing global responses to EN and LN events, similar to that shown in Figure 2.

Horel and Wallace (1981), Murphree and Reynolds (1995), and many others conducted observational studies that described a number of characteristic extratropical anomalies that occur during EN and LN events. Figure 3 shows an example of the characteristic 200 hPa anomalies in the northern winter during EN and LN events. Such characteristic anomalies describe the teleconnection patterns associated with EN and LN events. The strong resemblance between many observed teleconnection patterns and the modeled wave train responses (Matsuno 1966, Gill 1980, Hoskins and Karoly 1981) indicates that the teleconnections were the result of anomalous Rossby wave trains forced by the anomalous atmospheric heating in the tropical Pacific during EN and LN events.

C. TELECONNECTIONS FROM EAST ASIA

A number of studies have shown that relatively short term and small scale convective heating anomalies in the East Asian - western North Pacific region can generate anomalous midlatitude wave trains that extend from East Asia

across the North Pacific - North American - North Atlantic (NPNANA) region. Nitta (1987) linked intraseasonal to seasonal scale anomalies in western tropical Pacific SST and convection to anomalous upper tropospheric heights over Japan during the northern summer. He found that anomalously high SSTs and strong convection near the Philippines were associated with anomalously high heights over Japan, and vice versa. He also found that the height anomalies over Japan were part of a wave train that described a gentle zonal arch over East Asia and the North Pacific (Fig. 4). The anomalous western tropical Pacific SSTs and convective heating appeared to be the trigger for the anomalous wave train.

Such wave trains have also been found in observational and modeling studies of the Intraseasonal to seasonal response to tropical cyclone activity in the western North Pacific (Harr 1993, Woll 1993, Springer 1994, Jakus 1995, and Malsick 1995). These studies concluded that, through interactions with the East Asian – North Pacific jet, heating and vorticity anomalies in the tropical and mid latitude East Asian – western North Pacific region could generate anomalous wave trains that extend into the North Atlantic. Such wave trains could set up teleconnections that link the monsoon and TC activity of southern and eastern Asia and the western North Pacific to the NPNANA region, including the TC regions of the North Atlantic.

D. EN AND LN EVENTS AND WESTERN PACIFIC TCS

A number of studies have been conducted to identify what impacts, if any, EN and LN events have on TCs in the western North Pacific (Chan 1985, Lander 1994, Chen 1998). However, these studies have used a variety of data and

methods, and have come to opposite conclusions, so it is difficult to compare and apply their results.

Chan (1985) analyzed the temporal distribution of TCs in the western Pacific using spectral analyses and noted a peak centered near 3.5 years, which was thought to reflect the effects of the Southern Oscillation (SO, a tropical atmospheric phenomenon associated with EN and LN events and having a similar periodicity of about 3.5 years). This study suggested that there are fewer TCs during an EN event, and even fewer in the year following the event. Chan also concluded that EN (LN) events tend to produce a large number of TC formations east (west) of the climatological average formation location.

Lander (1994) found two statistically significant relationships existed between the number of western Pacific TCs and EN and SO phenomena. Lander concluded that a reduction in the number of early season TCs occurred when the eastern equatorial Pacific SST started out high and fell sharply by the middle of the year. Lander also reported a statistically significant relationship between the number of late season TCs and higher than normal eastern equatorial SST. Lander (1994) also found a significant difference in the formation regions for western North Pacific TCs for EN and LN periods. For EN periods, more TCs formed near the central tropical Pacific (near the intersection of the equator and dateline) than usual, while in LN periods, TCs tended to form farther to the north and east than usual. This study also examined the numbers of intense storms, (defined as storms with a central pressure of 920 hPa or

lower), and found no significant correlation with any EN index or the Southern Oscillation Index (SOI).

Lander and Guard (1999) performed cross correlations between the ocean basins that have TCs and found a weakly significant positive correlation between the annual number of TCs in the western North Pacific and the numbers of TCs in the southern hemisphere and the eastern North Pacific basins. This study also found the number of TCs in the North Atlantic to be positively correlated with the SOI, with the correlation being significant at the 99% level.

Chen et al. (1998) examined summertime western North Pacific monsoon trough disturbances and noted an anomalous 850 hPa anticyclonic circulation cell in the western subtropical Pacific north of 15°N and a anomalous cyclonic circulation in the western tropical Pacific south of 15°N at 850 hPa during EN events. During LN event summers, Chen et al. (1998) noted the opposite: a anomalous cyclonic circulation cell in the western subtropical Pacific north of 15°N and a anomalous anticyclonic circulation in the western tropical Pacific south of 15°N at 850 hPa. The authors suggested that these anomalous circulation patterns were the result of tropical synoptic-scale disturbances that occurred primarily south of 15°N during EN events but farther to the north during LN events.

Chen and Weng (1998) suggested summertime variations in the number of TCs occurring just north of the climatological location of the monsoon trough were associated with SST fluctuations in the NINO3 region. This work viewed the anomalous circulation cells noted in Chen et al. (1998) as the westernmost

cells in anomalous wave trains that originated in the western tropical Pacific and extended across the extratropical North Pacific.

Most of the above studies focused on statistical relationships between EN events and the numbers of TCs and their formation locations. The relationships with LN events were generally not emphasized or only indirectly addressed. Little attention was given to other aspects of TC activity, such as the impacts of EN and LN events on TC intensity, number of strong and weak TCs, tracks, or landfalls. Only Lander (1994) attempted to separate storms by intensity to compare with an EN signal, but found no correlation. Several of these studies agreed that EN and LN events alter formation locations. The major disagreement between these studies was in the correlation between the numbers of TCs and EN and LN events, with Chan (1985) proposing fewer numbers of TCs reaching tropical storm strength in EN. Subsequent studies refute Chan's findings. Additionally, none of these studies provided much insight on the mechanisms that might explain the relationships between EN and LN events and TC activity. In addition, these studies identified different years and TC seasons as ones that were impacted by EN and LN event periods (see section F below). This makes it difficult to compare their results and to determine which results best represent the impacts of EN and LN events on TCs. Finally, these studies were conducted too soon to consider the impacts of several recent major EN and LN events (the 1997-1998 EN and the 1998-2000 LN events). Thus, these studies leave unresolved some major questions about the links between western North Pacific TC activity and EN and LN events.

E. EN AND LN EVENTS AND NORTH ATLANTIC TCS

Links between EN and LN events and North Atlantic TC numbers have been identified in a number of studies. Gray (1984) showed a significant negative correlation between the frequency of North Atlantic hurricanes and SST anomalies in the eastern equatorial Pacific associated with strong to moderate EN events. This study also revealed a similar negative correlation between the number of Atlantic hurricanes and equatorial upper tropospheric wind anomalies in the western Atlantic and Caribbean basins.

Shapiro (1987) found that during EN events, the 200 hPa circulation in the North Atlantic and Caribbean resembled an equatorially-confined Walker circulation. This circulation was associated with strong 200 hPa anticyclonic vorticity at in the tropical North Atlantic and increased vertical shear in the region from 10° to 30°N.

Gray et.al. (1993) found that useful seasonal forecasts of Atlantic TC activity could be made by using selected predictors which included elements of the quasi-biennial oscillation, West African rainfall, EN, SO, and Caribbean upper tropospheric wind and sea level pressure anomalies.

Goldenberg et. al. (1996) found that Atlantic hurricane activity was related to western Sahelian rainfall and eastern equatorial Pacific SST anomalies through modification of upper and lower tropospheric winds in the equatorial Atlantic TC formation area. This study suggested vertical shear anomalies in the subtropics north of the formation area are unrelated, or out of phase with shear anomalies in the formation region. Goldenberg et al. (1996) also indicated that

North Atlantic basin shear anomalies associated with EN tend to be equatorially confined.

F. EN AND LN INDICES

Several indices have been developed to monitor EN and LN events. The most familiar and widely used of these is the Southern Oscillation Index (SOI). The SOI is calculated by subtracting the sea level pressure anomaly (SLPA) at Tahiti from the SLPA at Darwin in northern Australia. The Northern Oscillation Index (NOI) developed by Schwing et al. (2000) is similar to the SOI, but is calculated by subtracting the SLPA at the annual mean position of the North Pacific High in the subtropical northeast Pacific from the SLPA at Darwin. The NOI is an indicator of the role of the North Pacific in EN and LN events. The NINO3 index is another commonly used index that measures the strength of EN and LN events. It is the SST anomaly (SSTA) averaged over the box bounded by 5S, 5N, 150W, and 90W.

The Multivariate ENSO Index (MEI, Wolter and Timlin 1998) provides a means of monitoring EN and LN events using six environmental variables. Unlike the SOI, NOI, and NINO3 index, which are calculated using one variable (SLPA or SSTA) at just one or two locations, the MEI incorporates sea level pressure, zonal and meridional surface winds, sea surface temperature, surface air temperature, and total cloudiness fraction over a broad tropical Pacific region. Thus, the MEI provides a broader measure than the SOI, NOI, or NINO3 index of EN and LN events and their intensities.

MEI values are available from 1950 (Fig. 5) and the variations of the MEI are similar to those of the SOI, NOI, and NINO3 index. While the MEI and the other indices do not agree on some weak events, their agreement is very good with moderate and strong events. The MEI shows that EN and LN events tend to start in the northern spring (March-June). EN events reach their maximum intensity during the following northern winter (Dec-Mar), while LN events tend to reach their maximum intensity during the following late fall or early winter (Sep-Nov) (Fig. 6). Both EN and LN events tend to end in the following northern spring, about one year after they began. These typical EN and LN event evolutions are illustrated in Figure 5 for a number of individual events.

The typical evolutions of EN and LN events shown in Figure 5 indicates that two northern hemisphere TC seasons overlap in time with the typical EN or LN event such that: (1) the season that begins several months prior to the start of an event and the season that begins several months before the end of a event. Thus, there are two northern TC seasons that might be affected by EN and LN events. In most previous studies, the authors did not identify which of the two seasons that occur during EN and LN events they were examining. This two-season issue may explain why different studies used different years as EN or LN years, and why they came to different conclusions.

Previous studies of EN and LN impacts on TCs have used a variety of EN and LN indices. This has also led to some uncertainty about the results of these studies and may be the reason for some of the conflicting results For example, the MEI classifies 1978 as an EN event, however the SOI lists 1978 as neither

EN or LN. Gray (1993) and Goldenberg et al. (1996) list 1978 as an LN event, while Chen et al (1998), Chen (1993), Chu et al (1997), and Lander (1994) studies do not consider 1978. The different indices have a large number of disagreements about weak and moderate events. Thus, it may be important to focus on the stronger events when trying to identify EN and LN impacts on TCs.

Table 1 lists the EN and LN event years identified by several indices and used in various studies of EN and LN impacts on TCs. Note the disagreements about whether an event occurred, whether it was an EN or LN event, and whether it was a weak, moderate, or strong event.

Year	MEI	SOI	NOI	Lander 1994	Chen et al. 1998	Chen 1998	Gray 1984	Gray et al. 1993	Goldenberg et al 1997
49	LS								
50	LS	LS	LW					L	
61	EW	EM	EW					E	
52			LM					L	
5[illegible]		EM					EM	L	
54	LS	LM	LS						
5[illegible]	LS	LS	LM					L	
56	LS	LM	LW					L	
57	ES	EW	ES				ES		
5[illegible]	EW		LM					L	
5[illegible]		LM	LM					L	
60		LW	LW					L	
61	LS	LM	LM					E	

62	LS	LM						L	
63	EM	EW	LM	E				L	
64	LS	LW	LM	L				E	
65	ES	EM		E			EM	E	
66	LW	LM	LM						
67	LM	LW	LW					L	
68	EW		EW					L	EW
69		EW	EM	E				E	EW
70	LS	LS	LS	L				L	L
71	LS	LM	LM	L				L	L
72	ES	EM	EM	E			ES	E	ES
73	LS	LVS	LM	L				L	L
74	LS	LW	LM	L				L	L
75	LS	LS	LS	L				L	L
76	EW	LW	LS				EM	E	EM
77	EM	EM	ES	E				E	L
78	EW		LW					L	L
79	ES		ES					L	EM
80			EW					E	L
81		LW	EW		L	L		L	L
82	EES	EVS	EVS	E	E	E	ES	E	EVS
83		LW	LM		E	E	ES	E	EVS
84	LM	LW	LS			L		E	L
85		LW	EM		L	L		E	L
86	EVS	ES	EM					L	EW
87	EM		LW	E	E	E		E	EM

88	LS	LS	LS	L		L		L	L
89			LW	L	L	L		L	L
90			LM					L	L
91	EVS	EM	ES	E	E	E			
92	EM	EM	EM						EW
93	EW		LW						
94	ES	EM	EM		L	L			
95	LW	LW	EW						
96	LW	LM	LW						
97	EVS	ES	ES						
98	LS	LM	LS						

Table 1. EN and LN events as identified by different indices and by selected authors of studies of the impacts of these events on western North Pacific and North Atlantic TCs. Chan (1985) reported using the SOI for his study but did not specify years. Shapiro et al. reported using the ENI from Weare (1986). Key: first letter: L=LN, E=EN; following letters W=weak, M=moderate, S=strong, VS=very strong, ES=extremely strong.

G. DESIGN OF THIS STUDY

This study was motivated in part by the shortcomings of previous studies, and by several issues left unresolved by these studies:

1. As a group, past studies have used inconsistent means for identifying EN and LN events and the TC seasons that might have been affected by them. In this study, we use a new and

broad based index, the MEI, to help resolve some of these problems.

2. Most previous studies have focused on differences in the numbers of TCs occurring in EN or LN events, with little or no attention to differences in TC intensities or tracks. We attempt to address these other aspects of TC activity in this study.

3. Most past studies have taken mainly a statistical perspective, with little analysis of the physical mechanisms. In this study, we analyze the large scale circulation anomalies associated with EN and LN events and the roles they play in altering TC activity.

4. Most previous studies have focused on EN events and did not conduct any explicit analyses based on LN events. In this study, we consider both EN and LN events and use composites of both types of event to identify the impacts of each type on TC activity.

5. Most past studies were conducted too early to consider several strong EN and LN events that occurred in the 1990s. We consider all events during 1949-1999.

6. Very few previous studies have attempted to identify the links between EN and LN impacts on TC activity in different basins. In this study, we use teleconnection concepts to link the impacts in the western North Pacific to those in the North

Atlantic, and to identify possible wave train mechanisms for EN and LN impacts on North Atlantic TC activity.

The main purpose of this observational study is to clarify the role of EN and LN events on tropical cyclones, mainly western North Pacific TCs, but also North Atlantic TCs. We focus in this study on two main questions:

1. How was TC activity different during past EN and LN events?
2. What mechanisms caused these differences in TC activity?

Our basic hypotheses are:

1. Equatorial heating anomalies, attributable to EN and LN events, contribute to anomalous tropospheric circulations that resemble quasi-stationary equatorial Rossby-Kelvin waves. These anomalous circulations help alter the vertical shear and steering flow in the tropical Pacific. This leads to alterations of the formation sites, numbers, intensities, and tracks of TCs in the western tropical Pacific. All of these alterations tend to be opposite for EN and LN events, because their respective heating anomalies are opposite.
2. EN and LN events play a role in creating quasi-stationary anomalous wave trains extending from the East Asian - western North Pacific region across the North Pacific - North American - North Atlantic region. These wave trains alter the vertical shear and steering flow in the tropical North Atlantic, thereby altering the formation sites, numbers, intensities, and tracks of TCs in this area. All of these alterations tend to be opposite for

EN and LN events, because their respective heating anomalies are opposite.

We focus in this study on testing hypothesis 1. We hope that this work will help improve our ability to provide useful TC forecasts on weekly and longer time scales by identifying the lower frequency and large scale factors that affect TC activity.

H. ORGANIZATION

In the following chapter, our data and methods are presented. Chapter III presents our main results. Chapter four provides our summary of results, discussions and conclusions, and suggestions for future research.

THIS PAGE INTENTIONALLY LEFT BLANK

II. DATA AND METHODS

A. DATA

Much of our data for this study came from the National Centers for Environmental Prediction (NCEP) reanalysis data set (Kalnay et al. 1996). Most of these data were in the form of monthly mean fields at a 2.5° latitude x 2.5° longitude resolution provided by the NOAA-CIRES Climate Diagnostics Center (CDC), Boulder, Colorado, from their web site at http://www.cdc.noaa.gov. This set uses a fixed, state-of-the-art, global data assimilation system to create a global data set containing the major atmospheric thermodynamic and circulation fields and many surface oceanographic fields. The reanalysis data were available from January 1947 to March 2000 for most fields as of this writing. The reanalysis set includes some suspect fields, especially for earlier years and for areas in which observations were especially limited. These problems are outlined at http://www.cdc.noaa.gov/cdc/data.nmc.reanalysis. However, for most of the times and locations considered in this study, the reanalysis fields appear to be reliable indicators of the large scale thermodynamic and circulation fields (cf. Kalnay et al. 1996).

Liebmann and Smith (1996) interpolated OLR and reconstructed sea surface temperature (SST) fields (Reynolds et al.1995, Smith et al. 1995) were also used. The Liebmann and Smith OLR data set is available for June 1974 to March 2000 and is based on an interpolation scheme that estimates missing data in both the spatial and temporal domains. The Reynolds SST data reconstructs historical SST values using empirical orthogonal functions and is available for

1950-1992. Liebmann and Smith interpolated OLR was used for examination of OLR anomaly and climatology fields in this study. Reynolds reconstructed SST was used to examine SST anomaly and climatology fields.

The Pacific TC data, which contains 1536 TC files covering 1945-1999, comes from the best-track data collected continuously since 1945 by the Department of Defense Joint Typhoon Warning Center (JTWC), currently located in Pearl Harbor, Hawaii. The National Hurricane Center (NHC) in Miami, Florida provided the Atlantic TC data, which contain 571 TC files from 1945-1999. The JTWC data provides good positional fixes based on aircraft penetrations of known typhoons during 1945-1987. Prior to the advent of satellites, there is the possibility that TCs formed without being recorded by JTWC. The wide use of satellites to locate and classify TCs since 1974 probably provides more accurate TC data during the satellite era (Carr 1999). There are clear variations in the Pacific TC time series, with high TC numbers in the 60s, dropping to lower values in the 70s, and gradually increasing in the 80s (Lander 1994). These variations may be real, but some are likely due to variations in such human factors as reconnaissance tactics and operational warning philosophy (Lander, 1994).

The JTWC data lacks information on most TCs that formed east of 180° longitude. And for some TCs, the first best-track report is for a location on or near the dateline, even though the TC formed east of the dateline. These problems are the result of JTWC being responsible for reporting TCs at and west of the dateline, with the Central Pacific Hurricane Center responsible for reporting

east of the dateline. However, these problems with TCs east of the dateline do not affect our major results, as will be shown in Chapter 3.

B. INDEX SELECTION

As described in Chapter I, previous research differed significantly in their identification of when EN and LN events occurred and their strength (see Table 1). For this study, we used the Multivariate ENSO Index (Wolter and Timlin 1998) primarily because it provided a more complete depiction of EN and LN events. The MEI is based on six observed tropical Pacific fields: sea-level pressure, zonal surface wind, meridional surface wind, sea-surface temperature, surface air temperature, and total cloudiness fraction of the sky. All fields are derived from the Comprehensive Ocean-Atmosphere Data Set (COADS). The MEI is computed separately for each of twelve sliding bi-monthly seasons (Dec/Jan, Jan/Feb, ... Nov/Dec). Positive (negative) values of the MEI represent EN (LN) events.

We used the MEI to identify EN and LN events during 1949-1999 and to classify these events according to their strength. Periods for which the MEI was greater (less) than or equal to 0.3 (-0.3) for at least two consecutive bimonthly periods during the northern fall or winter were identified as EN (LN) events (Wolter and Timlin 1998). The northern fall and winter are the seasons in which EN and LN events tend to peak (see Fig. 6). Table 2 lists the EN and LN events since 1949, which were identified by this method. The asterisks in this table indicate the stronger events. Because of the disagreements between some indices among weaker events, we focused in this study on the stronger events

indicated in Table 2. Table 3 shows the categories used to classify the strength of EN and LN events.

First Year of EN Event	First Year of LN Event
1951	1949*
1957*	1954*
1958	1954*
1963	1956*
1965*	1956*
1968	1961*
1972*	1962*
1976	1964*
1977	1966
1978	1967
1979*	1970*
1982*	1971*
1986*	1973*
1987	1974*
1991*	1975*
1992	1984
1993	1988*
1994*	1995
1997*	1996
	1998*
	1999*

Table 2. EN and LN events since 1949 according to the MEI. "*" indicates events that were strong, very strong, or extremely strong, as explained in Table 3.

Strength	EN Events	LN Events
Weak	0.3 to 0.5	-0.3 to -0.5
Moderate	>0.5 to 1.0	<-0.5 to -1.0
Strong	>1.0 to 2.0	<-1.0 to -2.0
Very Strong	>2.0 to 3.0	<-2.0 to -3.0
Extremely Strong	>3.0	<-3.0

Table 3. MEI strength categories and corresponding MEI values for EN and LN events.

During 1949-1998, there were nine strong, very strong, or extremely strong EN events and fifteen such LN events. For comparisons of EN and LN impacts on TCs, we frequently used nine strong EN events and nine strong LN from the period because equal numbers of events are required. Inherent reanalysis and TC data problems appear to be minimized by selecting events after 1957. In the case of EN and LN, the nine selected events were drawn from recent events. The nine selected strong EN and LN events focused on in this study are listed in Table 4.

Nine Strong EN Event Years	Nine Strong LN Event Years
1957	1962
1965	1964
1972	1970
1979	1971
1982	1973
1986	1974
1991	1975
1994	1988
1997	1998

Table 4. List of nine strongest EN and LN events focused on in this study.

The sensitivity of our results to this selection of strongest events was tested by using several alternate selections of events, including all events during 1949-1998, all events during 1974-1998 (i.e., during the satellite era), etc. Our major results were very similar for each of these alternate event sets.

C. CALCULATIONS

1. Anomalies and Composites

We calculated anomalies for many fields in order to highlight the impacts of and differences between EN and LN events. The anomalies were calculated as the difference between the actual value for a period minus the climatological value for that period. For example, to calculate the anomalous 200 hPa geopotential height for August 1998, we subtracted the monthly mean 200 hPa height for August 1998 from the climatological monthly mean 200 hPa height for August. The climatological mean was based on the monthly means for 1968-1996, in order to be compatible with climatological mean used by the Climate Diagnostics Center.

Composites were calculated to identify average, or characteristic patterns. For example, to find the characteristic 200 hPa height anomalies in August during LN events, we averaged together the nine monthly 200 hPa height anomalies from the nine strongest LN events. Similarly, to find the characteristic LN anomalies during August-November, we averaged together the LN composite monthly anomalies for August, September, October, and November.

2. Vertical Shear

The vertical shear of the zonal wind was calculated by subtracting the monthly mean zonal wind at 850 hPa from the overlying monthly mean zonal wind at 200 hPa.

3. Correlations

Correlations between different global fields were used to help identify teleconnections. For this study, monthly mean time series of SST, sea-level pressure, and 200 hPa height were created for selected base locations for the 1949-1998. These time series were then correlated with time series for these and other fields for all locations using a linear correlation scheme provided at the CDC web site http://www.cdc.noaa.gov/correlations. The results were global correlation maps depicting areas of high and low correlation with the base location fields.

4. TC Time Series

Twenty-four month composite time series were calculated from several components of the TC data sets. The 24 month period spans the two calendar years over which EN and LN events typically occur (cf. Fig. 6) and includes the northern basin TC season that occurs just before and during the peak of EN and LN events, and the TC season that occurs in the following calendar year. These time series allowed us to study the impacts of EN and LN events over the full course of the two TC seasons that are most likely to be affected by the events. However, there are problems with using one continuous 24 month period to examine the impacts on the second of the two TC seasons. Many EN and LN events are followed by another event, either another EN or another LN event. This means that the data that goes into creating the second TC season composite may represent TCs occurring just before and during the peak of both EN and LN events. Thus, considerable care must be exercised when examining

the TC season following the event peak. Almost all the results of our study are based on the first of the two TC seasons in the time series; that is, the TC season that occurs immediately before and during the event peaks.

We calculated five types of TC time series:

a) average number of best-track reports per month, defined as a position report or TC warning which results in a line in a best-track data file.

b) total number of TCs per month

c) total number of strong TCs per month, defined as TCs with maximum sustained winds of 80 knots (41 m/s)

d) total number of weak TCs defined as TCs with maximum sustained winds of less than 80 knots (41 m/s)

e) average TC intensity per month, based on each TC's maximum intensity.

The numbers of best-track reports per month were used as proxies for overall TC activity (analogous to TC days per month) and for TC forecaster activity. The number of TC reports per month was calculated by averaging the number of TC reports for each calendar month for each event, with each report being assigned to the month in which it formed. A similar procedure was followed for the calculation of the other types of TC time series. For each type of time series, the EN and LN composite time series were compared with each

other and with the climatological time series. In addition to the time series, TC formation sites, tracks, point of maximum intensity, and westernmost longitude were plotted on maps for each month of the 24 month series, and then analyzed to identify patterns characteristic of EN and LN events.

THIS PAGE INTENTIONALLY LEFT BLANK

III. RESULTS

A. EN AND LN EFFECTS ON PACIFIC TCS

We began our assessment of EN and LN impacts on western North Pacific TCs by analyzing the five types of TC time series described in Chapter II. We then analyzed maps of formation sites, vertical shear, 200 hPa height anomalies, tracks, and westernmost positions. Our two main objectives were to identify: (1) the patterns in these fields that are characteristic of EN and LN events; and (2) the mechanisms that explain these characteristic patterns. For the reasons stated in Chapter II, the results presented in this chapter are based mainly on analyses of the nine strong EN and LN events listed in Table 4. We chose to analyze this limited set of events in order to minimize uncertainties in the identification of weak events, and so that we would have identical numbers of events to work with when comparing TC tracks and landfalls during EN and LN events. The results derived from these nine EN and nine LN events are very robust and similar to those we obtained when using several other sets of EN and LN events, including all EN and LN events and all events since the beginning of satellite observations. Although our focus was on the TC season that occurs just before and during the peak of the composite EN or LN event (cf. Fig. 6), we have presented below some results for the following TC season in order to make comparisons between the two TC seasons. Throughout this report, our statements about TC seasons and TC activity refer to the first of these two seasons, unless otherwise stated.

1. EN, LN, and Climatology

During the 51 year period between 1949-1999 the MEI record indicates that there were 19 EN events, 21 LN events, and 11 non-events (see Table 2). Thus, about 80 percent of the years were either EN or LN periods. Some of the 40 events in this record were weak events, but even considering only moderate and stronger events, the majority of years were either EN or LN periods. The analysis of EN and LN events involves comparisons of actual fields with climatological means in the calculation of anomalies. But, since the majority of years are either EN or LN periods, the climatological means embody both EN and LN features and may therefore be more statistical than real. Thus, in this study we focused on comparisons between composite EN patterns with composite LN patterns, rather than comparisons with climatological patterns. We did, however, use climatological means to calculate the characteristic EN and LN anomaly patterns. These means are based on the 1968-1996 period, when there were 14 EN events and 11 LN events (see Fig. 5 and Table 2). To test whether this small bias toward EN events affected our results, we did some anomaly calculations using a 1949-1998 climatological mean and found no appreciable differences.

2. EN and LN Effects on Forecaster Activity

Figure 7 displays the average number of reports per month that were issued by JTWC on Pacific TCs during the nine strong EN and LN events listed Table 4. A report, as defined for this study, is a warning, satellite fix report, or post-storm analysis position that resulted in a positional fix line in best track data

files. The number of reports is used as a proxy for the amount of forecaster activity at JTWC and can be thought of as analogous to TC days a measure of TC activity employed by NHC.

The horizontal axis in Figure 7 shows the two calendar years associated with typical EN and LN events. The red (blue) bar along this axis shows the typical EN (LN) event period, with the dark red (blue) portion indicating the event peak during December-March (September-November; cf. Fig. 6). The TC season in the western North Pacific extends from February through January, with TC activity being low during December-June and high during July-November. Thus, the high activity period of the first of the two calendar years occurs just before (during) the EN (LN) peak.

Figure 7 shows a clear difference in the average number of reports per month for the composite EN event (red curve) and LN event (blue curve). During June-November, strong EN events produced about 50 more reports per month than LN events, with peak differences in the months of July and September of 75 reports. These results suggest that TC seasons, and TC forecasters, are much more active during EN events than during LN events.

3. EN and LN Effects on TC Numbers

Although the results shown in Figure 7 indicate that EN and LN events might affect the numbers of TCs, the average number of TCs per month during the composite EN and LN events (Figure 8) does not support this conclusion. The number of TCs is very similar for both EN and LN events, as suggested by

several previous studies (e.g., Lander 1994). This result holds true whether comparing composites of nine strong events or all events during 1949-1999.

However, the impacts of TCs vary greatly with their strength, so we also examined the average number of strong TCs (maximum sustained winds greater than or equal to 80 knots [41 ms^{-1}]) and the average number of weak TCs (maximum sustained winds less than 80 knots [41 ms^{-1}]). Figure 9 shows that during the peak of the TC season, there were about 2.5 more strong TCs during the composite EN event than during the composite LN event. The results for weak TCs (Fig. 10) are just the opposite, with strong LN events producing an average of about 3.5 more weak TCs during the peak of the TC season. Figures 9 and 10 help explain the discrepancy between Figures 7 and 8. The effects of EN and LN events on the number of strong and weak TCs offset each other, so that the total number of TCs is similar for the two events. However, the number of TC reports is greater for EN events, since strong TCs tend to last longer.

4. EN and LN Effects on TC Intensity

To examine the effects of EN and LN events on the variation of TC strength through the TC season, we created composite time series based on the maximum intensity of each TC. Figure 11 shows that during the peak of the TC season, the composite EN TCs have an average strength that is 10-15 knots (5.0-7.5 ms^{-1}) greater than for the composite LN TCs.

The results shown in Figures 7-11 indicate that EN events favor strong TCs and LN events favor weak TCs. To investigate the mechanisms by which these impacts on TC activity occur, we examined the links between TC formation

sites and tracks, vertical shear, and tropospheric height anomalies. Our objective in these investigations was to test our hypotheses that attribute much of the EN/LN differences in TC activity to the major changes in large scale circulation that occur during EN and LN events.

5. EN an LN Effects on TC Formation Sites

Chan (1985) and Lander (1994) found that TC formation sites during EN events tend to be farther east and south (closer to the dateline and equator) than during LN events. The composite EN and LN formation sites for May-December (Figs. 12-19) confirm these findings. To investigate why these formation differences occurred, we examined the corresponding vertical shear and the anomalous 200 hPa heights (Figs. 12-19). During May-December of both the EN and LN composites, most (85%) of the TCs formed within regions having a shear of -10 to $+10$ ms^{-1}. Figures 12-19 also indicate that formations were strongly affected by the month-to-month variations in the low shear region, and the large EN/LN differences in the low shear region. These results agree with the well-known idea that TC formation is very sensitive to shear and occurs mainly in low shear regions (e.g., Gray 1979).

The largest differences between the EN and LN composites in western North Pacific shear occur in two regions: (1) the tropics, east of New Guinea, within about 15 degrees of the equator and east of 150°E; and (2) the subtropics, south and east of Japan, at about 15°N-35°N and 135°E-180°E. In the tropical region, the low shear area extends much farther to the east in the EN composite than in the LN composite. Examinations of the corresponding composite total

lower tropospheric height fields (not shown) indicate that these differences in the tropical low shear area are the result of an east-southeastward extension of the monsoon trough during EN events and the reverse during LN events (discussed further in Chapter 3, section B; also cf. Chen et al 1998). In the subtropical region, the low shear area extends much farther to the east-northeast in the LN composite than in the EN composite. The total composites (not shown) reveal that these differences correspond to a deepening and westward shift of the tropical upper tropospheric trough (TUTT) during LN events, and the reverse during EN events. The positive (negative) 200 hPa height anomalies in the subtropical region in the EN (LN) composites (Figs. 12-19) support this conclusion.

Figure 20 schematically displays the zonal winds in the tropical and subtropical regions for the peak of the TC season during August-September. For the subtropical region (Fig. 20a), the climatological shear is relatively large, with weak upper tropospheric easterlies and strong lower tropospheric easterlies. In the LN composite, the upper tropospheric easterlies are strengthened while the lower-level winds stay close to climatological values. This results in a reduced vertical shear and enhanced subtropical TC formations. However, in the EN composite, the climatological shear is enhanced, making TC formations less likely. In the tropical region, the upper-tropospheric easterlies are slightly stronger than the lower-level easterlies creating a small shear. This shear is reduced during EN events due to an increase in the low level easterlies, part of an enhanced northeasterly trade wind flow into the monsoon trough that extends

east-southeastward into the region of anomalously high convection near the dateline during EN events (discussed further in Chapter III, section B). The shear in the tropical region is increased during LN events by a reversal of the upper tropospheric winds and a large increase in the trade wind flowing toward the enhanced convection near the maritime continent (discussed further in Chapter 3, Section B).

The 200 hPa height anomalies in Figures 12-19 indicate some of the reasons for these shear differences. Note that the height anomalies between about 15°S and 30°N are approximately opposite for the EN and LN composites throughout the May-December period, and approximately opposite in all regions during September-December. Note also the positive (negative) height anomalies centered near 20°N and between the dateline and Hawaii in the EN (LN) composites. These height anomalies are the North Pacific Rossby wave components of the Rossby-Kelvin wave response to the anomalous equatorial tropospheric warming (cooling) shown in Figure 1. The South Pacific components of this response are indicated by the matching height anomalies south of the equator in Figures 1 and 12-19. The tropospheric warming (cooling) anomalies linked to these responses are located near the equator and dateline and are discussed further in Chapter III, section B. Figures 16-19 also show anomalous extratropical Rossby wave trains similar to those shown in Figure 4. These wave trains are indicated by the alternating positive and negative height anomalies that extend from China into the central North Pacific north of 30°N. The opposite signs of the Rossby-Kelvin and the extratropical Rossby wave

patterns indicate that both patterns are characteristic of EN and LN events. The occurrence of these patterns in the western North Pacific during the TC season suggests that both may be part of large-scale circulation changes that alter TC activity in this region.

This idea is supported by noting that the low vertical shear contours in Figures 12-19 tend to parallel the height anomaly contours, so that: (1) the tropical low shear area extends eastward along the south flank of the positive height anomaly centered near 20°N and between the dateline and Hawaii in the EN composites; and (2) the subtropical low shear area extends east-northeastward along the north flank of the corresponding negative height anomaly in the LN composites. The upper- and lower-tropospheric winds associated with these shear differences (e.g., Fig. 20) are consistent with those expected from the Rossby-Kelvin wave response (Fig. 1) and implied by the composite height anomalies (Figs. 12-19).

Put together, the results shown in Figures 1 and 12-20 indicate that the Rossby-Kelvin wave response during EN and LN events strongly alters vertical shear and TC formation in the western North Pacific. The result is that EN formations occur closer to the equator and further to the east, where SSTs and circulations are more favorable for subsequent strengthening as the TCs track to the west and north. Thus, the circulation differences that lead to formation site differences may indirectly lead to the TC strength differences shown in Figures 9-11.

6. EN and LN Effects on TC Tracks

Figures 21-28 show the composite EN and LN tracks for May-December, along with the corresponding 200 hPa height anomalies. Note that these figures also clearly reveal the formation site differences shown in Figures 12-19. Due to formation site differences, there are areas strongly affected by TCs during EN events but almost unaffected during LN events. For instance, in July and August the area near 15°N 155°E, near the Marianas and Marshall Islands, is quite active during strong EN events but almost free of TCs during strong LN events. Such differences are due not only to the vertical shear differences that produce the formation site differences but also to the impacts of the shear differences on the ability of TCs to intensify.

Obvious EN and LN differences in TC track types (e.g., recurving tracks, with a clear northward turn, and straight-running tracks, with no clear northern turn) are not apparent in the early and middle parts of the TC season (March-August, Figs. 21-24). However, during September-November, and especially in October, track differences are relatively clear, with the EN composite showing a high percentage of recurving tracks and the LN composite having a predominance of straight running tracks (Fig. 25-28). These track differences appear to be strongly connected to the anomalous heights and circulation in the western North Pacific.

The October composite (Fig. 26) is a good example of how the circulation anomalies affect the tracks. In the October EN composite (Fig. 26a), the western portion of the Rossby-Kelvin response extends westward from Hawaii to about

140°E and also extends throughout the troposphere (see Chapter 1 and Section B of this chapter). This provides an anomalous steering flow that favors recurvature. In addition, the negative height anomaly centered near Korea and the positive height anomaly east of Japan also extend throughout the troposphere and provide anomalous steering flows that favor recurvature. The reverse is true for the October LN composite (Fig. 26b). Note that in the October LN composite, the formation sites are centered well to the west of those in the corresponding EN composite. Thus, as the LN TCs move westward, they quickly become positioned south of the anomalous high centered near Korea. This indicates that the formation site differences are part of the reason for the track differences. The net result is that TC tracks are altered by the anomalous large-scale circulations associated with EN and LN events. These alterations occur both directly via anomalous steering flows, and indirectly via anomalous vertical shears that alter the formation sites and initial positioning of TCs within the steering flow.

Note that both the anomalous Rossby-Kelvin and extratropical wave patterns strengthen as the TC season progresses (Figs. 21-28). This may explain why the track differences are most apparent in the last four months of the TC season. The October track differences may be especially apparent because by that time in the TC season, the numbers of TCs are still high and the anomalous wave patterns have become quite strong.

Note also that the anomalous wave patterns in the subtropical western North Pacific are co-located with the subtropical ridge in this region. Thus, the

height anomalies that define the wave patterns add to or subtract from the strength of the ridge, according to the sign of the height anomalies. For example, in the October EN composite, the height anomalies strengthen the ridge south and east of Japan but weaken it over eastern China and Korea. In order to recurve, TCs must move north of the ridge axis. The negative height anomalies over eastern China, Korea, and southern Japan indicate that the ridge in this area is relatively weak, thus making conditions more favorable for TCs to move through the ridge axis. The reverse is true for the LN case. In addition, TCs during EN events tend to be stronger and thus more capable of moving through the ridge. This may be the result of TCs during EN events forming farther east and experiencing a longer exposure to conditions favorable to strengthening, such as warm SSTs and the east-southeastward extension of the monsoon trough discussed in the preceding subsection.

The large-scale circulation anomalies that help create large track differences in October are even stronger in November and December (Figs. 27-28). However, there are fewer TCs in these months, which may help explain why the track differences seen in October are not so apparent in the following two months.

7. EN and LN Effects on TCs' Westernmost Locations and Landfalls

The westernmost locations of western North Pacific TCs are usually the locations at which the TCs are near their maximum strength. These locations can also be a convenient way to identify landfalls, especially for straight running

TCs. Figures 29-32 show the westernmost locations over the western Pacific and the South China Sea (SCS) for the August-November EN and LN composites. Note that in the coastal regions from Shanghai to southern Vietnam, more TCs made landfall during LN events than EN events, with many of the LN TCs penetrating far inland. These differences are most apparent late in the TC season (September-November). During October-November, the number of LN TCs making landfall in Vietnam is especially high. This is consistent with straight-running TCs being more common in LN events during September-November (Figs. 26-28).

The September composites indicate that landfalling TCs are 65% more likely along the south China and Vietnam coasts during strong LN events than during strong EN events (Fig. 30). For October, this figure area rises to 285%. And for November, the mainland coast has nine LN landfalls but almost no EN landfalls.

Similar results appear to apply farther to the north (e.g., northern China, Korea and Japan), where recurving TCs may make landfalls more likely during EN events.

8. Summary of EN and LN Effects on Western Pacific TCs

The changes in tropospheric circulation linked to strong EN and LN events impact western North Pacific TC activity in several ways that is summarized in Table 5. Similar impacts occur when all EN and LN events are considered, but the magnitude of the impacts are somewhat reduced (not shown).

TC Features	Effects During August-November Before and During EN or LN Event Peak	
	Strong EN	Strong LN
Average Number of TC Reports per Month	740	540
Average Number of Strong TCs per Month	11	8
Average Number of Weak TCs per Month	9	13
Average TC Intensity	90 kts (46 ms^{-1})	80 kts (41ms^{-1})
TC Formation Sites	Further east and south	Further west and north
TC Tracks	Tendency for recurving tracks late in season (Sep-Nov)	Tendency for straight tracks late in season (Sep-Nov)
TC Landfalls along China/Vietnam coasts	Large decrease late in season (Sep-Nov)	Large increase late in season (Sep-Nov)

Table 5. Summary of the effects of strong EN and LN events on western North Pacific TCs.

B. LARGE-SCALE EN AND LN ANOMALIES AFFECTING WESTERN NORTH PACIFIC AND NORTH ATLANTIC TCS

A great deal of insight into EN and LN effects on western North Pacific TCs can be gained by using a local perspective. However, to fully explain the mechanisms at work, a near-global view must be adopted. In doing so, we can go beyond *what* the effects are, and get a better sense of *why* these effects are taking place.

Figure 33 shows the near-global August-November EN and LN composite anomalies for SST, OLR, 200 hPa geopotential heights, tropical and subtropical zonal winds, and vertical shear. The August-November period was chosen for closer examination because the results of the previous section showed that EN

and LN events have their greatest impacts on TCs during these months. These figures are based on all EN and LN events since 1949, which includes 19 EN events and 20 LN events (see Table 2), since these results are not sensitive to having identical numbers of events. Similar figures were prepared for nine strong events (Table 4), but they were not appreciably different with the exception of the magnitude of the anomalies. Stronger events produced greater absolute anomaly values with anomaly sign and placement remaining very similar. We also analyzed the July-December EN and LN composite anomalies in order to span a larger portion of the TC season in which EN and LN impacts are indicated in previous figures (e.g., Figs. 7-11). These results are very similar to those shown in Figure 33 and thus are not shown here.

1. SST Anomalies

The August-November EN composite SST anomalies (SSTAs) show a strong positive anomaly in the central and eastern tropical Pacific, negative SSTAs in the western tropical Pacific, and mainly positive SSTAs in the tropical North Atlantic (Fig. 33a). The corresponding LN SSTAs are approximately opposite (Fig. 33b). Note that in most of the western North Pacific, where most of the TCs of this region form and spend the majority of their existence, the SSTAs are negative in EN events and positive in LN events. This suggests that western North Pacific SSTAs do not directly lead to stronger (weaker) TCs during EN (LN) events. The anomalously cool (warm) SSTs would be expected to produce unusually weak (strong) TCs during EN (LN) events, rather than the unusually strong (weak) TCs actually observed (Figs. 9-11). SSTs in this region

are very warm, even during EN events, which suggests that the explanation for the TC strength differences is probably the track differences (Figs. 21-28). Characteristic EN tracks provide more exposure to warm SSTs and low-level vorticity regions that favor TC intensification. Thus, EN and LN effects on TCs seem to have more to do, in a direct sense, with tropospheric circulation anomalies than SSTAs. Of course, these circulation anomalies are in part the result of SSTAs (cf. Gill 1981), but the connection between these SSTAs and TC activity changes appears to be through the circulation anomalies described in the previous subsection.

2. OLR Anomalies

In order to understand how these circulation anomalies develop during EN and LN events, we need to consider the anomalous thermal forcing of the tropical atmosphere that occurs during these events. Figures 33c, d show OLR anomalies (OLRAs), with negative OLRAs representing areas of unusually deep and high clouds, and unusually high precipitation and latent heating, while positive OLRAs indicate the opposite. Note that the areas of largest absolute OLRA roughly coincide with the largest absolute SSTAs (Figs, 33a, b), with the positive and negative OLRA areas forming a dipole over the tropical Indian and Pacific ocean basins. Note also that the OLRAs centered near the maritime continent extend into the south and east Asian regions. There are also negative OLRAs in the tropical northern African region, and positive OLRAs in the tropical South American and Caribbean region, in the EN composite. The reverse of these OLRAs occurs in the LN composite. The negative (positive) tropical

OLRAs represent anomalous forcing of the troposphere, similar to the warming (cooling) shown in Fig. 1.

3. 200 hPa Anomalies

The corresponding 200 hPa height anomalies (Fig. 33 e, f) show tropical Rossby-Kelvin wave responses similar to those in Figure 1. The EN composite (Fig. 33e) shows these responses especially well over the Pacific in association with the negative OLRA near the equator and dateline. Additional but weaker responses are seen in association with the OLRAs near the maritime continent, tropical Africa, and South America - Caribbean regions. Similar but opposite and somewhat weaker responses are seen in the LN composite (Fig. 33 f).

The extratropical 200 hPa height anomalies in Figure 33 e, f show the near-global extent of the anomalous extratropical Rossby wave trains seen in Figures 12-28. These anomalous wave trains, indicated by the alternating positive and negative height anomalies, extend in a gentle arch from south and east Asia across the North Pacific and North America into the North Atlantic. These wave trains are similar to those in Figure 4 but with a greater zonal extent. Note that the anomalous extratropical wave trains originate near anomalously low heights over south Asia in the EN composite. The Asian height anomalies correspond to anomalously low summer monsoon convective activity during EN events, as documented in a number of studies (e.g., Meehl 1993). The height anomalies in the south Asian and African regions also indicate anomalously weak flow in the tropical easterly jet (TEJ) over the Indian Ocean and Africa.

Similar but opposite anomalies in the heights, monsoon convection, and TEJ are indicated by the LN composite.

Note that the tropical and subtropical western North Pacific height anomalies shown in Figure 33 e, f are very similar to those shown in Figures 12-28 and represent the large scale circulation changes through which EN and LN events impact TC activity. The near-global extent of the anomalous extratropical wave trains indicates that some of the processes that impact western North Pacific TC activity extend into the North Atlantic and impact TCs there as well. The EN and LN composite height anomalies in the North Atlantic are approximately opposite to each other and similar in magnitude to the height anomalies in the western North Pacific. This suggests that the North Atlantic circulation anomalies may alter TC activity there, perhaps via vertical shear anomalies, as in the western North Pacific. For example, the LN composite height anomalies (Fig. 33 f) indicate that upper-tropospheric easterlies are increased over the main TC formation region in the North Atlantic at about 10-20°N, 60-20°E. Given the climatological upper- and lower-level winds (weak upper-tropospheric easterlies over stronger lower-tropospheric easterlies, not shown), this would tend to produce a decrease in vertical shear and favor increased TC activity during LN events, as reported in several studies (e.g., Goldenberg et al. 1996).

4. Zonal Wind Anomalies

The results shown in Figures 12-20 indicate that there are two regions in which important vertical shear changes occur during EN and LN events, the

tropical and subtropical regions on the southern and northern flanks of the upper tropospheric height anomalies that are part of the Rossby-Kelvin wave response to EN and EN events. Figure 33 e,f indicates that similar regions may also be important in producing EN and LN impacts on North Atlantic TC activity. To examine how shear anomalies in these regions might develop and be related to each other, we constructed two sets of August-November EN and LN composite vertical profiles of the anomalous zonal wind averaged over 5-15°N and 20-30°N (Fig. 33 g-j). These profiles highlight the profound global effects that EN and LN events can have on circulation throughout the troposphere.

The EN composite tropical profile (Fig. 33 g) shows anomalously strong lower tropospheric confluence and upper tropospheric difluence in the central tropical Pacific, corresponding to anomalously strong convection near the equator and dateline (cf. Fig. 33 c). A similar wind anomaly pattern is found near east Africa (45°E), and reverse patterns are found over the maritime continent (135°E) and South America (60°W). Taken together, these wind anomalies represent the topical convection indicated by Figure 33 c and the corresponding anomalous Walker circulation that develops throughout the tropics during EN events. The corresponding LN profile is shown in Figure 33 h. Note in particular that the tropospheric wind anomalies are approximately opposite to those in the EN composite from the Indian Ocean to South America (45°E-45°W).

The EN composite subtropical profile (Fig. 33 i) shows a striking region of upper-tropospheric westerly anomalies extending eastward from North Africa to the Gulf of Mexico, with a small region of upper tropospheric easterlies over the

subtropical North Atlantic. These westerlies occur along the flanks of the subtropical and midlatitude height anomalies shown in Figure 33 e. These anomalies indicate a strengthening and southward shift of the subtropical jets for all regions except the North Atlantic during EN. In the North Atlantic, the anomalous upper-tropospheric easterlies oppose the climatological winds and tend to reduce the vertical shear. The anomalies in the LN composite subtropical profile (Fig. 33j) are almost opposite, indicating that the subtropical jet is weaker and farther north for all regions with the exception of the North Atlantic.

5. Vertical Shear

The EN composite vertical shear anomaly map (Fig. 33 k) shows negative (easterly) anomalies in the tropical western and central Pacific and positive (westerly) anomalies in the subtropical western North Pacific. The LN composite (Fig. 33 l) shows the opposite. These results agree with those for total vertical shear shown in Figures 12-20. In the LN composite, the subtropical and tropical North Atlantic shear anomalies are similar to those in the EN composite in the western North Pacific. That is, the tropical Atlantic during LN and the tropical western Pacific during EN are both dominated by negative (easterly) shear anomalies, while the subtropical regions are dominated by positive (westerly) shear anomalies. This suggests that the mechanisms that enhance TC activity in the North Atlantic during LN events may be dynamically similar to those that enhance it in the western North Pacific during EN events.

6. Correlation of Western Pacific SLP with Worldwide SLP

To further clarify the possible teleconnections between the Pacific and Atlantic, we correlated SLP in the Philippine Sea region (5-15°N, 120-160°E) with SLP everywhere else. The base site was chosen because it is near the location of the summer monsoon trough and much of the western North Pacific's convective activity throughout the year, and has been shown to be well correlated with SLP in the subtropical eastern Pacific (Schwing et al. 2000). The results (Fig. 34) show that the western North Pacific is well correlated with many other parts of the globe, including the North Atlantic. The sign of the correlations indicates that during EN (LN) events, when SLP at the base site tends to be anomalously high (low), SLP tends to be anomalously high (low) in the main TC formation region of the North Atlantic (10-20°N, 60-20°W) and low (high) in the secondary formation region over the Gulf of Mexico and Caribbean. This is consistent with the results of Goldenberg et al. (1996) and others of how North Atlantic TC activity is tied to EN and LN events.

C. EN AND LN EFFECTS ON NORTH ATLANTIC TCS

Our investigations of the effects of EN and LN events on global tropospheric circulation, especially in the northern hemisphere led us to conduct some preliminary studies of EN and LN impacts on North Atlantic TCs. These studies provide an initial test of our hypothesis that through anomalous extratropical wave trains, EN and LN events may create circulation anomalies in

the North Atlantic that are dynamically similar to those in the western North Pacific and thereby alter North Atlantic TC activity.

Our results indicate that EN and LN impacts on the western North Pacific and North Atlantic are dynamically similar in that anomalous tropical and extratropical wave patterns that are part of the EN and LN circulation anomalies alter the vertical shear in the tropical and subtropical parts of both basins. The results presented in the preceding section indicate that in the North Atlantic during LN events, there are more TC reports, more tropical TC formations, more strong TCs, less weak TCs, and higher average TC intensities compared to EN events.

We explored these possibilities using time series constructed in the same way as those for the western North Pacific shown in Figures 7-11. As expected, there are more TC reports and more forecaster activity in the North Atlantic during LN events (Fig. 35). There are also more TCs during LN events as previously noted by Gray (1984). An explanation for this trend probably lies in the mechanisms outlined in this study. During LN events, the shear is reduced in the tropical North Atlantic, where other factors (e.g., SSTs) tend to be favorable for TC formation. However, during EN events, the shear reduction occurs in the subtropical North Atlantic, where other factors are less favorable. Thus, the net result may be a larger number of TCs during LN events.

Figures 37 and 38 indicate that there are greater numbers of strong TCs in the North Atlantic during LN events, but the numbers of weak TCs do not vary appreciably between EN and LN events. For consistency, the division of weak

versus strong storms was 80 knots ($41ms^{-1}$), the same value used for western Pacific storms. Because Atlantic storms are generally weaker overall, in future work a better division value could perhaps be selected. Figure 39 shows that LN events produce stronger storms for most of the TC season.

D. 1999 CASE STUDY

The preceding results were based on composites developed before data for 1999 was available. When the 1999 data became available, we used it to test the composite results. The MEI indicates that 1999 was a strong LN event (Table 2). The 1999 results are shown in Figures 40-44 which are identical to Figures 7-11 except that the 1999 values are overlaid in black. In general, the 1999 Pacific TC season fit the strong LN composite, with the exception of a very active August which showed up as a spike in forecaster activity (Fig. 40) and total number of storms (Fig. 41). However when considering strong and weak TCs (Figs. 42-43), the 1999 results were very much in line with the LN composite, with the August spike being the result of a large number of weak TCs, as might be expected during a strong LN. In average intensity, the 1999 Pacific season generally fell below even the composite strong LN case (Fig. 44).

The 1999 results for the North Atlantic are shown in Figures 35-39. This North Atlantic TC season produced more TC reports (Fig. 35), more TCs per month (Fig. 36), and more strong TCs (Fig. 37) than even the strong LN composite for the North Atlantic. Aside from a large number of weak TCs in October 1999, the pattern of weak TC activity was similar to that for the strong LN composite (Fig. 38). Figure 39 shows that the average maximum intensity for

1999 was somewhat below the composite LN and EN cases for the majority of the TC season. As with the western North Pacific, the 1999 TC season in the North Atlantic was typical for strong LN periods.

THIS PAGE INTENTIONALLY LEFT BLANK

IV. SUMMARY AND CONCLUSIONS

A. SUMMARY

We have studied the impacts of EN and LN events on TCs, especially western North Pacific TCs, and the mechanisms by which these impacts occur. We examined TC data from 1945-1999 and global reanalysis fields from 1949-1999. We used a multivariate index of EN and LN events, and focused our attention on nine strong events from 1957-1999. In addition, we emphasized the impacts that occur during the TC season that occurs just before and during the peak of EN and LN events.

B. IMPACTS ON WESTERN NORTH PACIFIC TCS

We found the following major differences between western North Pacific TC activity during EN and LN events.

1. EN events require greater forecaster effort than LN events as measured by number of reports.

2. During EN events, the TC formation region shifts to the south and east, with formations occurring closer to the equator and dateline. In LN events, the formation region shifts to the north and west, with more formations occurring in the subtropics southeast of Japan.

3. EN events tend to produce greater numbers of strong TCs than LN events. LN events produce greater numbers of weak TCs. The result of

these off-setting effects is that EN and LN events produce about the same total number of TCs.

4. Late in the TC season (September-October-November), TCs tend to be recurvers in EN events and straight-runners during LN events.

5. During September-November of LN events, the chances of TCs making landfall along the south China and Vietnam coasts are dramatically increased. During EN events, the reverse is true.

6. All of these impacts are most apparent late in the TC season, during August-November.

C. THE MECHANISMS OF EN AND LN IMPACTS ON TCS

A major goal of this study was to explore the mechanisms behind the five major impacts listed above. A number of mechanisms were identified by examining the large-scale circulation changes that occur during EN and LN events. We concluded that a major way in which EN and LN events alter TC formation sites, strengths, and tracks was by setting up anomalous wave patterns that alter the circulation throughout the troposphere. A simple chain of events that summarizes the mechanisms that we have identified is given below.

1. Large-scale circulation changes lead to changes in vertical shear and steering flow.
2. Vertical shear changes alter formation sites.
3. Changes in vertical shear, formation sites, and steering flow alter tracks.

4. Changes in tracks alter intensities and landfalls.

During EN (LN) events, anomalous tropospheric warming (cooling) near the equator and dateline produce an anomalous Rossby-Kelvin wave response that shows up in the tropical and subtropical western North Pacific as an anomalous upper level anticyclone (cyclone) and lower level cyclone (anticyclone). These circulation anomalies produce vertical shear anomalies in two critical TC formation regions, the tropical and subtropical western north Pacific. The opposing circulation anomalies during EN and IN events mean that the vertical shear changes during EN and LN events are also opposite to each other. The net result is reduced vertical shear and increased formation in the tropical region, and increased vertical shear and reduced formations in the subtropical region, during EN events. For LN events, these results are reversed.

The changes in vertical shear cause formations during EN events to occur closer to the equator and dateline, where other factors, such as SSTs and low level relative vorticity, tend to be favorable for TC formation and intensification. These formation sites also allow long TC tracks over warm SSTs. The more northward and westward formation sites that are favored during LN events would tend to have the opposite effects on TC intensification. Thus the differences in formation sites may explain why TCs tend to be stronger during EN events than during LN events. The greater strength of TCs during EN may also help explain their tendency to recurve. TCs during EN (LN) events tend to be stronger (weaker) and thus more (less) capable of moving through the ridge.

Anomalous extratropical Rossby wave trains are also part of the anomalous circulations that develop during EN and LN events. A key aspect of these anomalous circulations is that, near Korea and Japan, they favor recurvature during EN events but straight running during LN events. Both the anomalous wave patterns (the tropical-subtropical Rossby-Kelvin and the extratropical Rossby wave patterns) strengthen from summer into fall and winter. This may explain why the impacts of EN and LN events are strongest during August-November, and especially during September-October. Climatologically, this is a time when TC activity is still high so the overlap of strong TC activity with strengthening EN and LN induced circulation anomalies would be expected to produce the largest impacts on TCs during these months.

It is interesting to note that SST *anomalies* do not provide a direct explanation of the TC intensity differences we have found. During EN events, TCs spend the majority (if not all) of their existence over anomalously cool water, while the reverse is true during LN events (compare Figs. 21-28 with Fig. 33). Thus it is difficult to attribute the stronger TCs found during EN events to the SST anomalies. Of course, SSTs, as opposed to SST anomalies, will still be important in determining TC strength. These observations coupled with our examination of large-scale circulation mechanisms, suggest that circulation anomalies, not SST anomalies, play a dominant role in EN and LN modifications of TC activity.

The impacts and mechanisms we have identified are schematically presented for EN and LN events in Figure 45. Note the large differences in wave related circulation anomalies, vertical shear, formation sites, tracks, and landfalls.

The mechanisms operating in the western North Pacific are part of a global scale process that also impacts TCs in the North Atlantic. The anomalous wave trains and circulations that link EN and LN events to the western North Pacific and the North Atlantic are schematically presented in Figures 46 and 47.

D. 1999 CASE STUDY

The results of this study are based primarily on composites of nine strong EN and LN events. However, these results are consistent with those found when studying an individual LN event, the strong event of 1999. In both the western North Pacific and North Atlantic basins, the 1999 season showed characteristics of a strong LN event in forecaster activity, numbers of weak and strong TCs, and TC intensities.

E. RECOMMENDATIONS FOR FURTHER RESEARCH

In all studies of EN and LN impacts, we recommend that researchers use consistent schemes for identifying event years, event strength, and the TC season being examined (e.g., the TC season before and during the event peak or the TC season that follows the event peak), and that they carefully document their schemes.

Our study focused on the impacts of EN and LN events on the TC season that occurs just before and during the peak of the event. But our results revealed

some interesting features in the TC season following the EN or LN peak that should be studied further. However, there are problems with examining this second TC season, in particular that some events are followed by the opposite event (e.g., EN followed by LN), while others are followed by a continuation of the same event (e.g., EN followed by EN), or a non-event year. A study of the TC season that follows an event will have to distinguish between these three types of follow-on years and will require an additional sorting level that our study did not employ.

We recommend additional research into the EN and LN impacts on North Atlantic TCs and their mechanisms. There is strong evidence that EN and LN events impact TCs via the development of anomalous extratropical wave trains. However these mechanisms should be explored in a more complete study that focuses on wave train dynamics. These wave trains also create anomalous circulations over the extratropical North Pacific, North America, and North Atlantic and potentially impact temperature, precipitation, winds, and severe storm activity in these regions. Some of our preliminary analyses indicate that summer and fall storm activity and precipitation in the eastern U.S. and the extratropical northwestern Atlantic may be especially affected by these wave trains.

The results of this observational study should be tested in modeling studies using: (1) global atmospheric models to simulate the anomalous tropical and extratropical wave patterns and their impacts on global scale circulations and

vertical shear; and (2) high resolution regional models to simulate the impacts of these wave patterns on TC activity.

One of the most exciting areas of future research is adapting the results of this study to TC forecasting efforts. The potential for this adaptation is especially clear for forecasting systems that involve the identification and use of large scale circulation features to predict TC formations and tracks (e.g., Carr et al. 1997). These systems typically identify features in the total circulation fields, so there would need to be a translation between the anomaly fields used in this study and the total fields used in these forecast systems. For example, the anomalous heights associated with recurving (straight running) tracks during EN (LN) events might be translated into total heights to identify the characteristic total heights associated with recurving (straight running) tracks. The remarkable differences in southeast Asian landfalls between EN and LN events indicates there is a strong potential for improving TC track forecasts in this area. Since EN and LN events occur over several seasons, the potential for using the results of this study to improve medium and long range forecasts of TC is especially high.

There is exciting work being conducted to identify the characteristic behavior of TCs under different regional scale circulation regimes. The results of this work are being exploited to develop a systematic approach to TC forecasting. Such systems may be improved by identifying the mechanisms that produce the different circulation regimes, perhaps using the methods of this study to clarify what those mechanisms are. Since EN and LN events produce especially large circulation anomalies with clear impacts on TCs, and with

identifiable mechanisms, it seems likely that systematic TC forecasting schemes could be improved by accounting for the occurrence of EN and LN events. This might be done, for example, by conducting hindcast studies to identify the seasonal biases that should be applied to existing systematic forecasting methods when an EN or LN event is occurring.

APPENDIX A - FIGURES

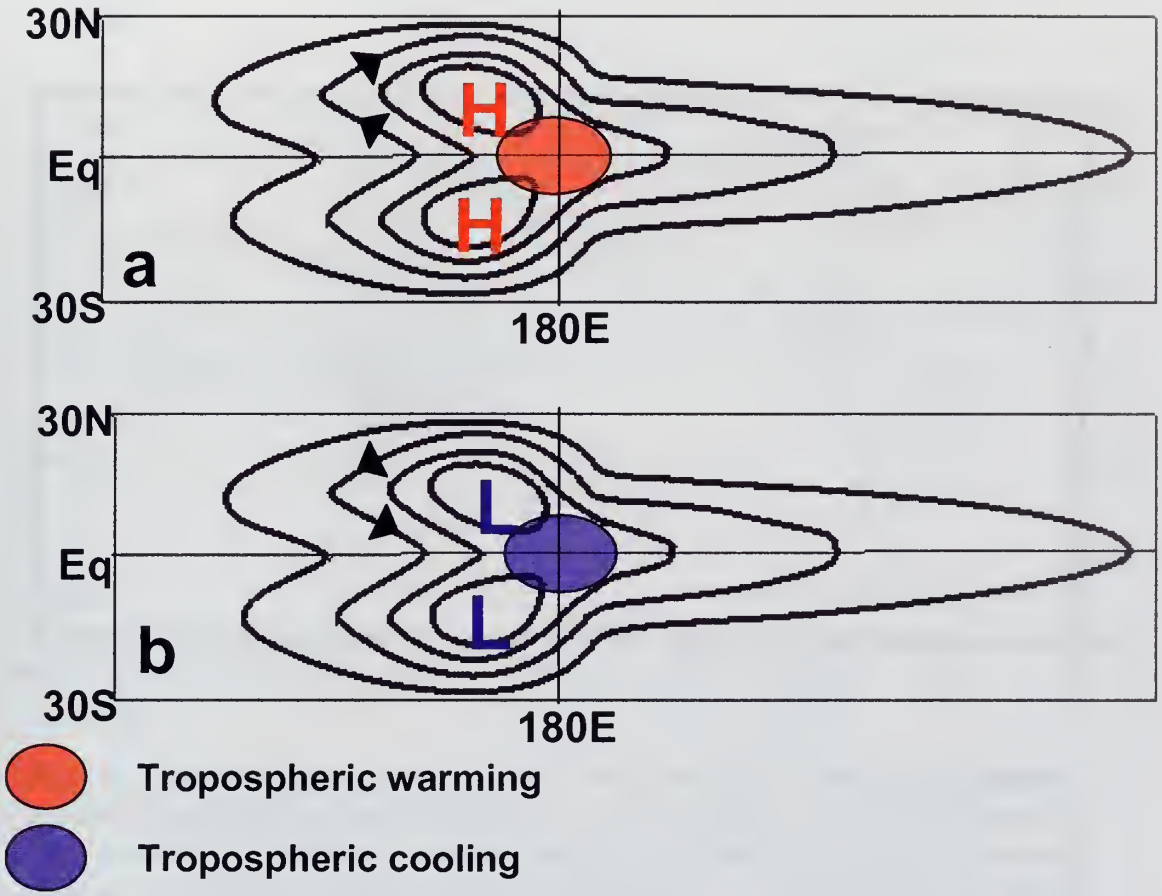

Figure 1. Solution for anomalous warming and cooling about the equator. (a) and (b) are contours of perturbation pressure. There is a ridge in (a) and a trough in (b) at the equator in the regime to the east of the forcing region. On the other hand, the pressure to the west of the forcing region, is different relative to its value off the equator. Two circulations are found on the north-west and south-west flanks of the forcing region (from Gill 1980).

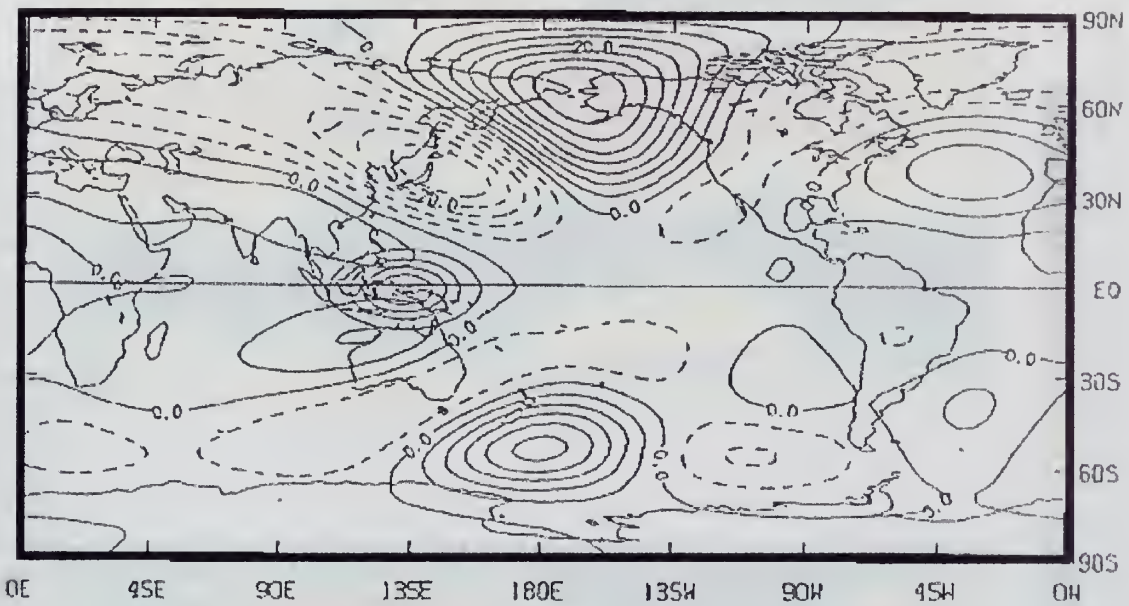

Figure 2. Modeled geopotential height response at 200 hPa to a positive tropical heating perturbation centered on the equator at 130E (indicated by oval contours). Positive (negative) height responses are indicated by solid (dashed) contours. Height contour interval = 5 m. The background flow is zonally symmetric with 25 ms^{-1} jets at 25°N and 32°S. The arching pattern of positive and negative height responses over the East Asian – North Pacific – North American – North Atlantic region reveals a quasi-stationary wave train initiated by the perturbation heating. A similar wave train occurs over the Australian – South Pacific – South Atlantic region.

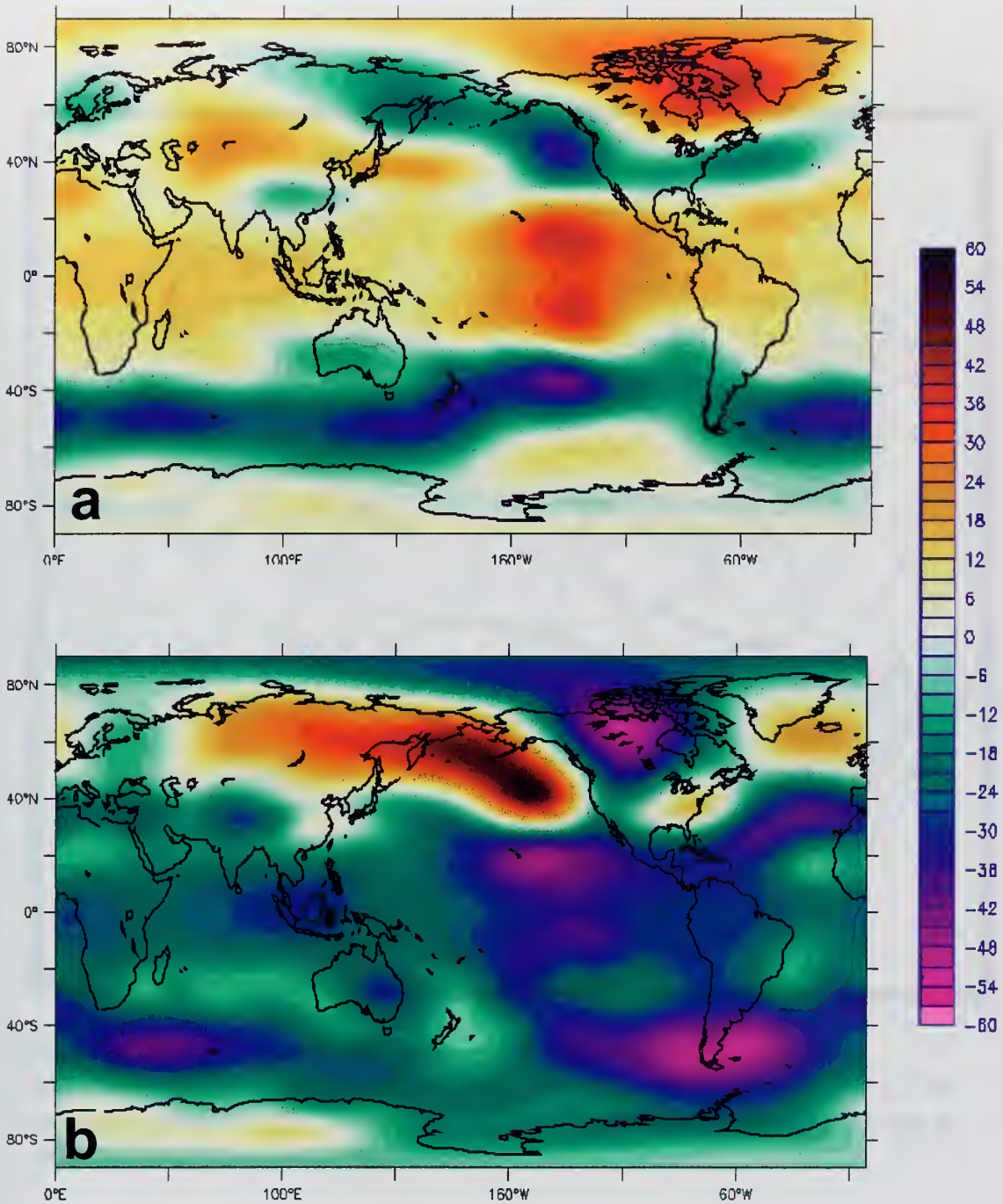

Figure 3. Composite 200 hPa height anomalies (in m) for Dec-Jan-Feb during (a) El Niño and (b) La Niña events. Composites based on Multivariate ENSO Index (MEI) for all events during 1949-1998.

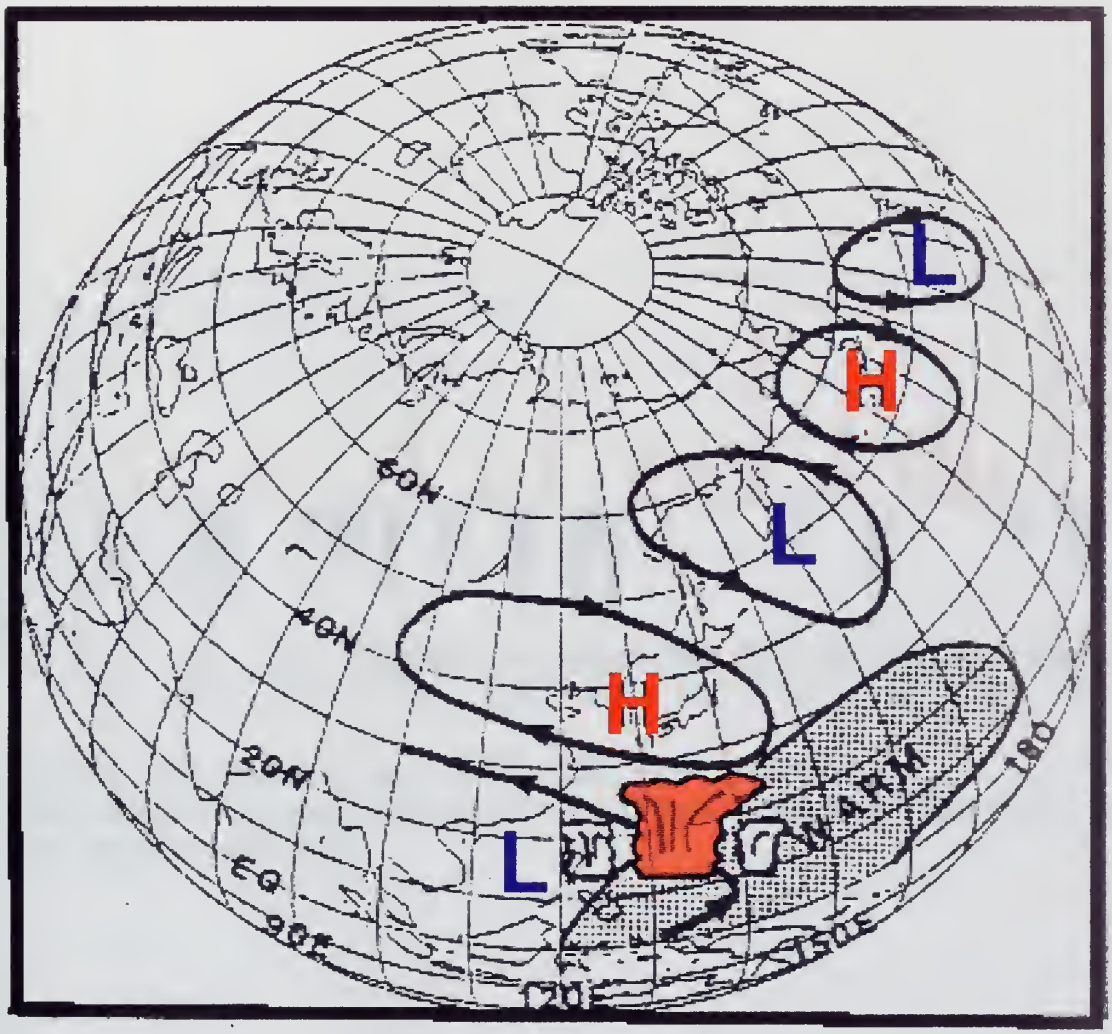

Figure 4. Schematic of northern summer 500 hPa height anomalies associated with increased convection over warmer than normal SST in the tropical western Pacific. H denotes a positive height anomaly, L denotes a negative height anomaly (from Nitta 1987).

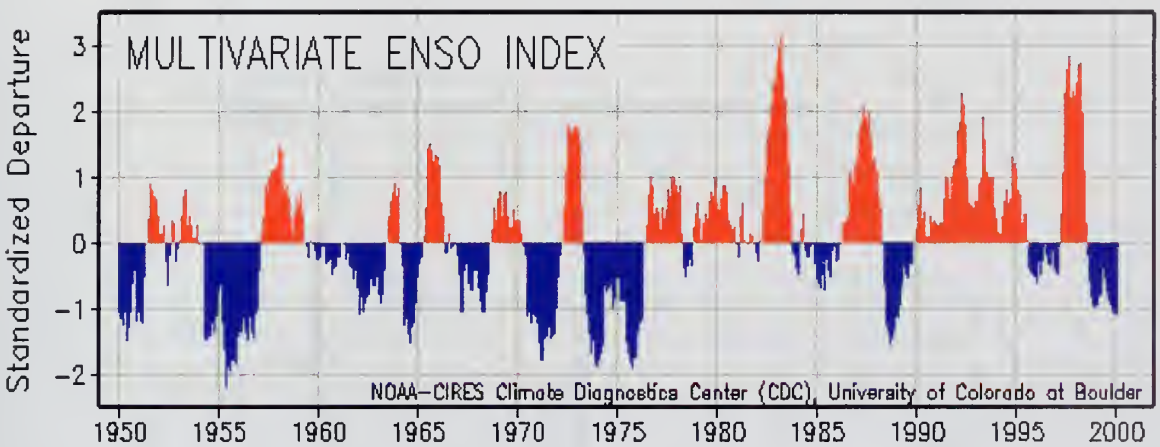

Figure 5. MEI values, January 1950 – April 1999. Figure from http://www.cdc.noaa.gov/~kew/MEI/mei.html. See Wolter and Timlin (1993) for more information on MEI.

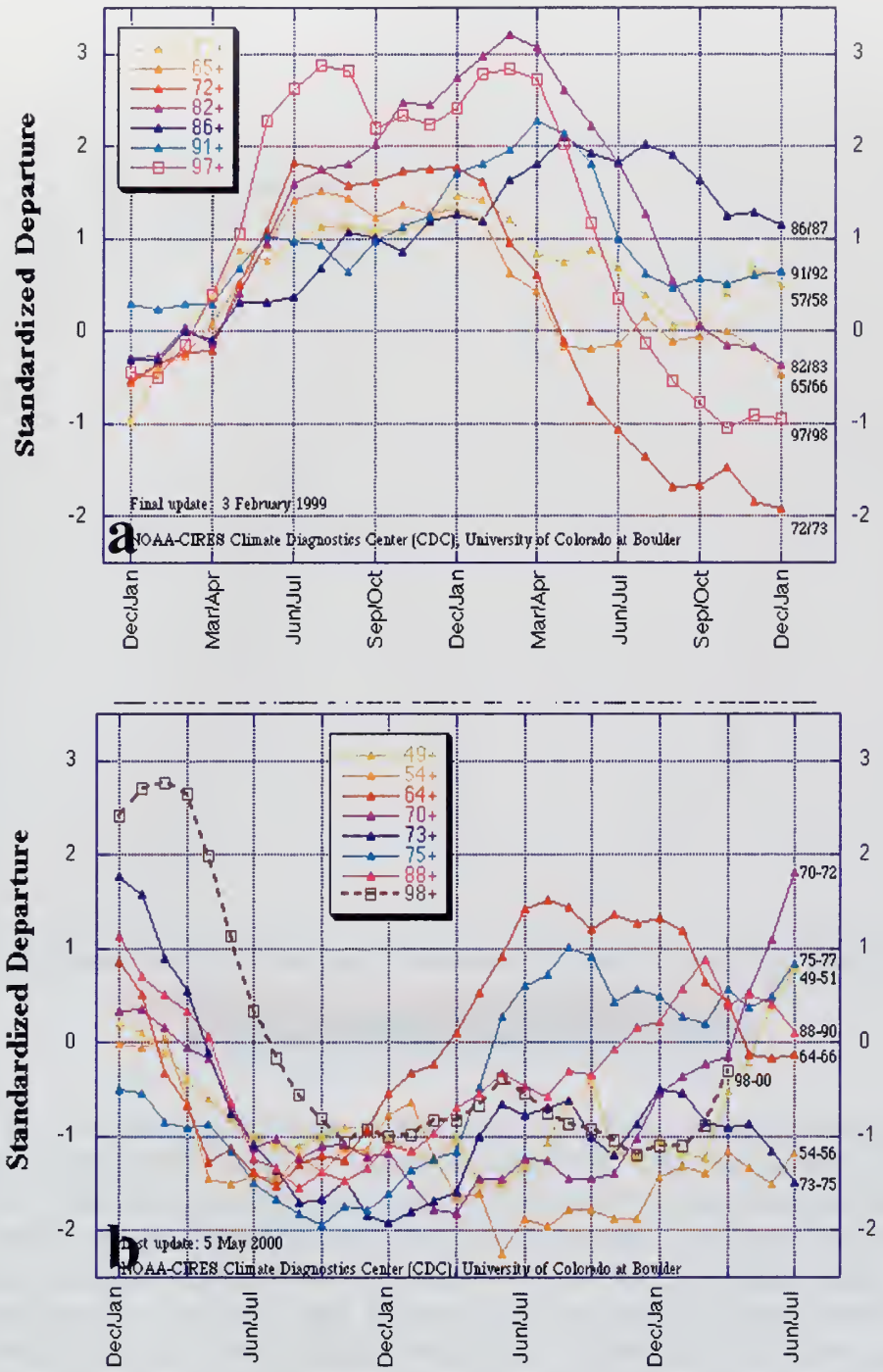

Figure 6. Multivariate ENSO index for the seven strongest historic El Niño (a) and La Niña (b) events since 1950. Figure from http://www.cdc.noaa.gov/~kew/MEI/mei.html. See Wolter and Timlin (1993) for more information on MEI.

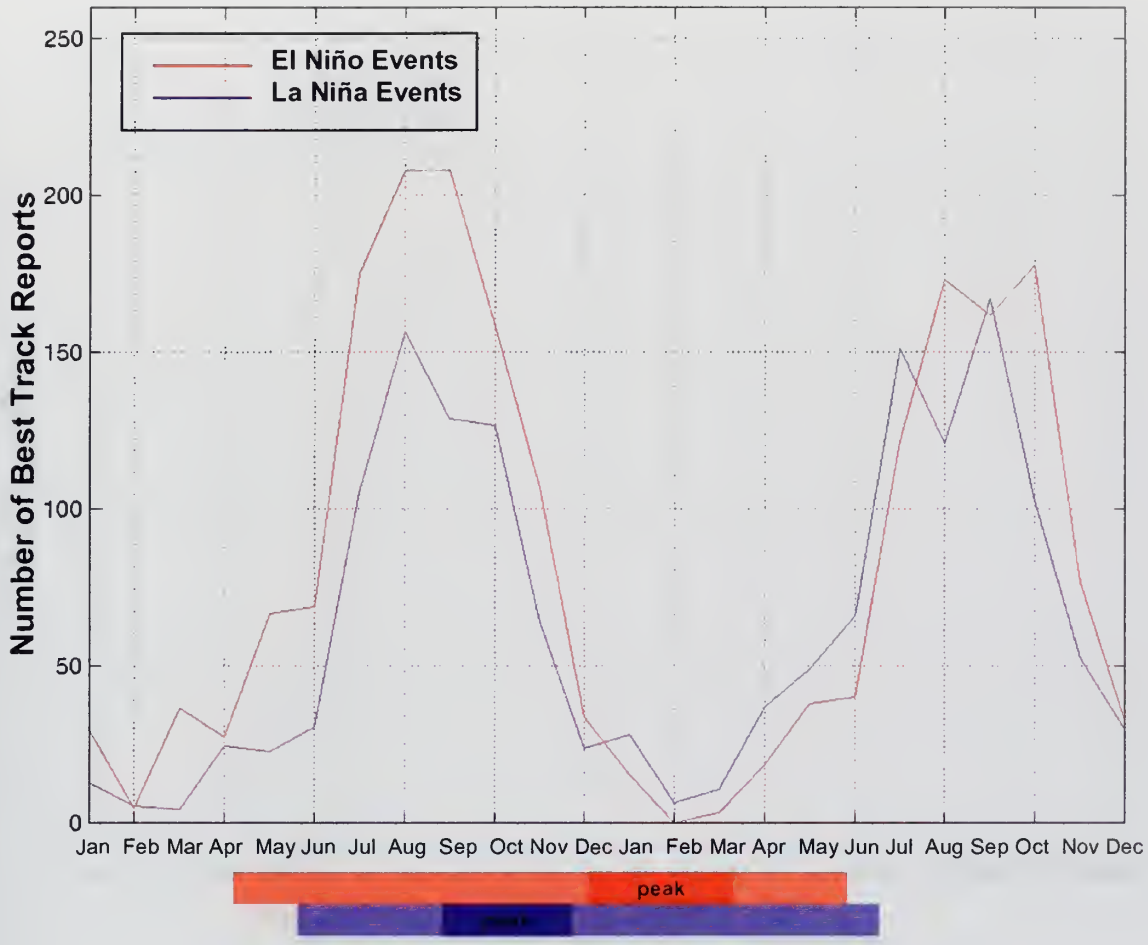

Figure 7. The average number of best track reports for western North Pacific TCs per month for the nine strongest composite El Niño and La Niña events, *based on nine strong events*. Red and blue bars at bottom of figure indicate the duration of composite El Niño and La Niña events, with event peaks indicated in darker colors. The TC season in this region extends from February through January. This study focuses on the first season shown in this figure, the season that occurs during and immediately before the event peaks (see Chapter 2 for rationale). See Chapter 2 for information on evolution of events and selection of event years.

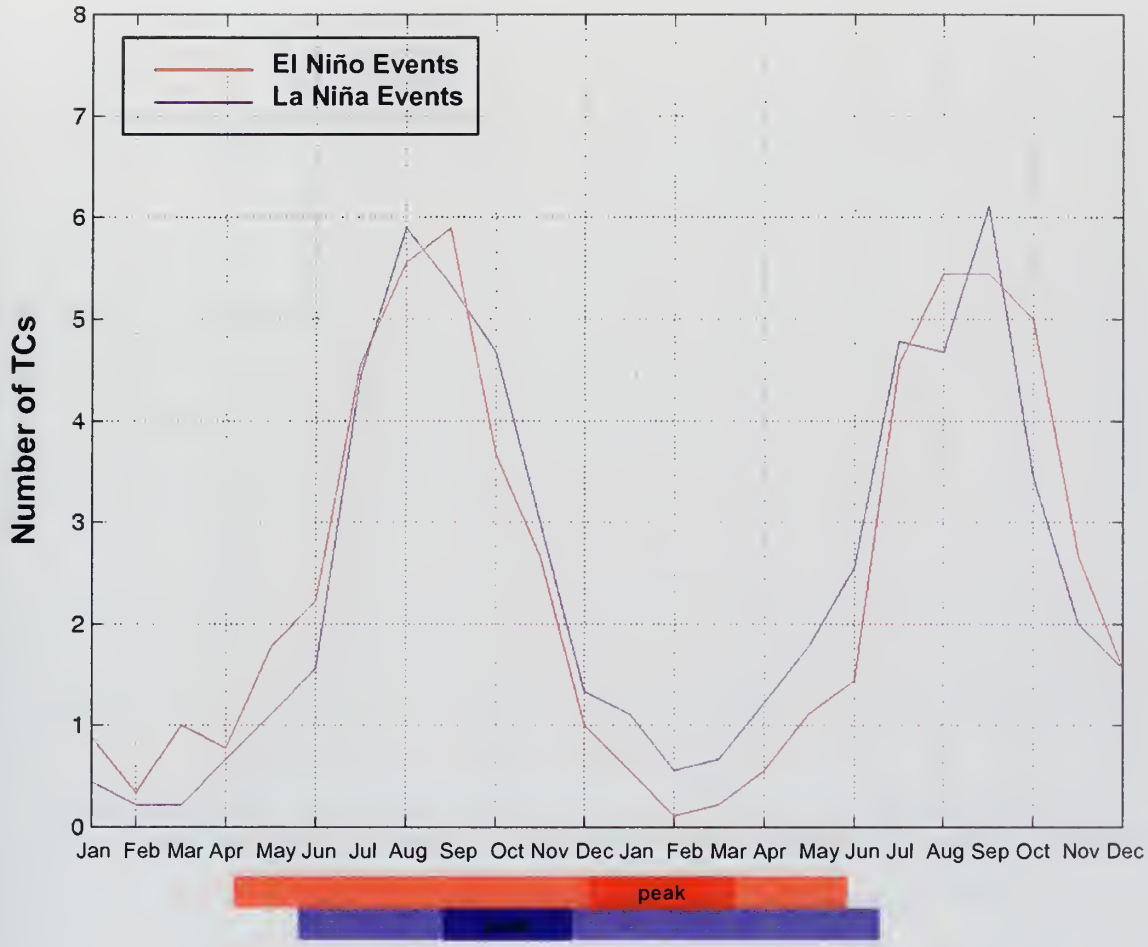

Figure 8. The average number of western North Pacific TCs per month for composite El Niño and La Niña events, *based on nine strong events*. Red and blue bars at bottom of figure indicate the duration of composite El Niño and La Niña events, with event peaks indicated in darker colors. The TC season in this region extends from February through January. This study focuses on the first season shown in this figure, the season that occurs during and immediately before the event peaks (see Chapter 2 for rationale). See Chapter 2 for information on evolution of events and selection of event years.

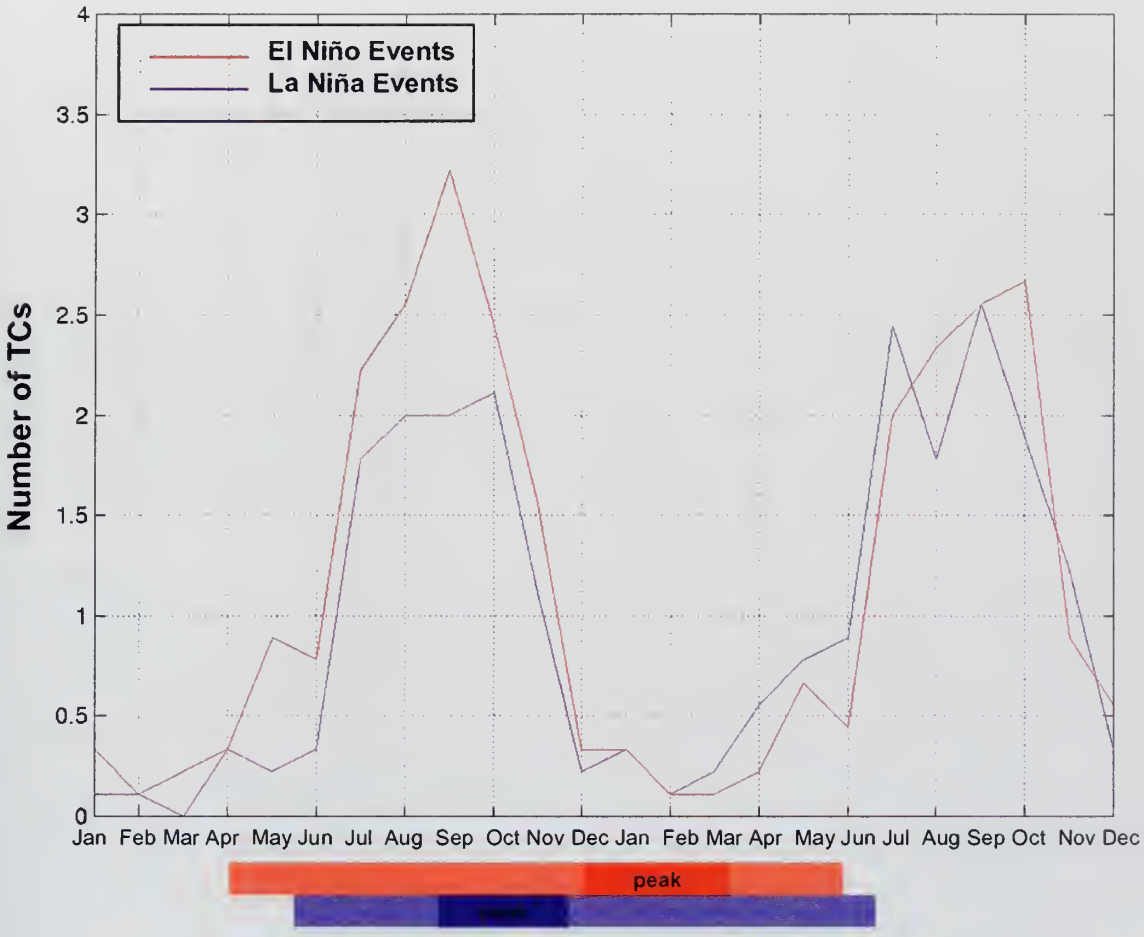

Figure 9. The average number of strong (>80 knot (41 ms^{-1}) maximum intensity) western North Pacific TCs per month for composite El Niño and La Niña events, *based on nine strong events*. Red and blue bars at bottom of figure indicate the duration of composite El Niño and La Niña events, with event peaks indicated in darker colors. The TC season in this region extends from February through January. This study focuses on the first season shown in this figure, the season that occurs during and immediately before the event peaks (see Chapter 2 for rationale). See Chapter 2 for information on evolution of events and selection of event years.

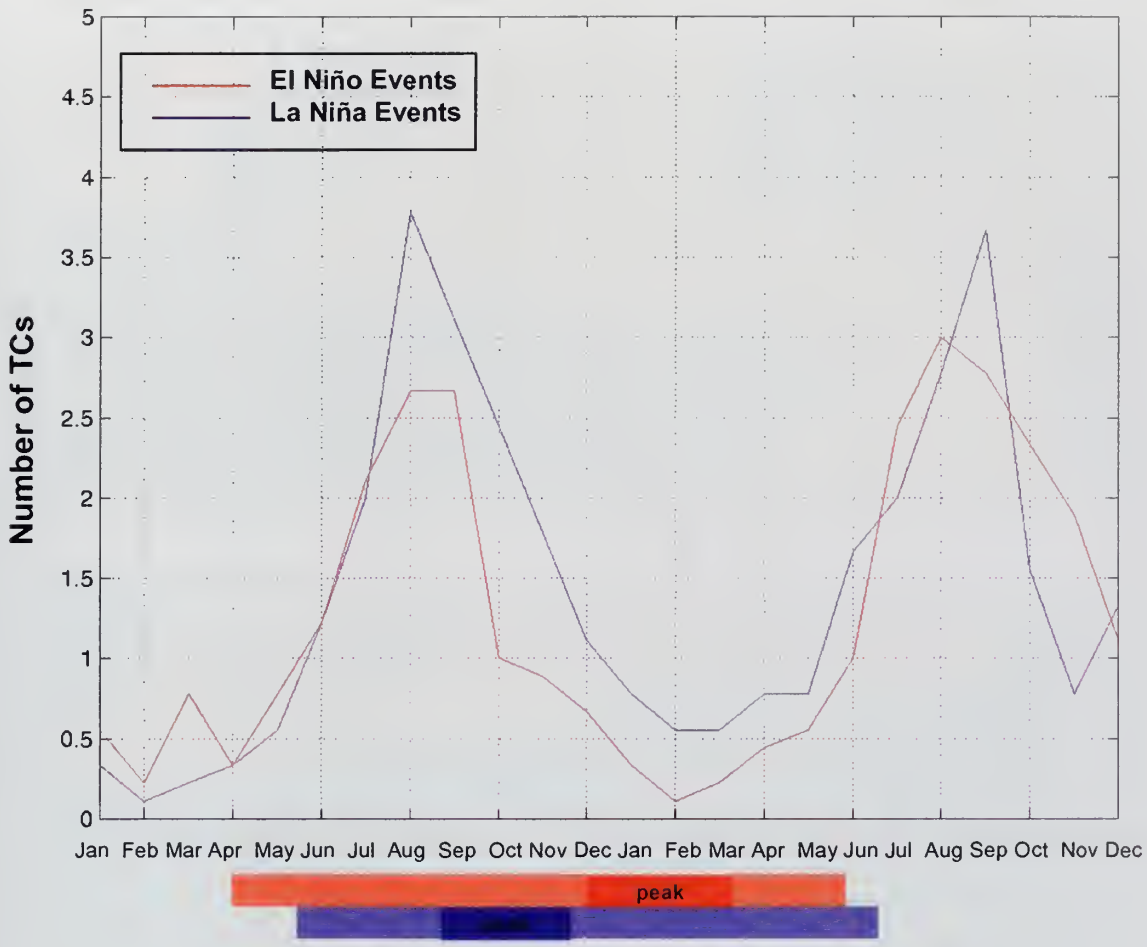

Figure 10. The average number of weak (<80 knot (41 ms^{-1}) maximum intensity) western North Pacific TCs per month for composite El Niño and La Niña events, *based on nine strong events*. Red and blue bars at bottom of figure indicate the duration of composite El Niño and La Niña events, with event peaks indicated in darker colors. The TC season in this region extends from February through January. This study focuses on the first season shown in this figure, the season that occurs during and immediately before the event peaks (see Chapter 2 for rationale). See Chapter 2 for information on evolution of events and selection of event years.

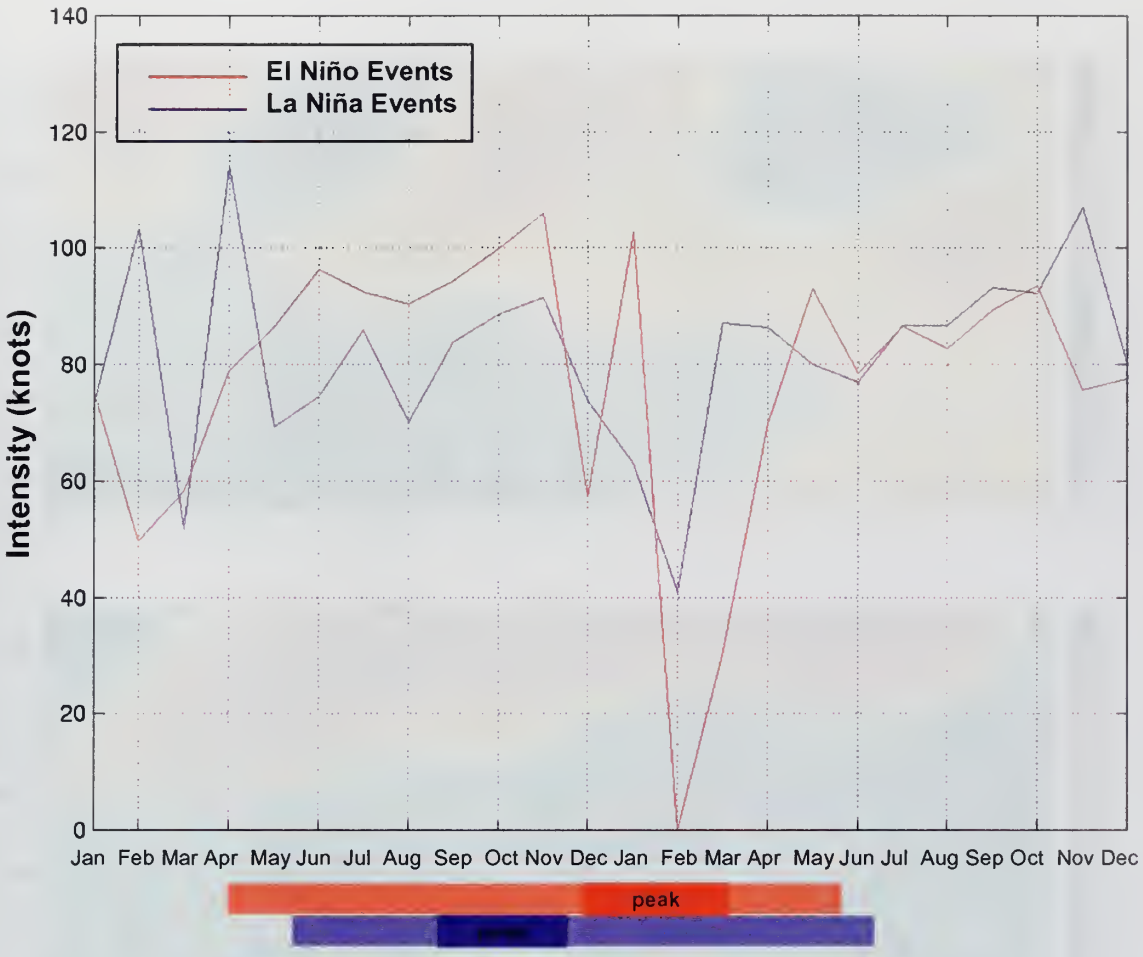

Figure 11. The average maximum intensity of western North Pacific TCs per month for composite El Niño and La Niña events, *based on nine strong events*. Red and blue bars at bottom of figure indicate the duration of composite El Niño and La Niña events, with event peaks indicated in darker colors. The TC season in this region extends from February through January. This study focuses on the first season shown in this figure, the season that occurs during and immediately before the event peaks (see Chapter 2 for rationale). See Chapter 2 for information on evolution of events and selection of event years.

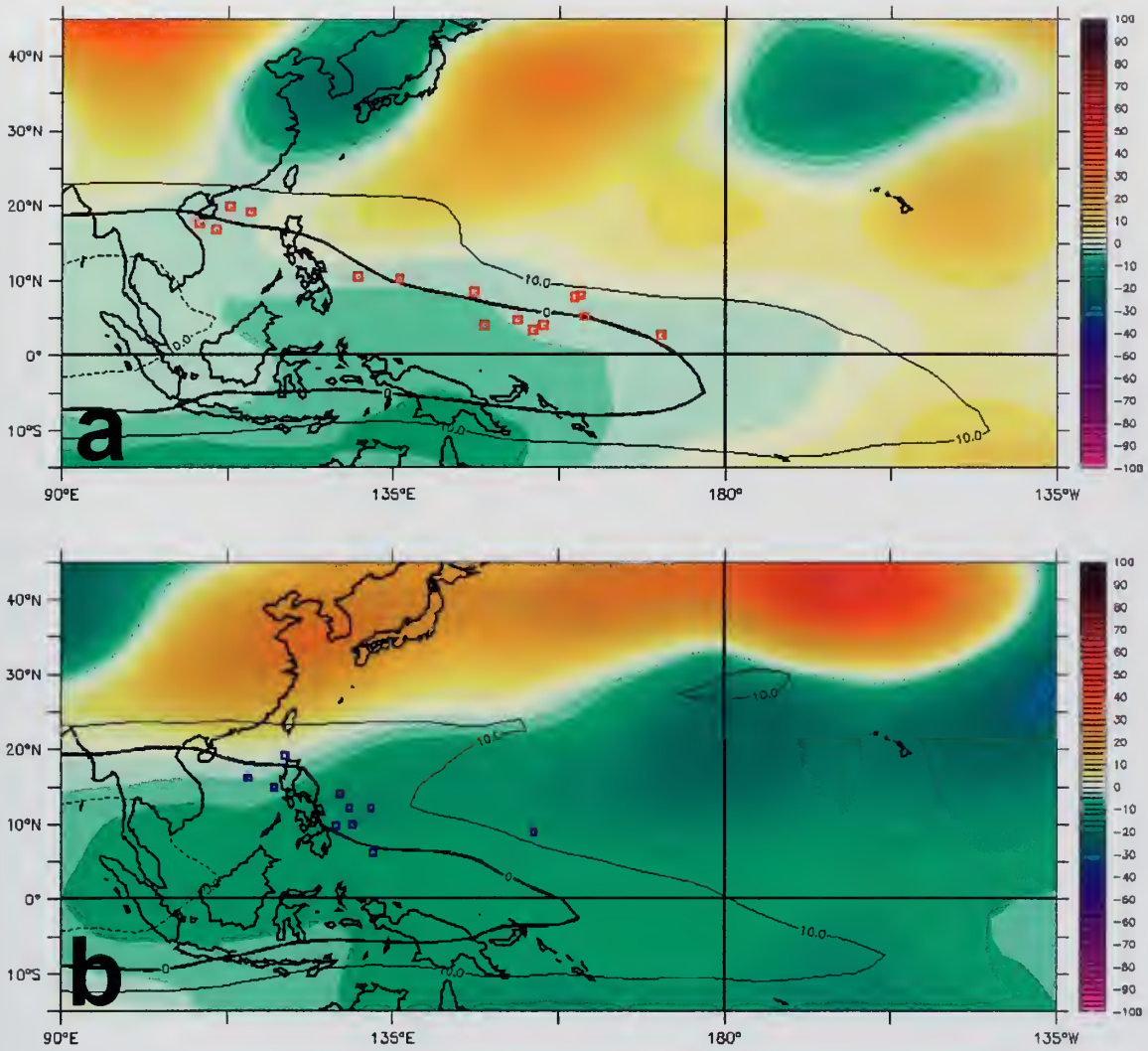

Figure 12. May tropical cyclone formation sites with composite 200 hPa anomalous geopotential heights (filled color in m) and actual shear (contour lines in ms^{-1}) *based on nine strong events* for: (a) El Niño and (b) La Niña .

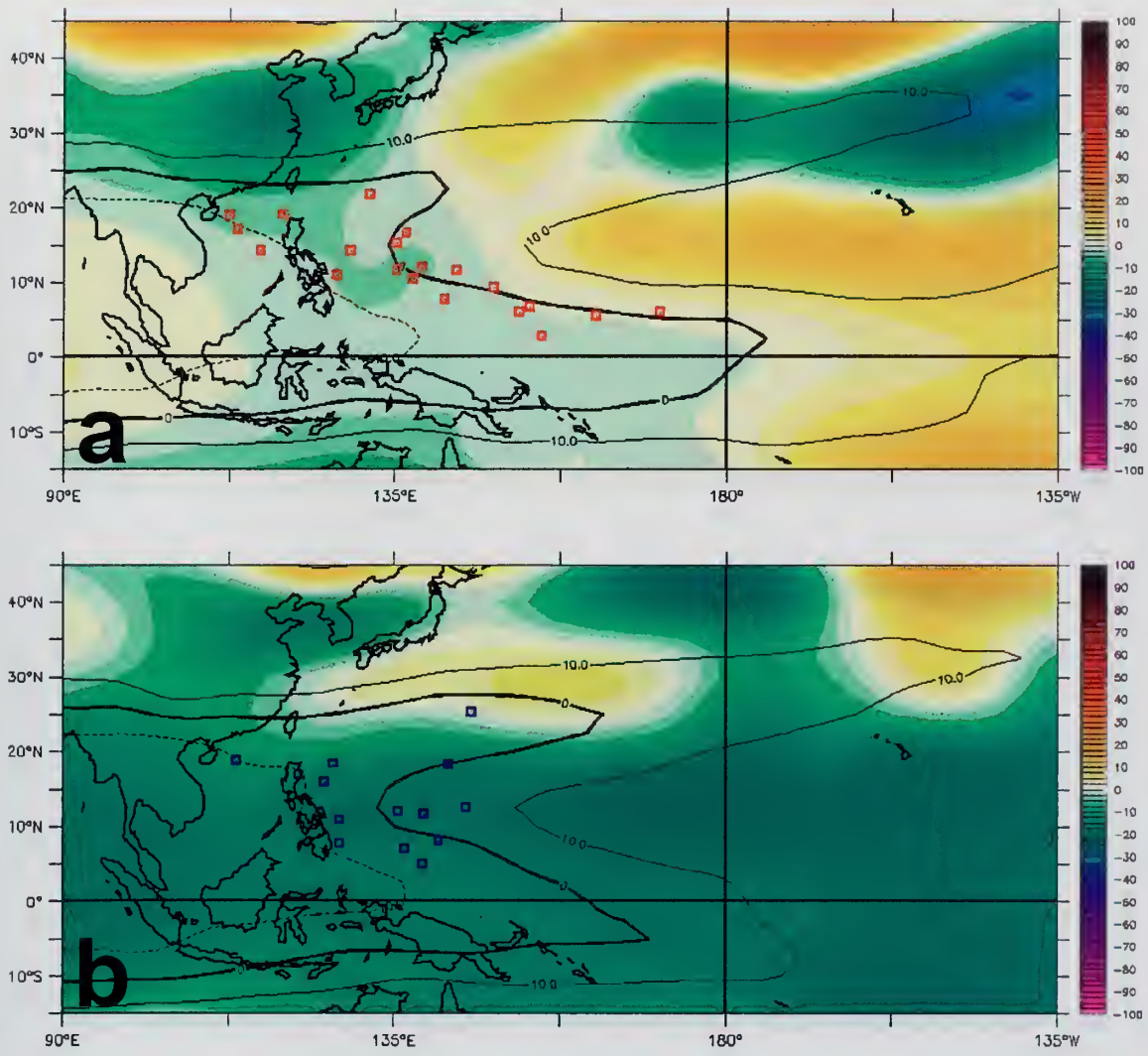

Figure 13. June tropical cyclone formation sites with composite 200 hPa anomalous geopotential heights (filled color in m) and actual shear (contour lines in ms^{-1}) *based on nine strong events* for: (a) El Niño and (b) La Niña .

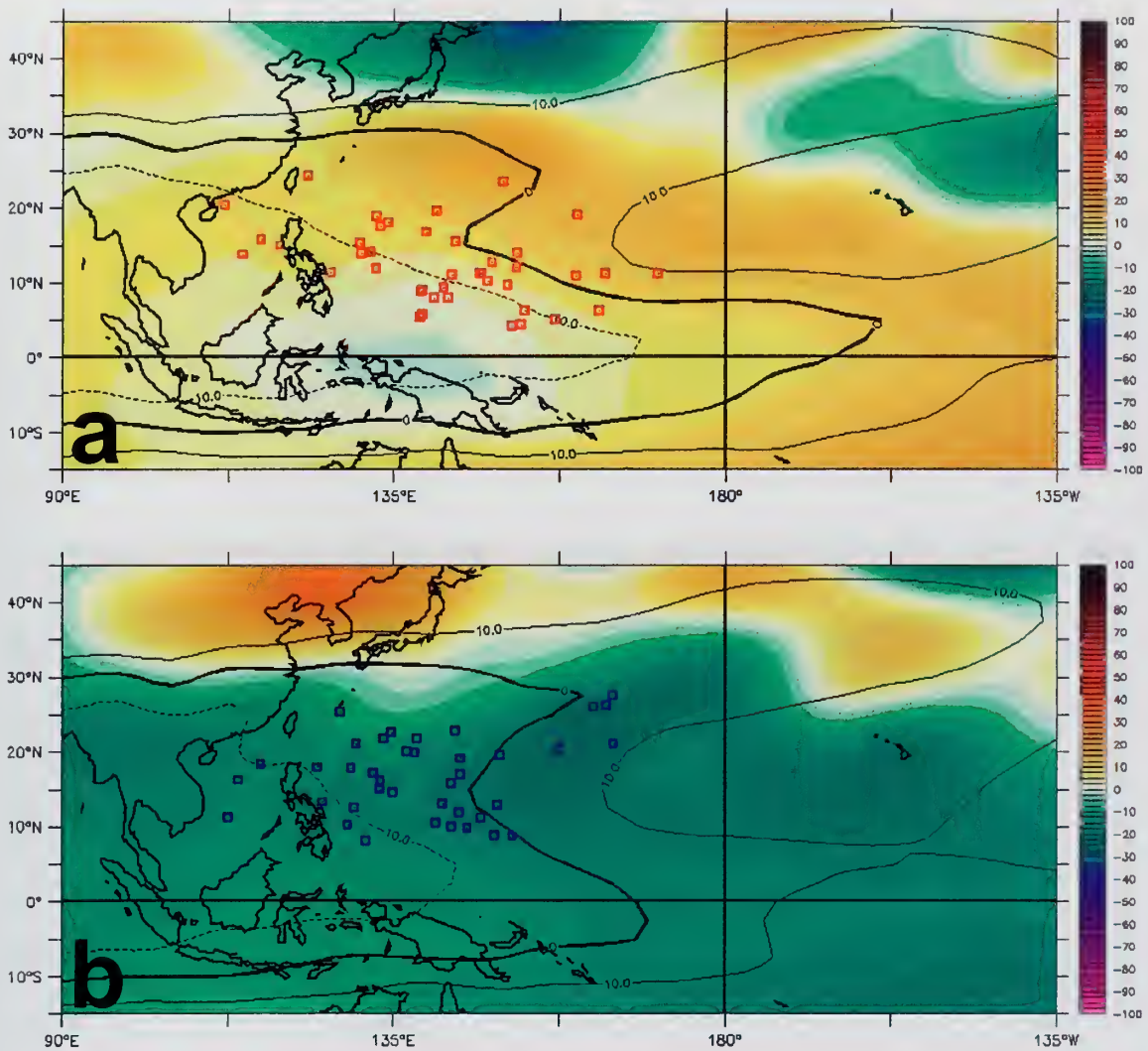

Figure 14. July tropical cyclone formation sites with composite 200 hPa anomalous geopotential heights (filled color in m) and actual shear (contour lines in ms^{-1}) *based on nine strong events* for: (a) El Niño and (b) La Niña .

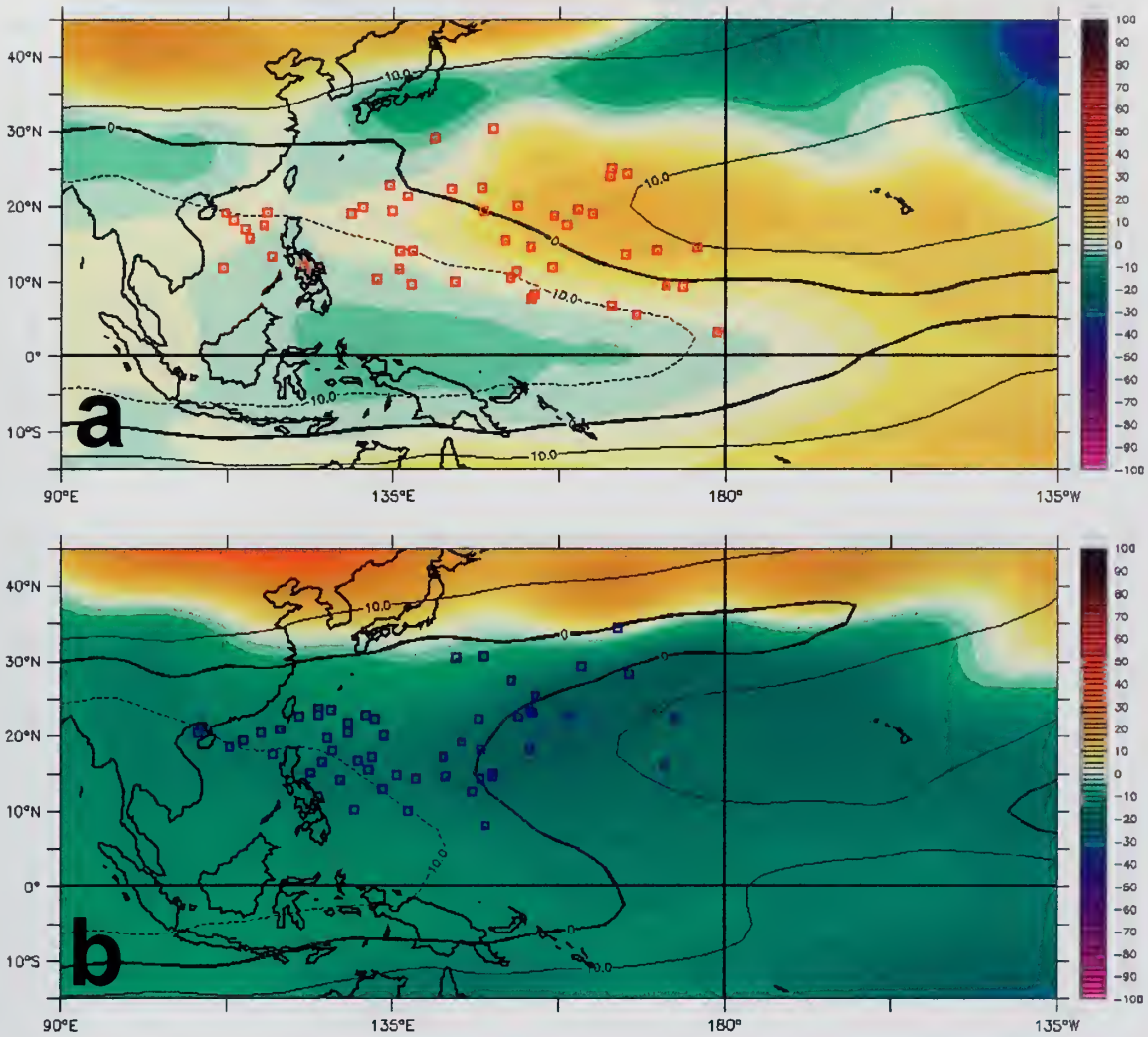

Figure 15. August tropical cyclone formation sites with composite 200 hPa anomalous geopotential heights (filled color in m) and actual shear (contour lines in ms^{-1}) *based on nine strong events* for: (a) El Niño and (b) La Niña .

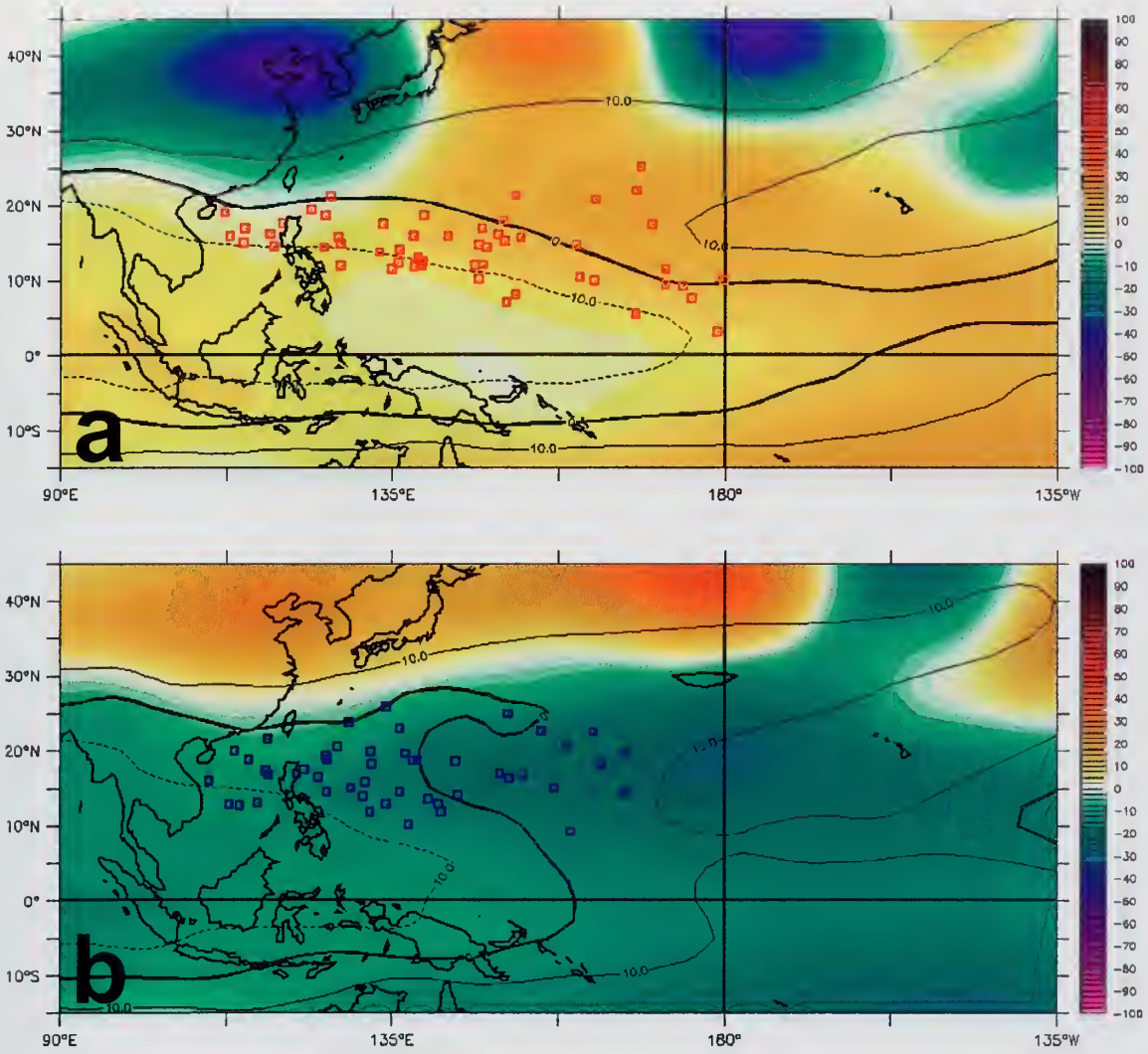

Figure 16. September tropical cyclone formation sites with composite 200 hPa anomalous geopotential heights (filled color in m) and actual shear (contour lines in ms^{-1}) *based on nine strong events* for: (a) El Niño and (b) La Niña .

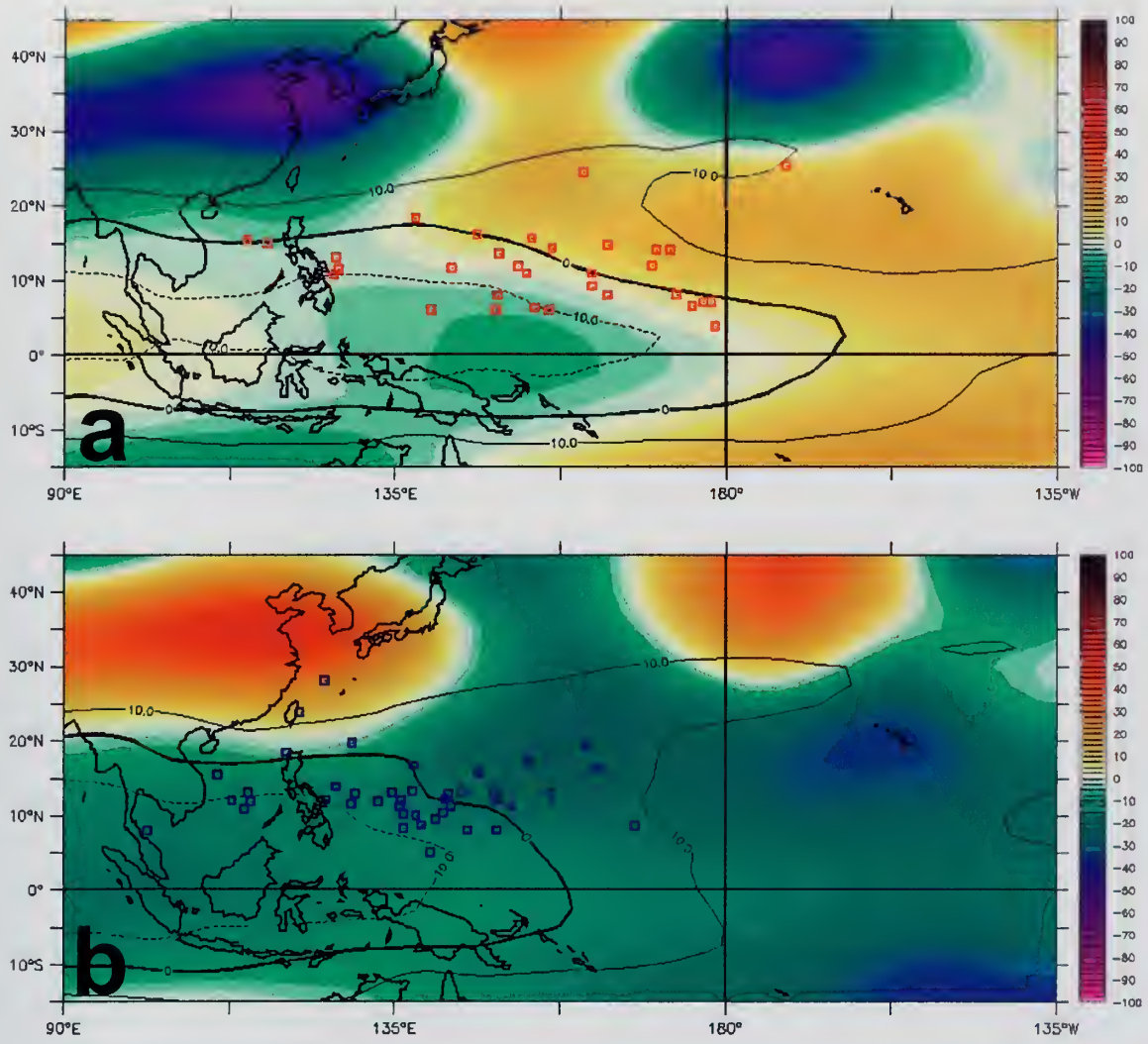

Figure 17. October tropical cyclone formation sites with composite 200 hPa anomalous geopotential heights (filled color in m) and actual shear (contour lines in ms^{-1}) *based on nine strong events* for: (a) El Niño and (b) La Niña .

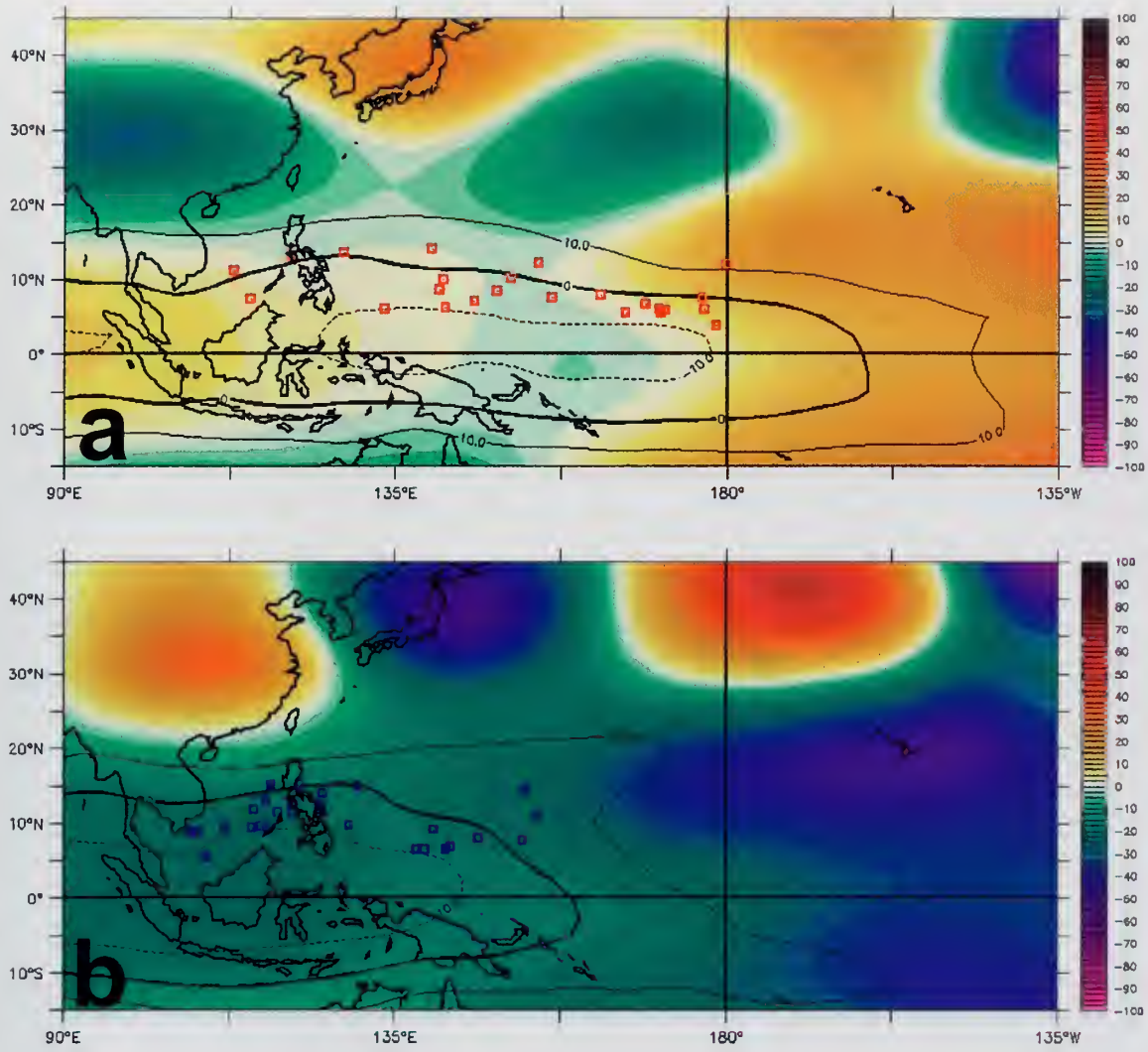

Figure 18. November tropical cyclone formation sites with composite 200 hPa anomalous geopotential heights (filled color in m) and actual shear (contour lines in ms^{-1}) *based on nine strong events* for: (a) El Niño and (b) La Niña .

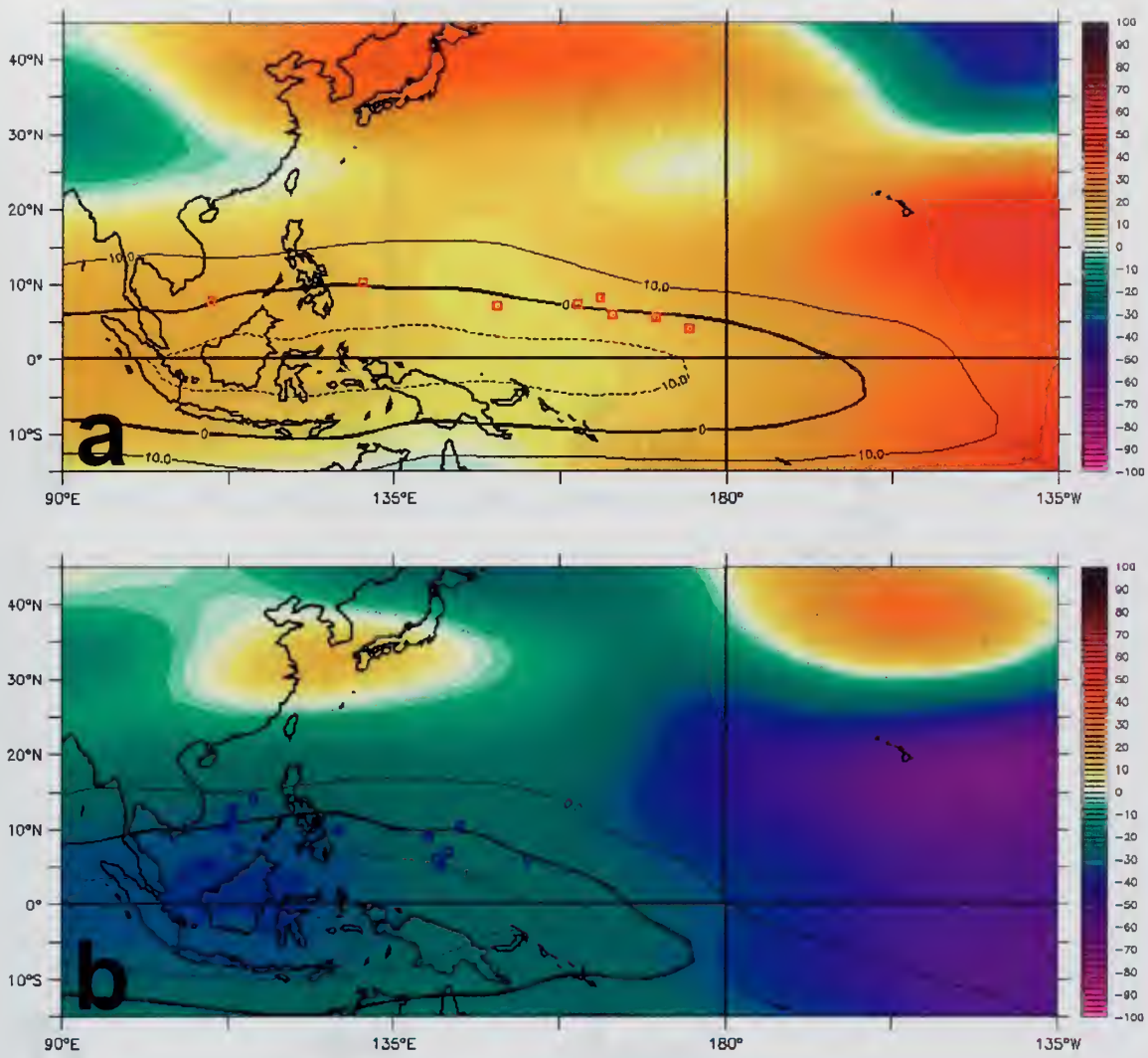

Figure 19. December tropical cyclone formation sites with composite 200 hPa anomalous geopotential heights (filled color in m) and actual shear (contour lines in ms^{-1}) *based on nine strong events* for: (a) El Niño and (b) La Niña .

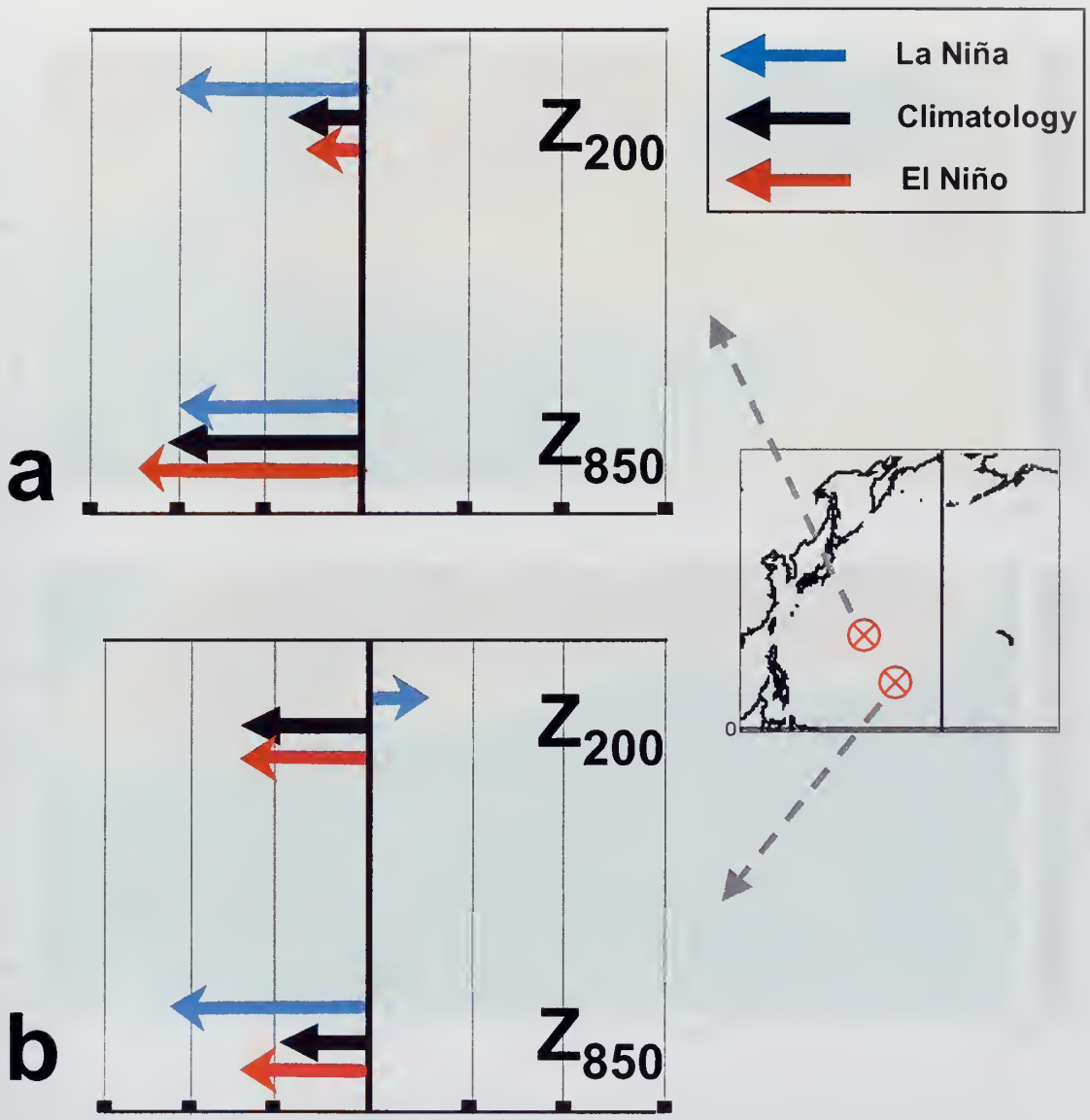

Figure 20. Schematic diagram of August-September zonal wind for 1968-1996 climatology, and the composite of the *nine strong events* for (a) 20°N 150°E and (b) 15°N 165°E.

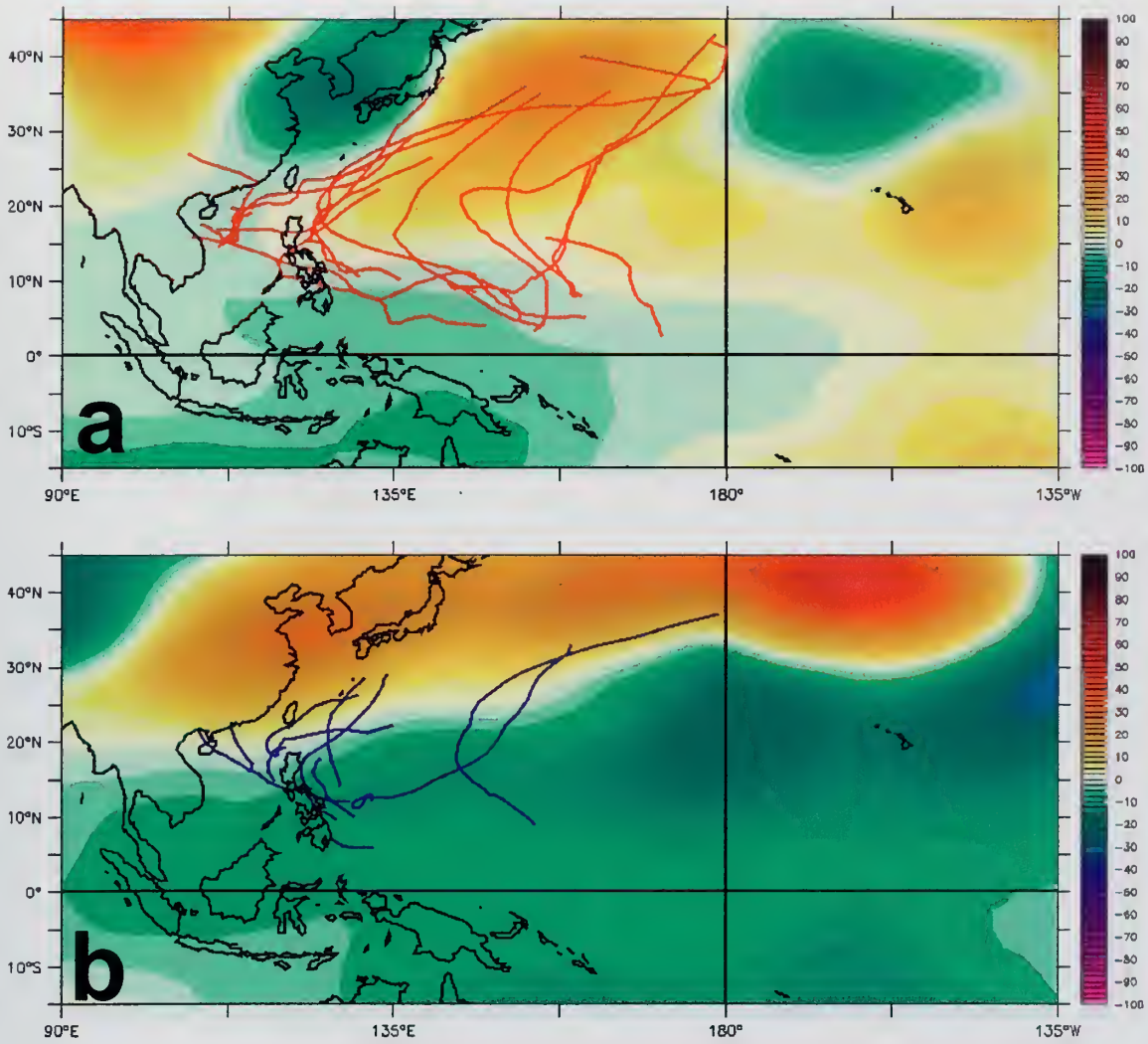

Figure 21. May tropical cyclone tracks with composite 200 hPa anomalous geopotential heights (filled color in m) *based on nine strong events* for: (a) El Niño and (b) La Niña .

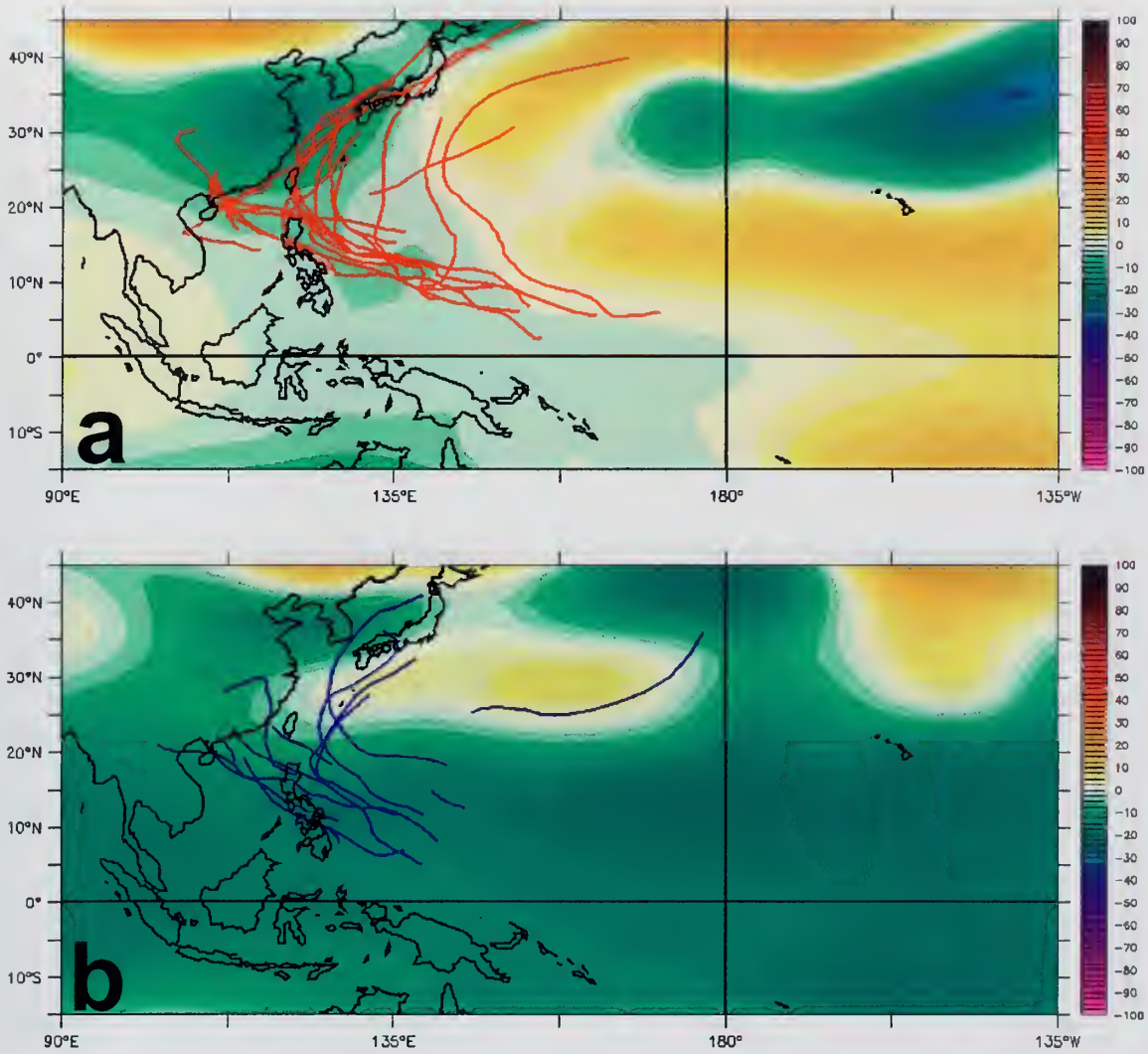

Figure 22. June tropical cyclone tracks with composite 200 hPa anomalous geopotential heights (filled color in m) *based on nine strong events* for: (a) El Niño and (b) La Niña .

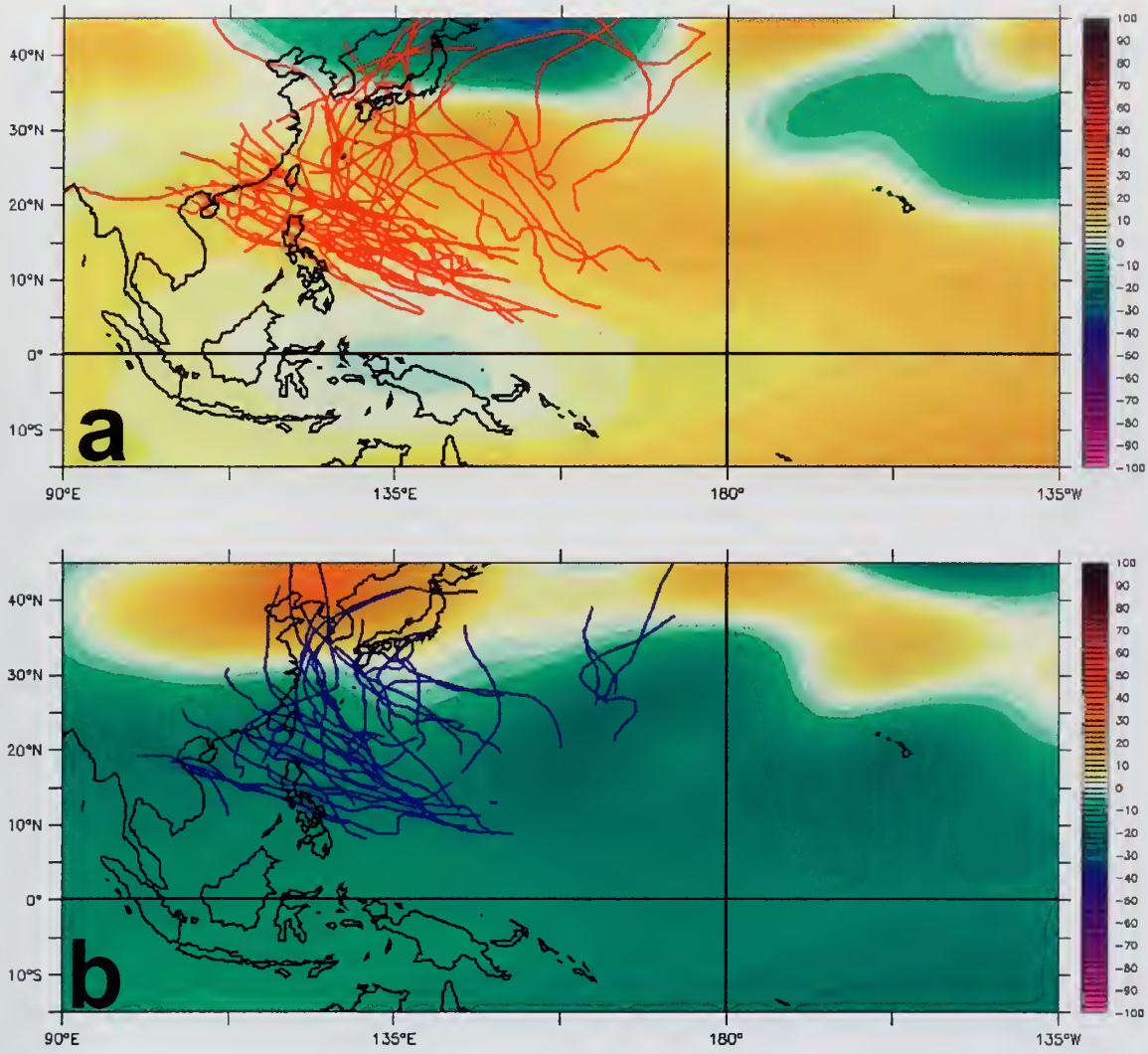

Figure 23. July tropical cyclone tracks with composite 200 hPa anomalous geopotential heights (filled color in m) *based on nine strong events* for: (a) El Niño and (b) La Niña .

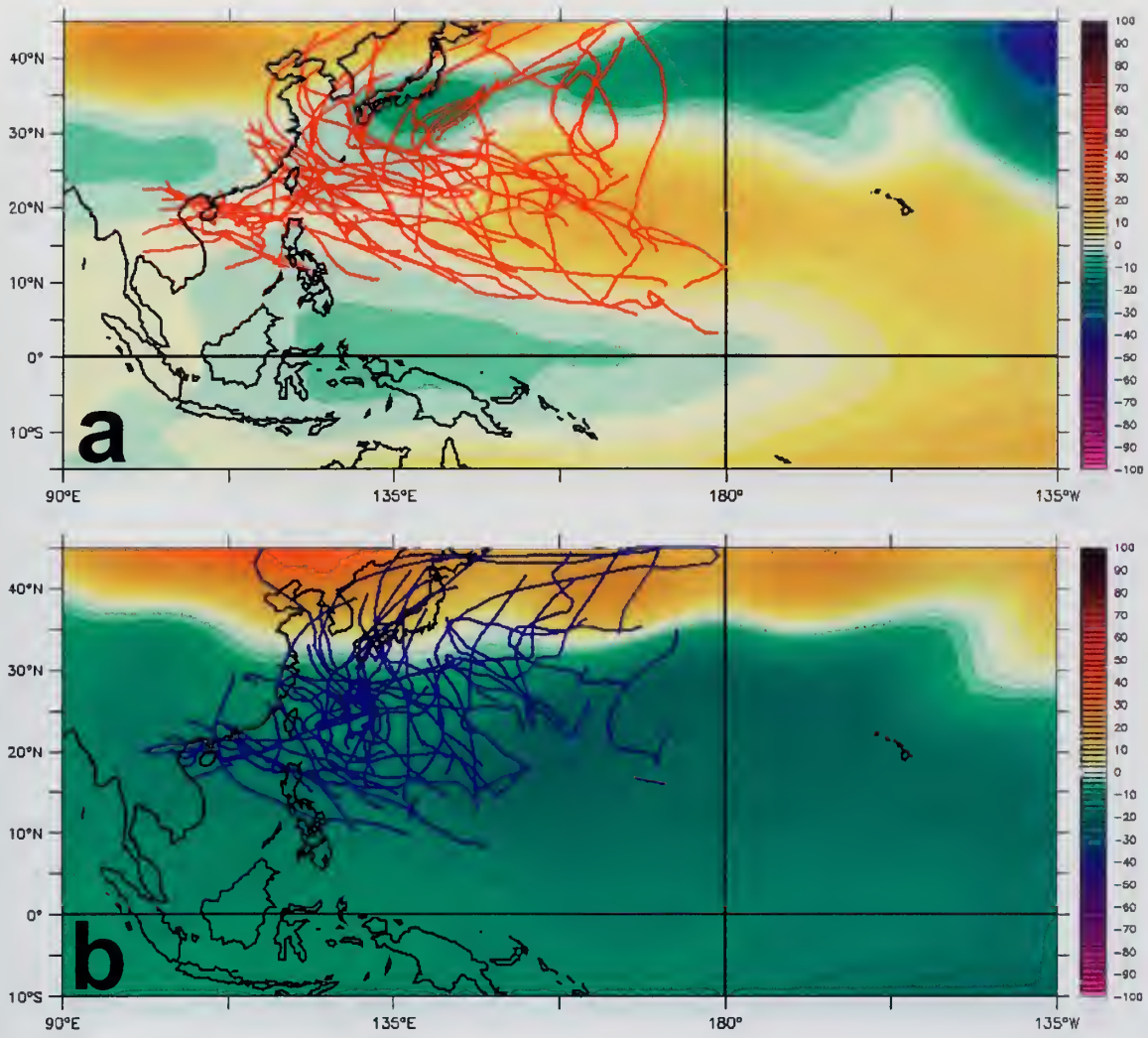

Figure 24. August tropical cyclone tracks with composite 200 hPa anomalous geopotential heights (filled color in m) *based on nine strong events* for: (a) El Niño and (b) La Niña .

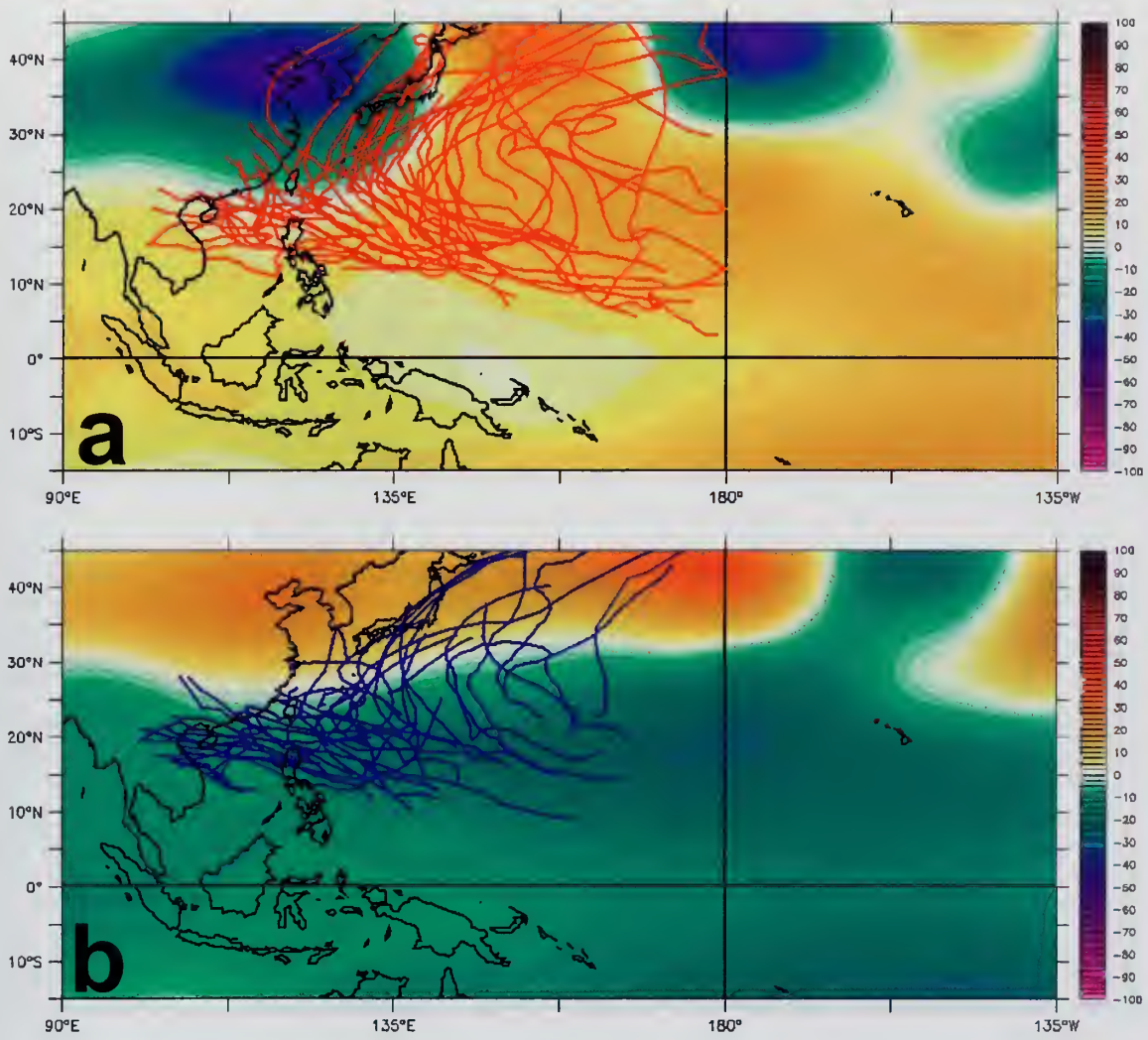

Figure 25. September tropical cyclone tracks with composite 200 hPa anomalous geopotential heights (filled color in m) *based on nine strong events* for: (a) El Niño and (b) La Niña .

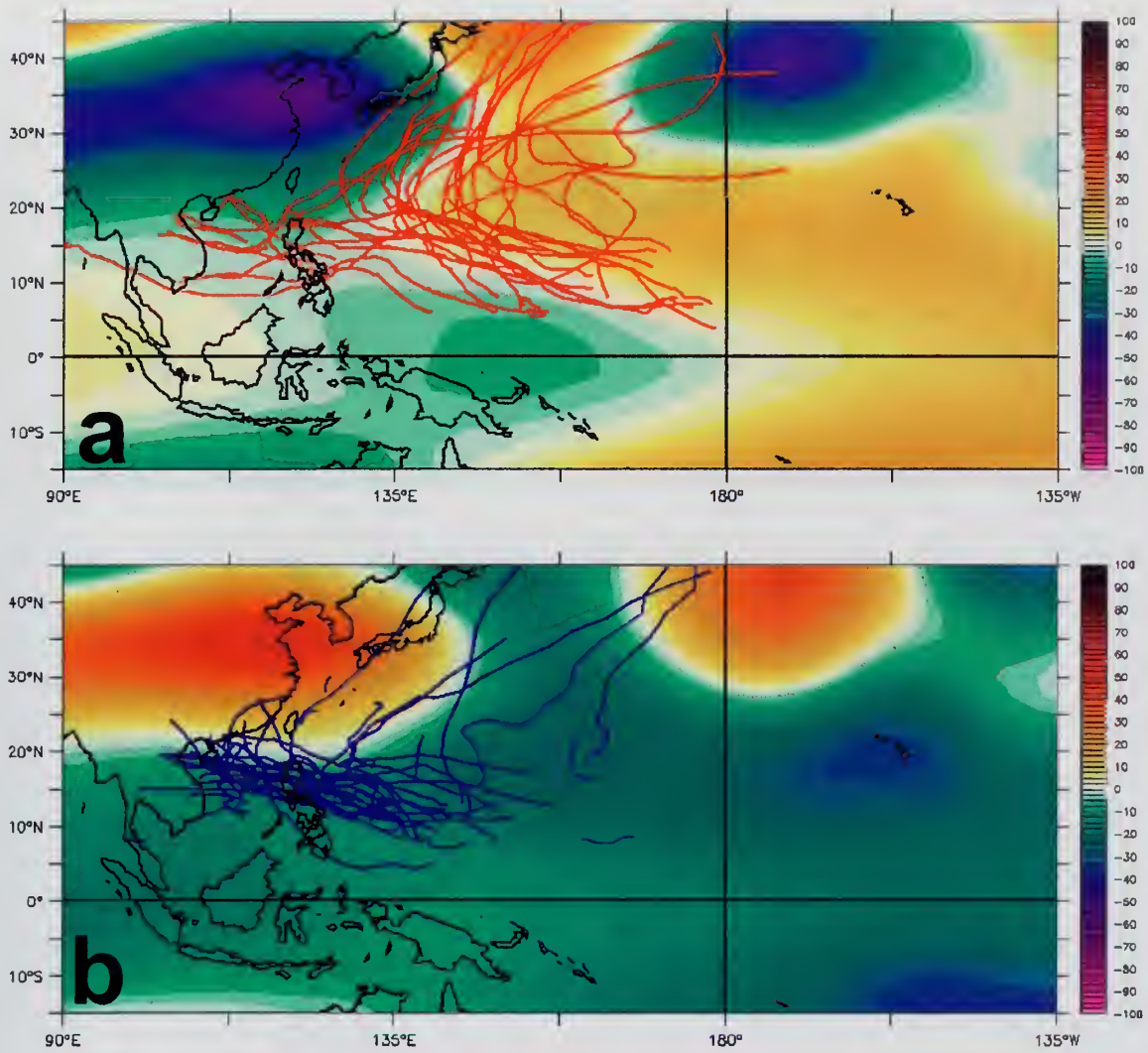

Figure 26. October tropical cyclone tracks with composite 200 hPa anomalous geopotential heights (filled color in m) *based on nine strong events* for: (a) El Niño and (b) La Niña .

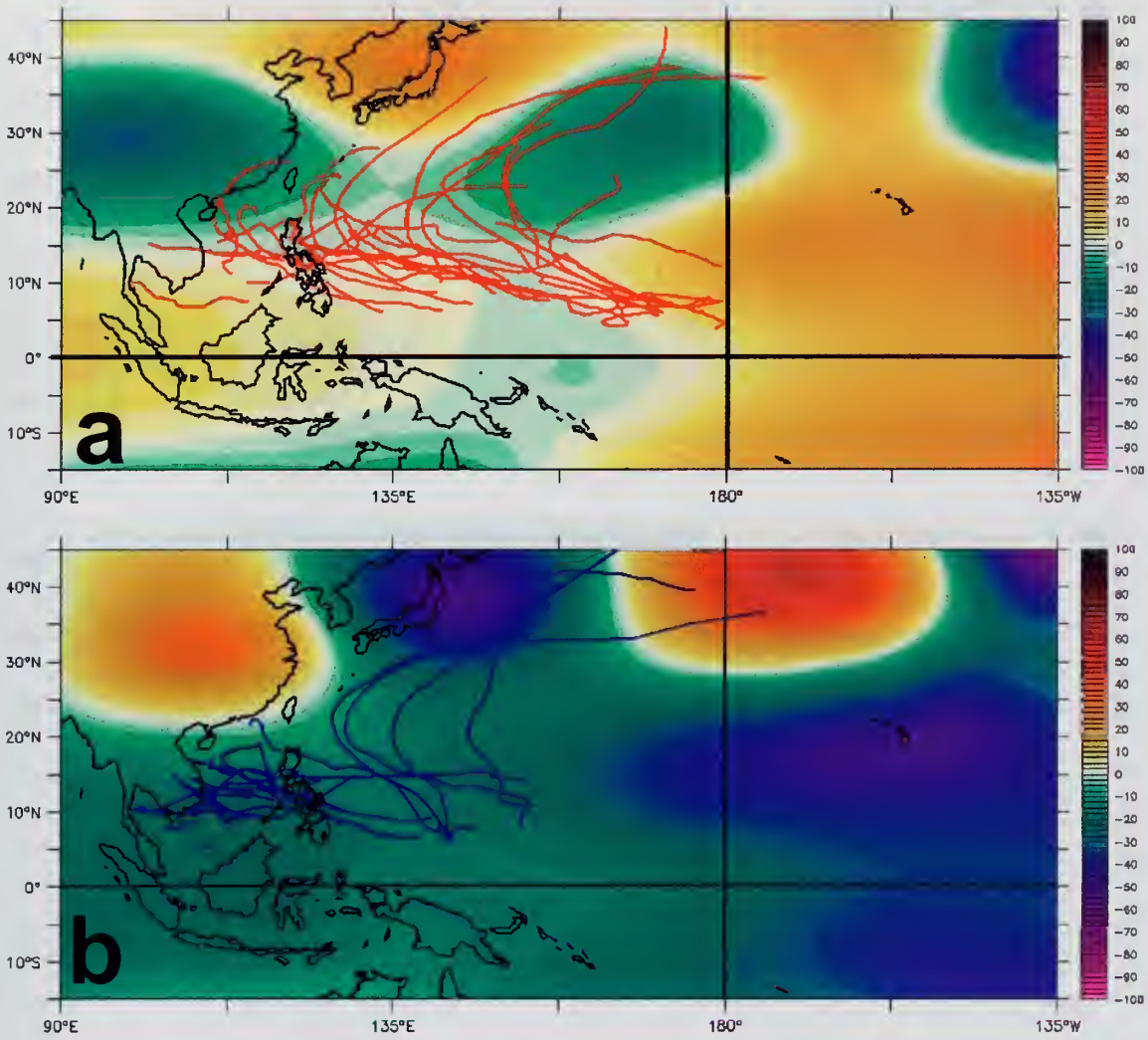

Figure 27. November tropical cyclone tracks with composite 200 hPa anomalous geopotential heights (filled color in m) *based on nine strong events* for: (a) El Niño and (b) La Niña .

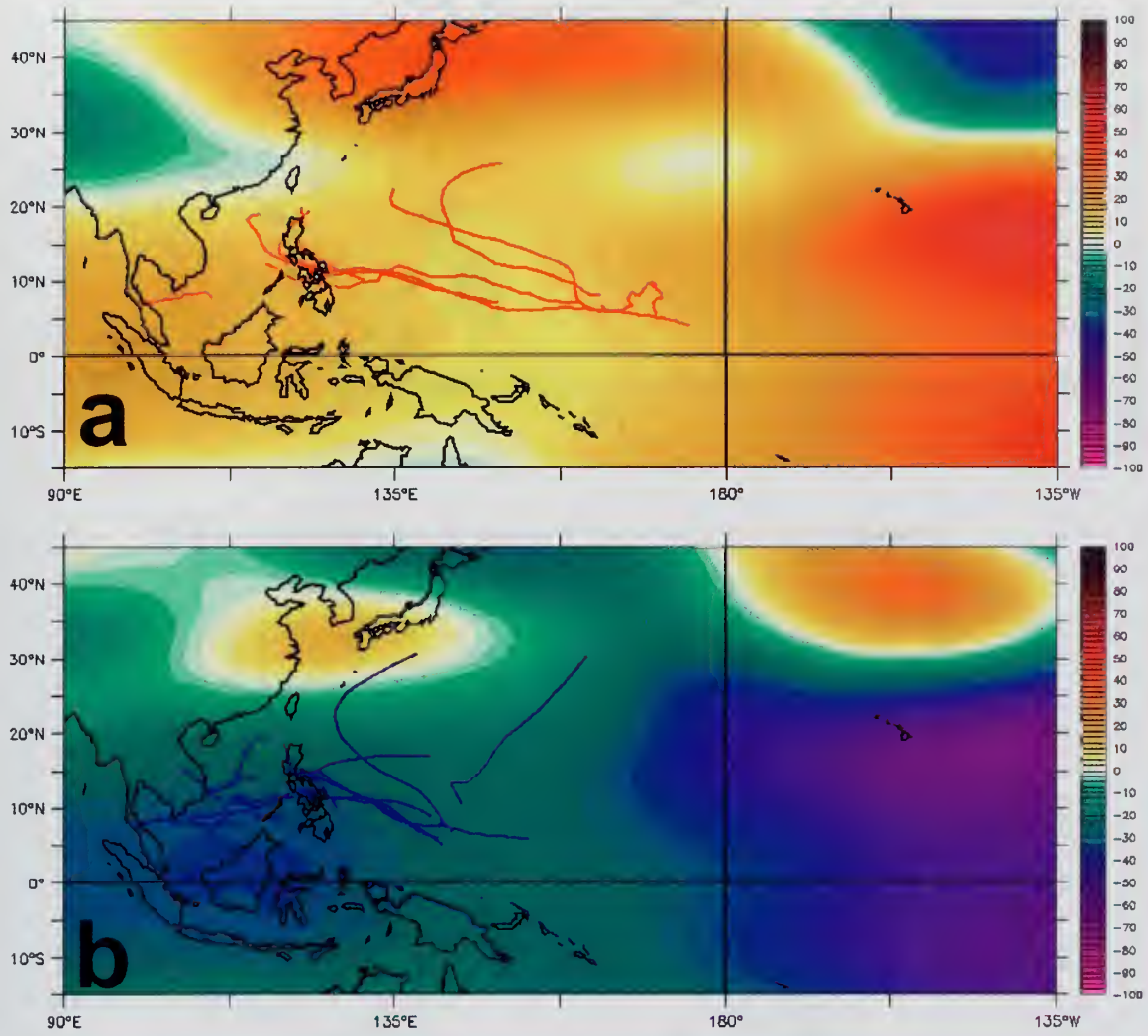

Figure 28. December tropical cyclone tracks with composite 200 hPa anomalous geopotential heights (filled color in m) *based on nine strong events* for: (a) El Niño and (b) La Niña .

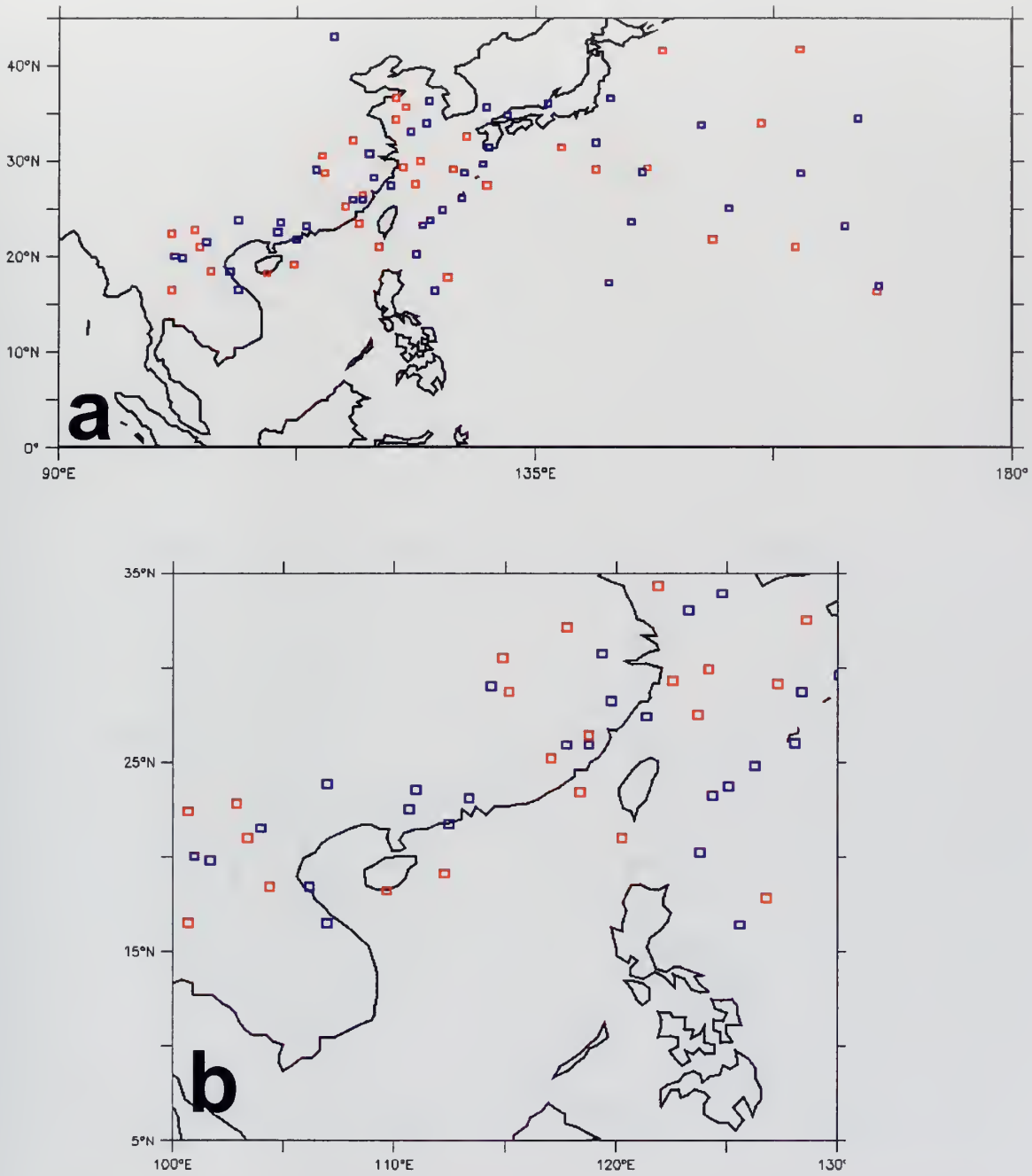

Figure 29. August tropical cyclone points of westernmost longitude for *nine strong events*. Red squares indicate El Niño storms and blue indicates La Niña storms for (a) the western Pacific and (b) the South China Sea.

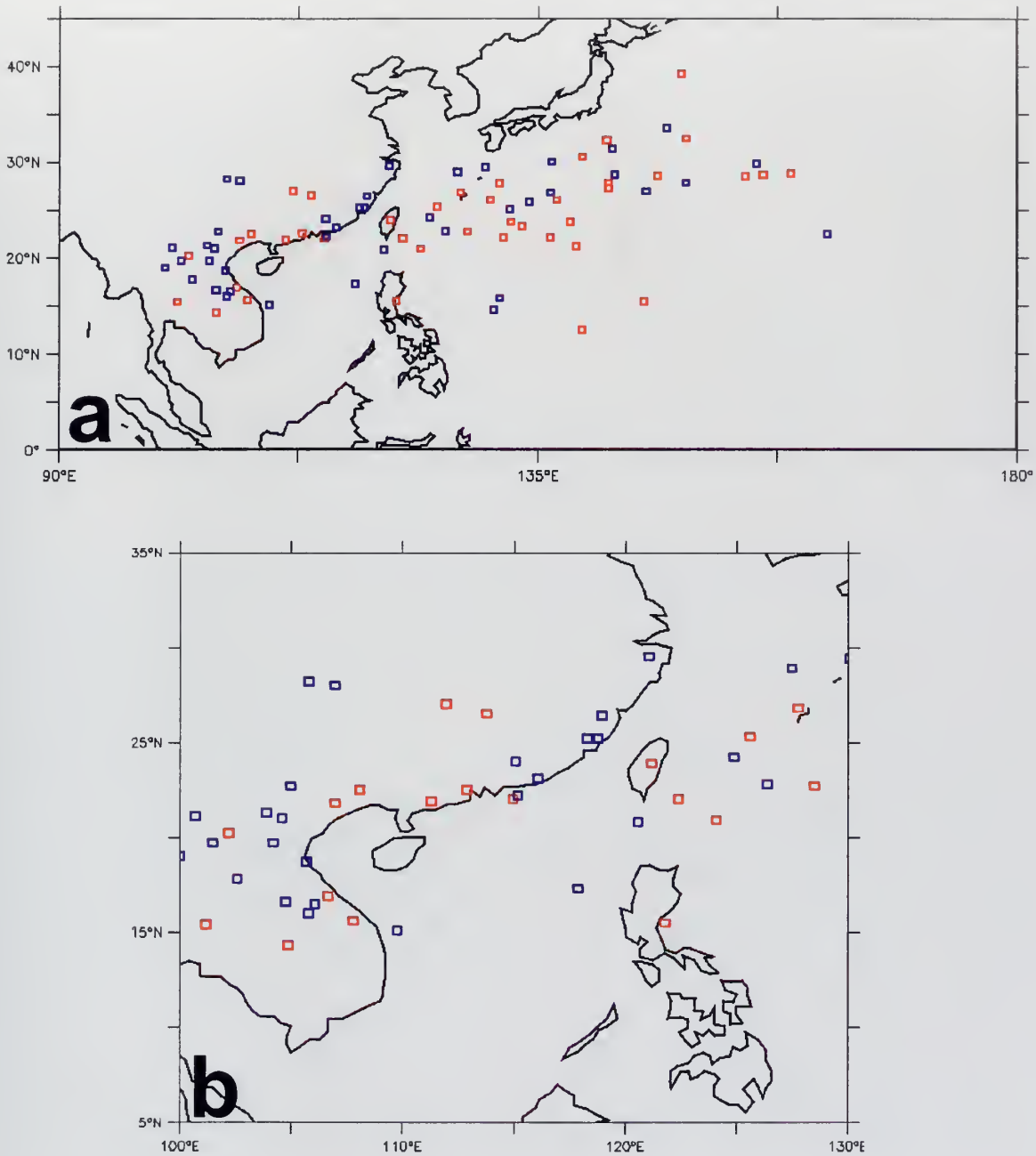

Figure 30. September tropical cyclone points of westernmost longitude for *nine strong events*. Red squares indicate El Niño storms and blue indicates La Niña storms for (a) the western Pacific and (b) the South China Sea.

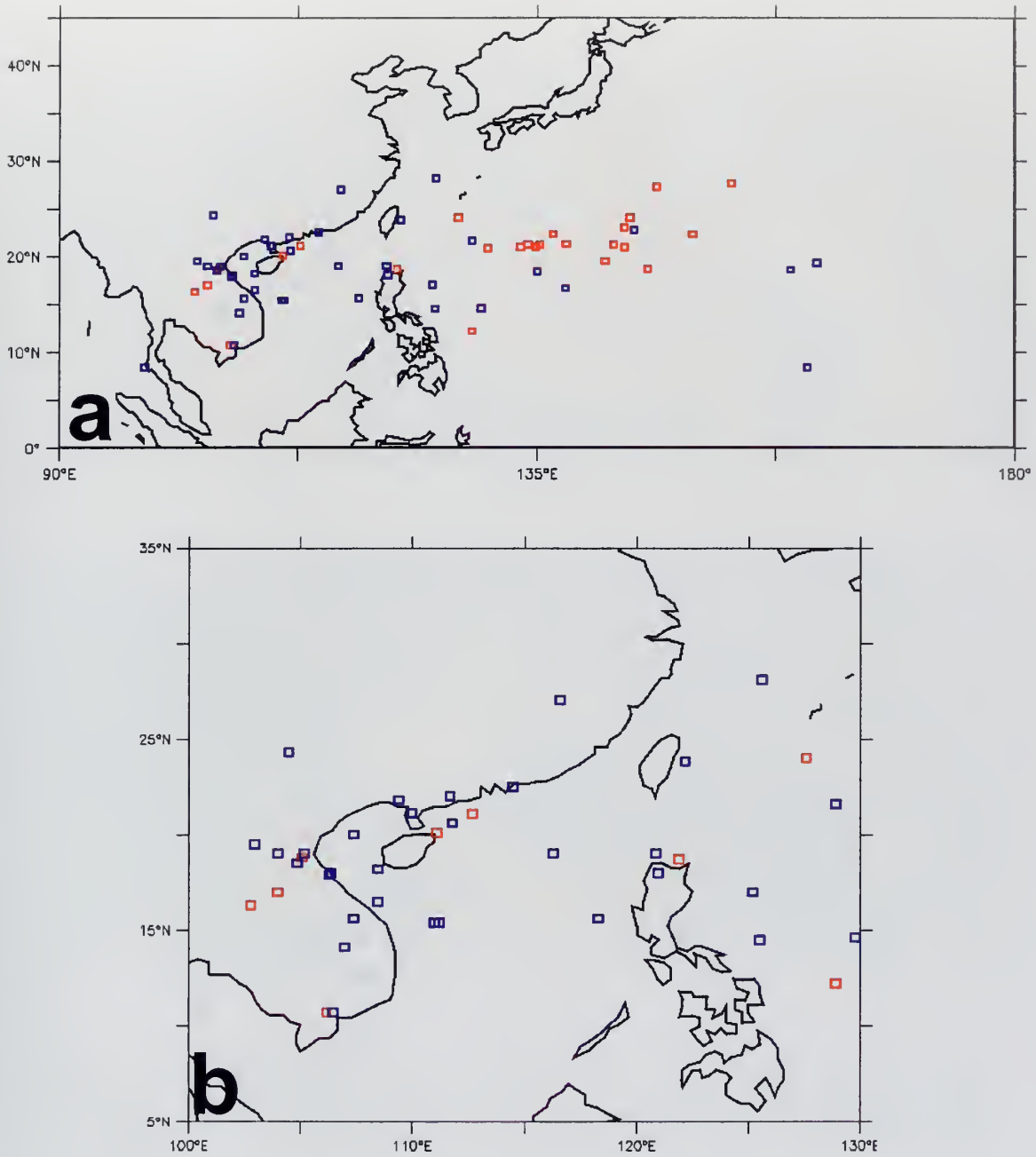

Figure 31. October tropical cyclone points of westernmost longitude for *nine strong events*. Red squares indicate El Niño storms and blue indicates La Niña storms for (a) the western Pacific and (b) the South China Sea.

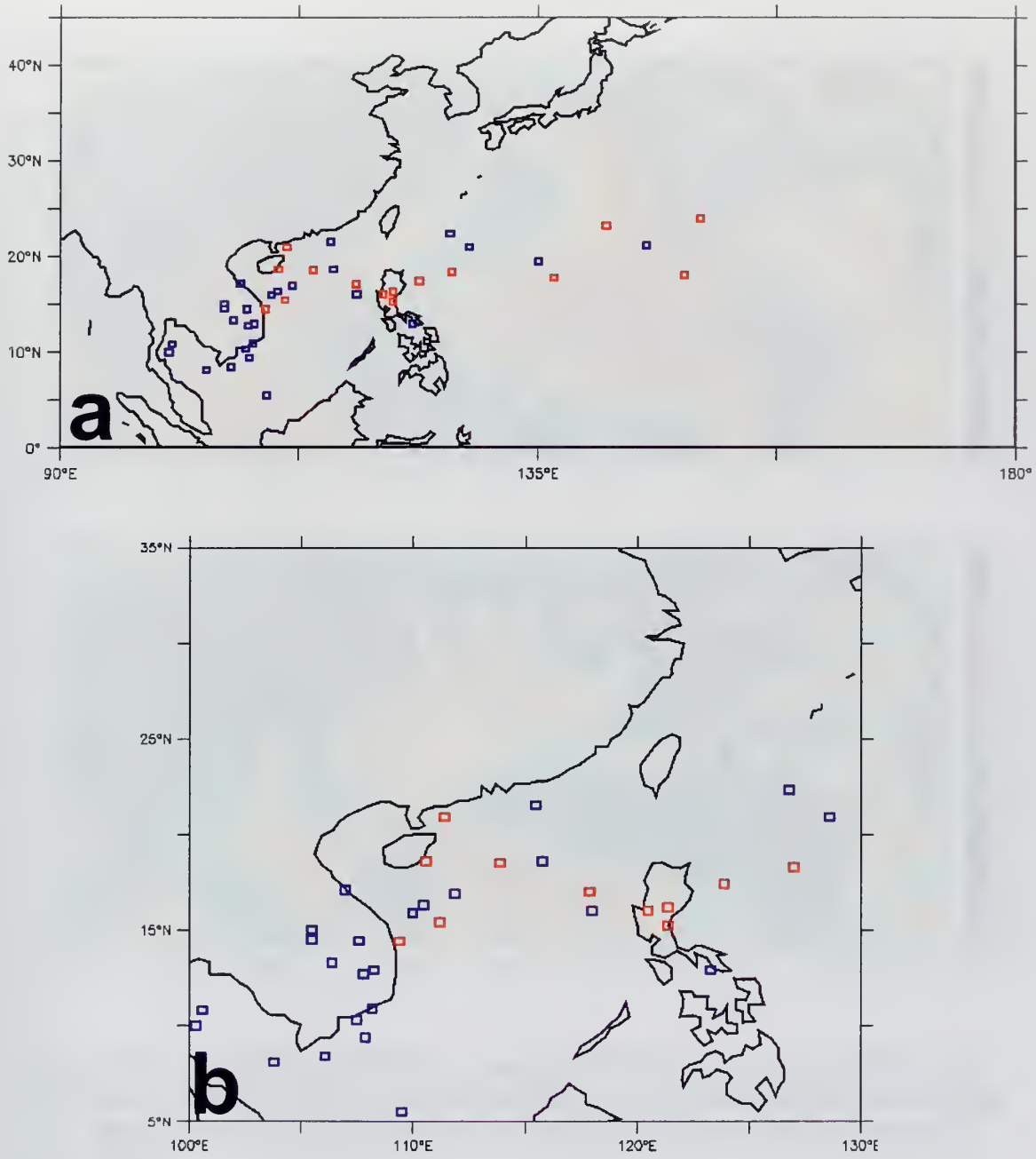

Figure 32. November tropical cyclone points of westernmost longitude for *nine strong events*. Red squares indicate El Niño storms and blue indicates La Niña storms for (a) the western Pacific and (b) the South China Sea.

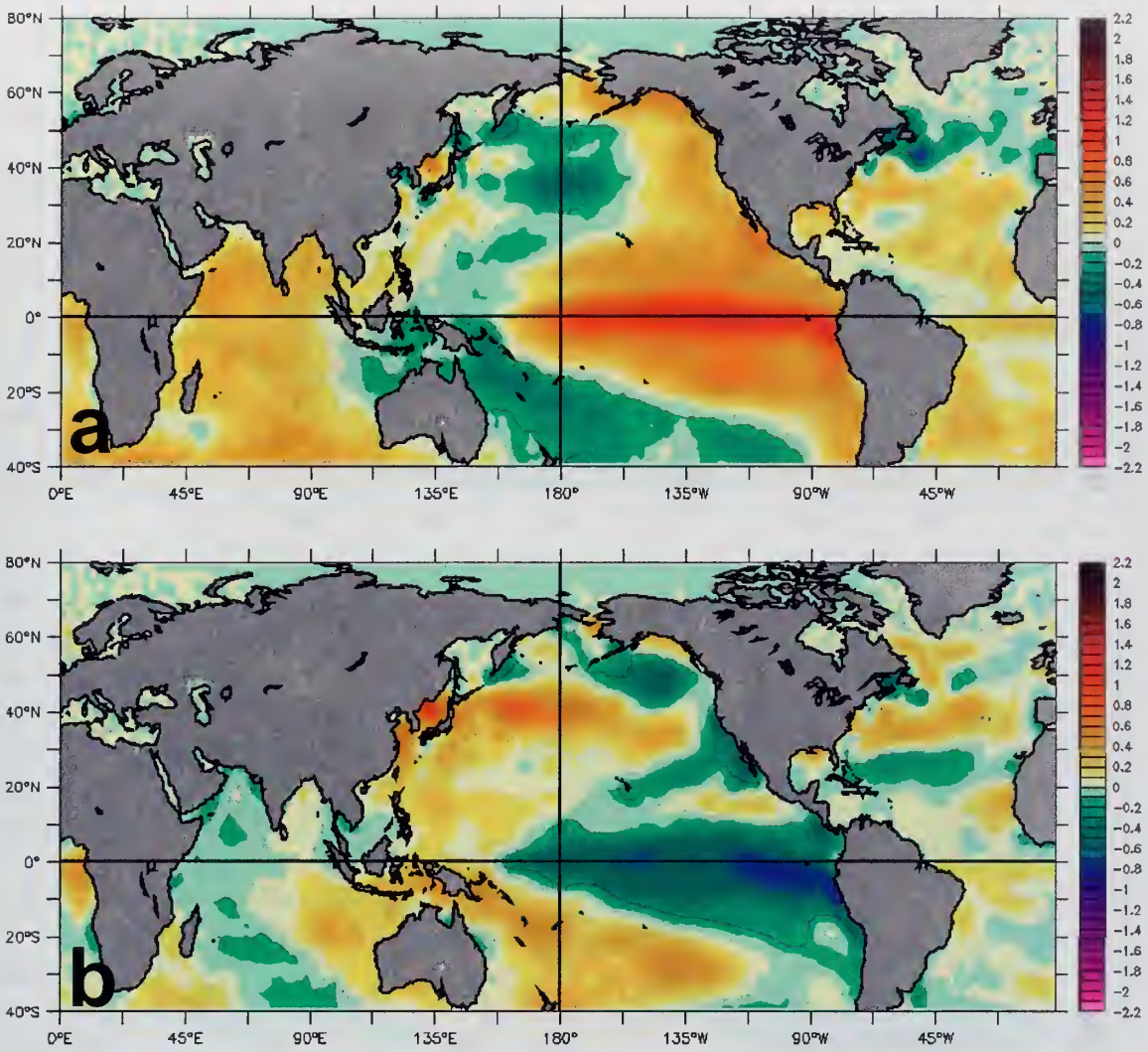

Figure 33. Composite anomalies for August-November prior to El Niño or La Niña event peak: (a) El Niño SST anomalies in °C; (b) La Niña SST anomalies in °C. See Chapter 2 for information on evolution of events and selection of event years.

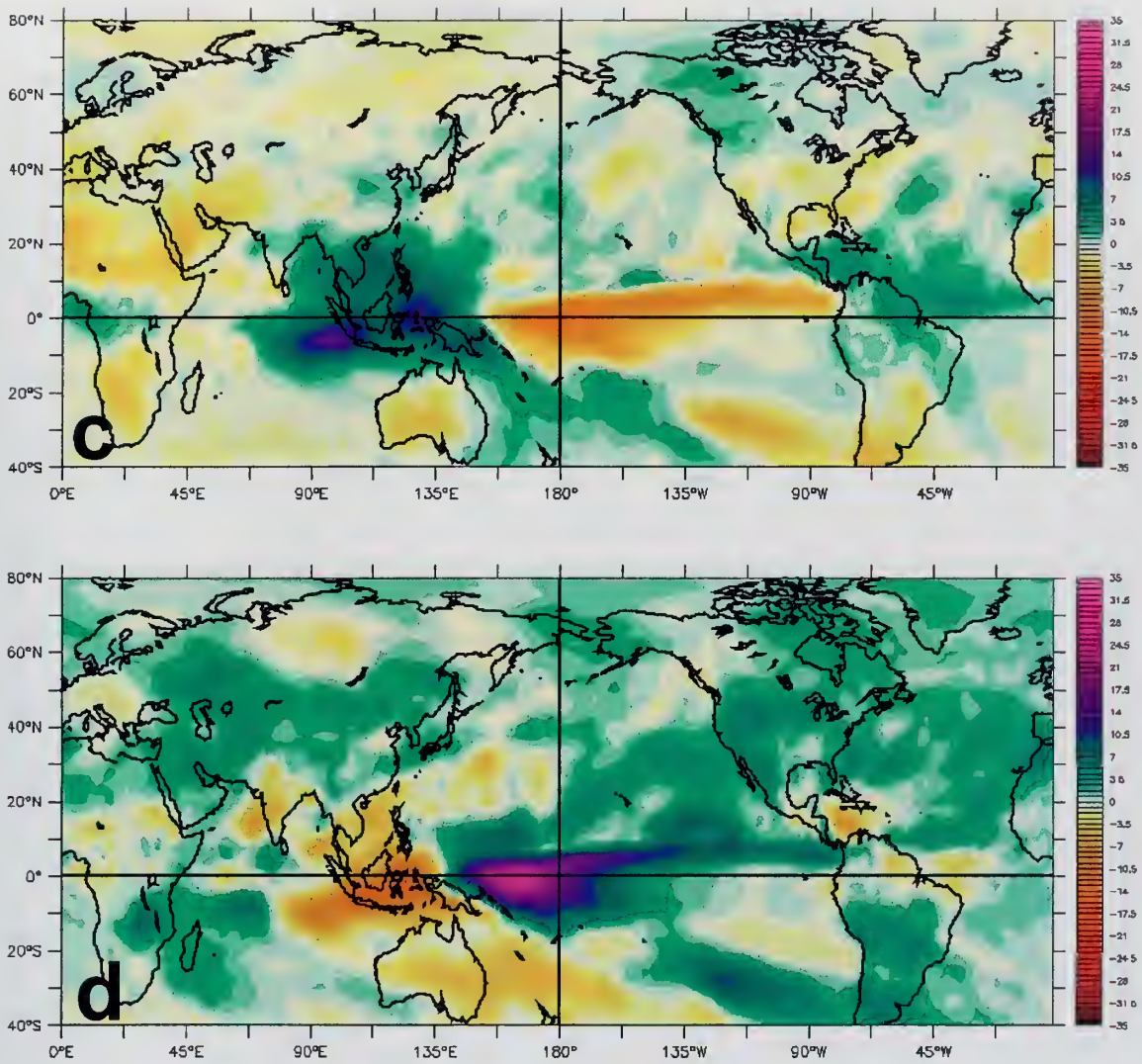

Figure 33 (continued). Composite anomalies for August-November prior to El Niño or La Niña event peak: (c) El Niño OLR anomalies in Wm^{-2}; (d) La Niña OLR anomalies in Wm^{-2}. See Chapter 2 for information on evolution of events and selection of event years.

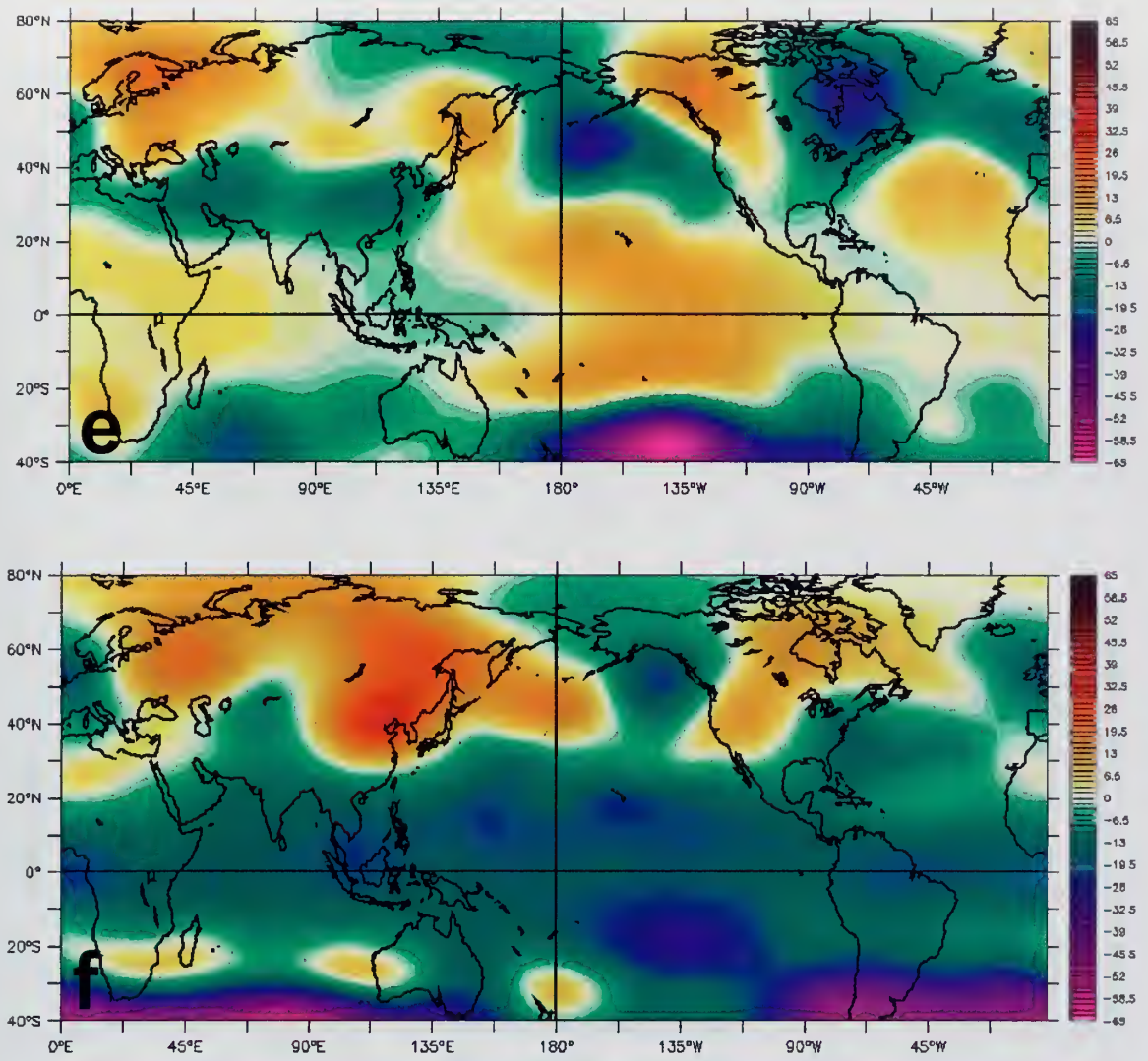

Figure 33 (continued). Composite anomalies for August-November prior to El Niño or La Niña event peak: (e) El Niño 200hPa geopotential (Z_{200}) height anomalies in m; (f) La Niña 200hPa geopotential height anomalies (Z_{200}) in m. See Chapter 2 for information on evolution of events and selection of event years.

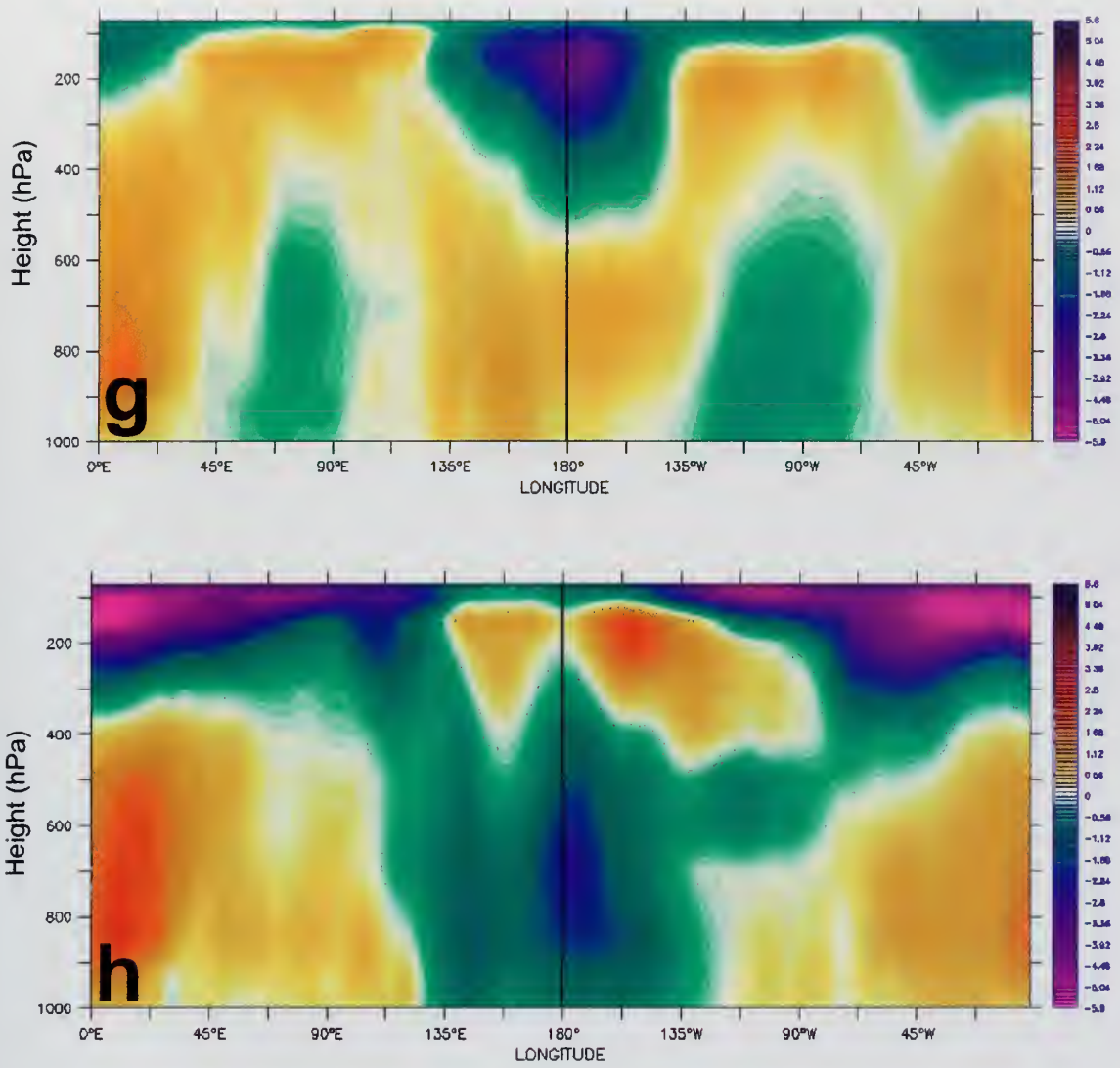

Figure 33 (continued). Composite anomalies averaged from 5°N-15°N for August-November prior to El Niño or La Niña event peak: (g) cross section of El Niño zonal wind anomalies in ms $^{-1}$; (h) cross section of La Niña zonal wind anomalies in ms^{-1}. See Chapter 2 for information on evolution of events and selection of event years.

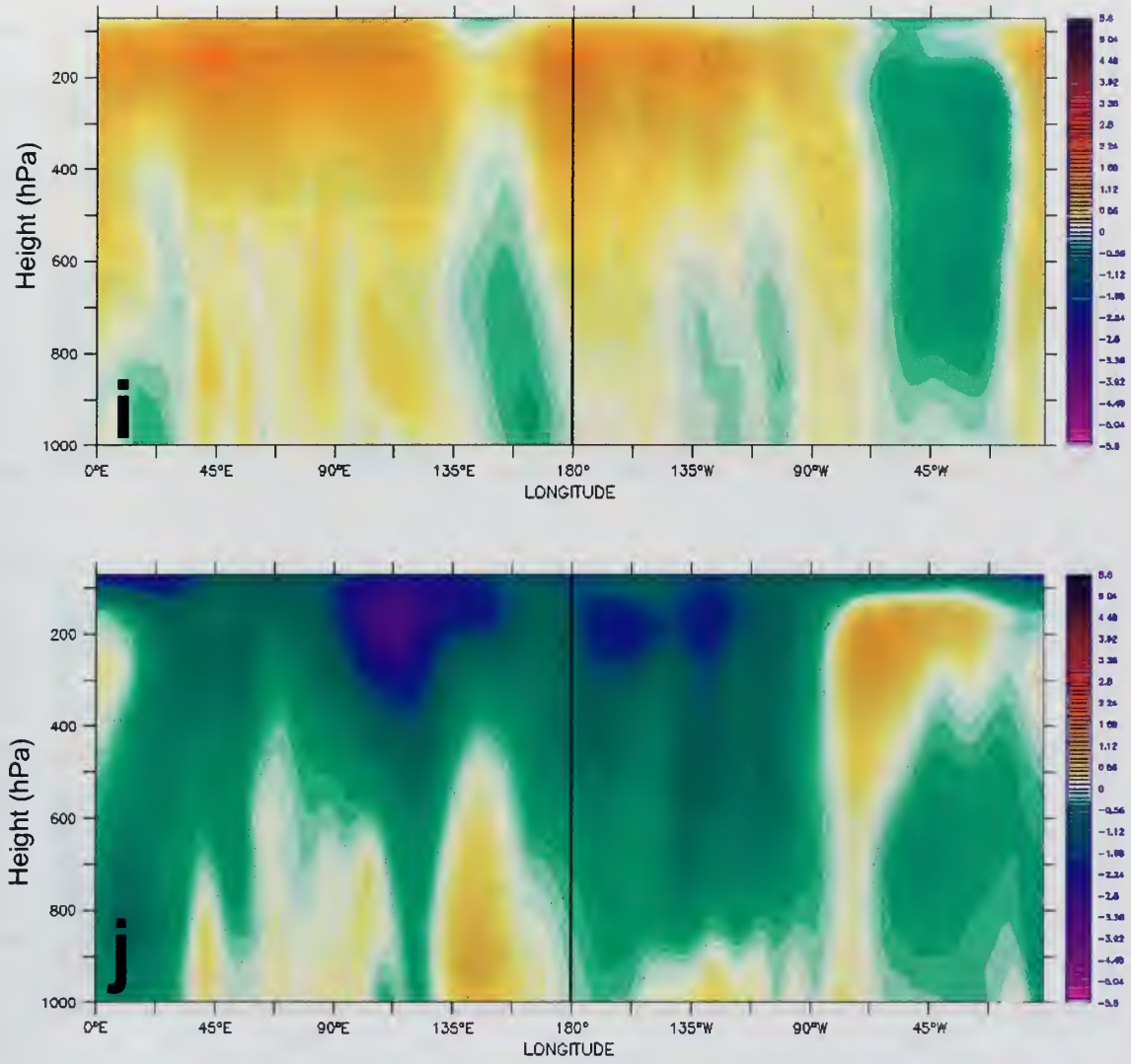

Figure 33 (continued). Composite anomalies averaged from 20°N-30°N for August-November prior to El Niño or La Niña event peak: (i) cross section of El Niño zonal wind anomalies in ms $^{-1}$; (j) cross section of La Niña zonal wind anomalies in ms^{-1}. See Chapter 2 for information on evolution of events and selection of event years.

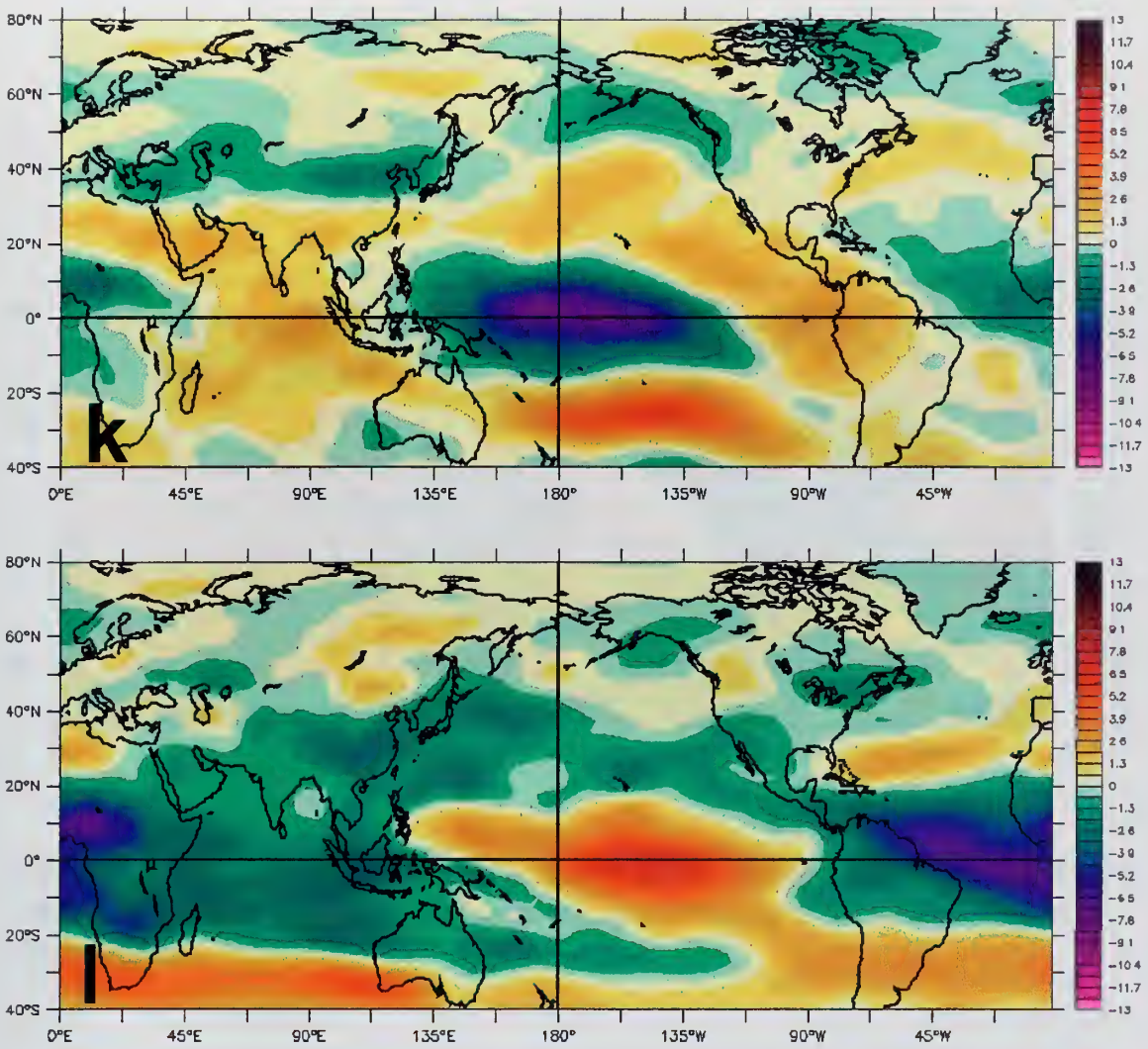

Figure 33 (continued). Composite anomalies for August-November prior to El Niño or La Niña event peak: (k) El Niño vertical shear (U_{200}- U_{850}) anomalies in ms^{-1}; (l) La Niña vertical shear (U_{200}- U_{850}) anomalies in ms^{-1}. See Chapter 2 for information on evolution of events and selection of event years.

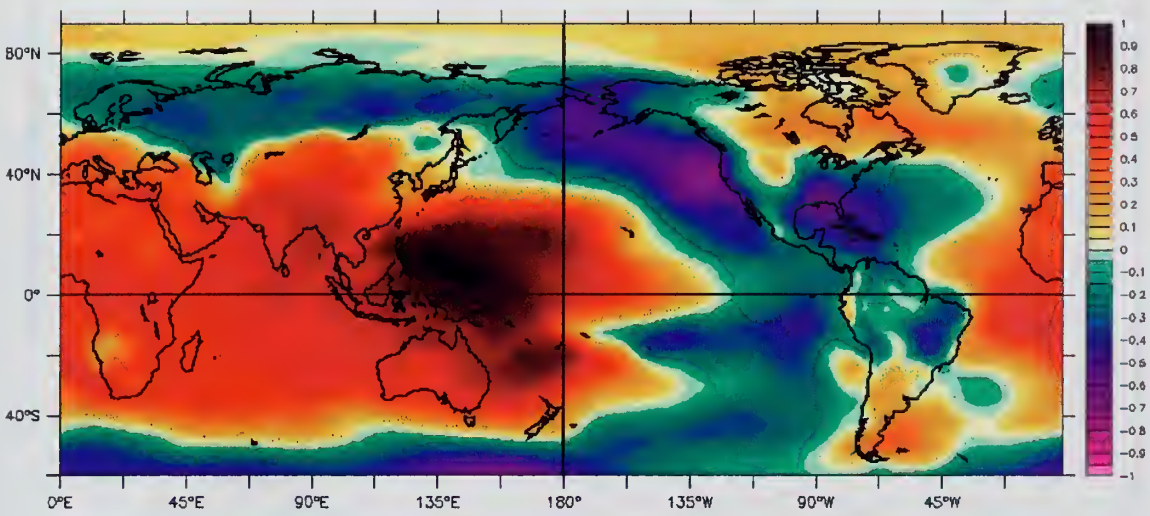

Figure 34. Correlation of sea level pressure in the Philippine Sea (**5-15N, 120-160E)** with sea level pressure elsewhere. See Chapter 2 for information on correlations.

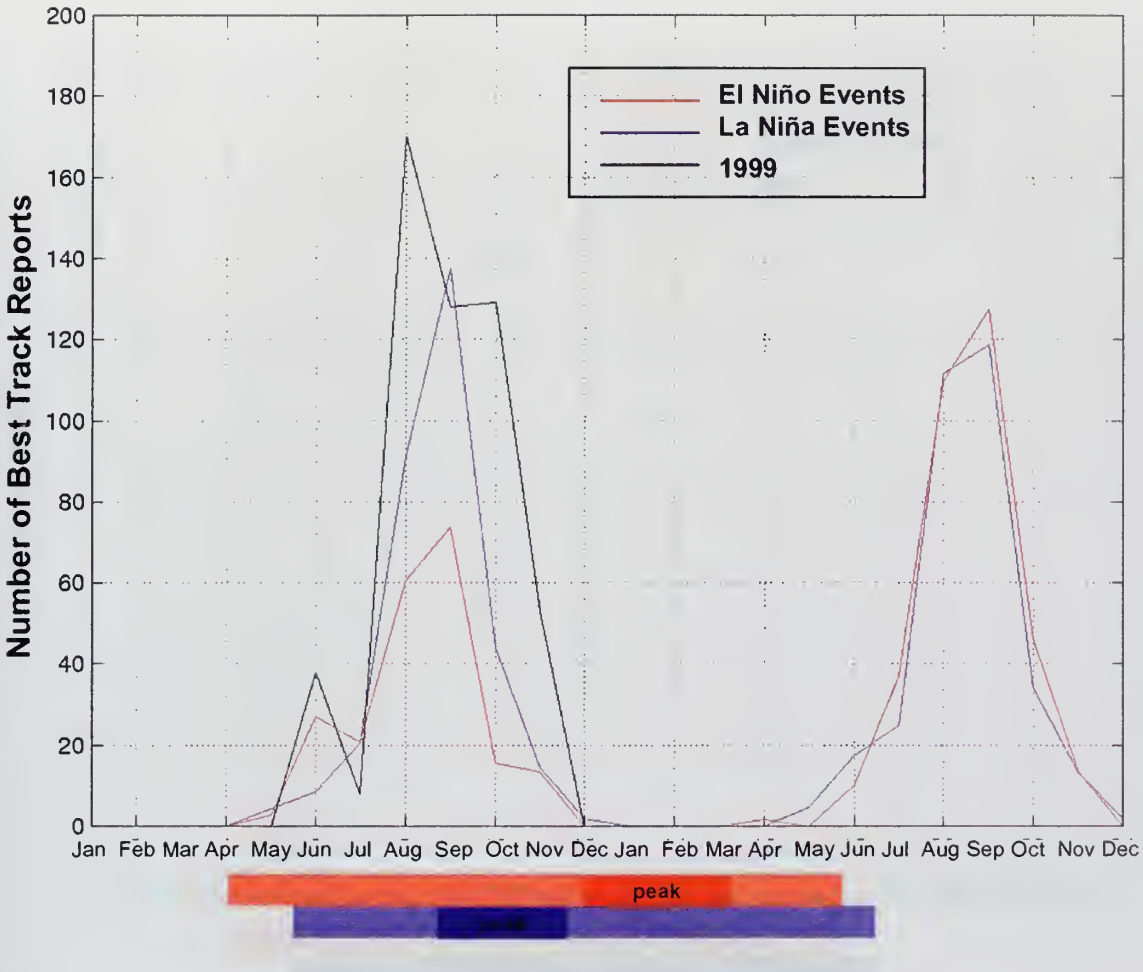

Figure 35. The average number of best track reports for Atlantic TCs per month for El Niño and La Niña events, *based on nine strong events and for 1999*. Red and blue bars at bottom of figure indicate the duration of composite El Niño and La Niña events, with event peaks indicated in darker colors. The TC season in this region extends from April to December. This study focuses on the first season shown in this figure, the season that occurs during and immediately before the event peaks (see Chapter 2 for rationale). See Chapter 2 for information on evolution of events and selection of event years.

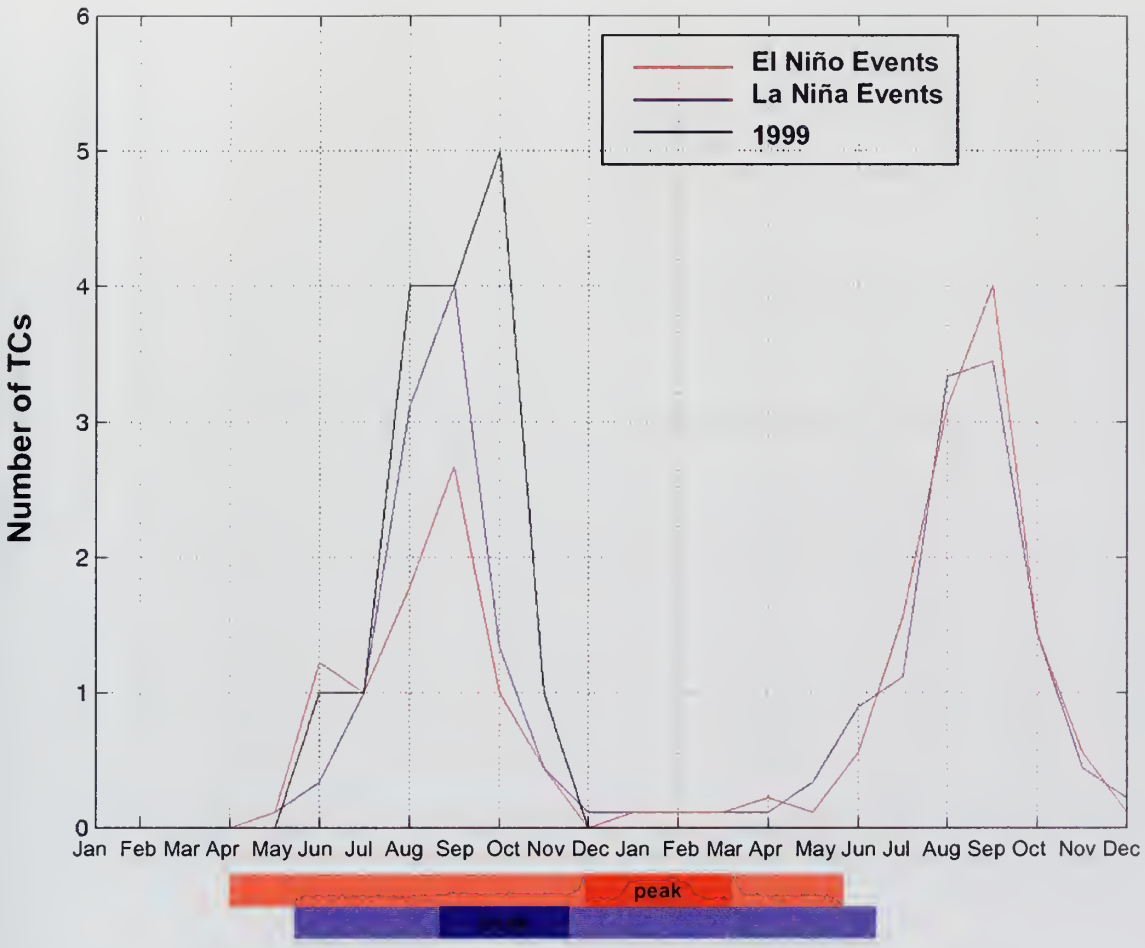

Figure 36. The average number of Atlantic TCs per month for composite El Niño and La Niña events, *based on nine strong events and for 1999*. Red and blue bars at bottom of figure indicate the duration of composite El Niño and La Niña events, with event peaks indicated in darker colors. The TC season in this region extends from April to December. This study focuses on the first season shown in this figure, the season that occurs during and immediately before the event peaks (see Chapter 2 for rationale). See Chapter 2 for information on evolution of events and selection of event years.

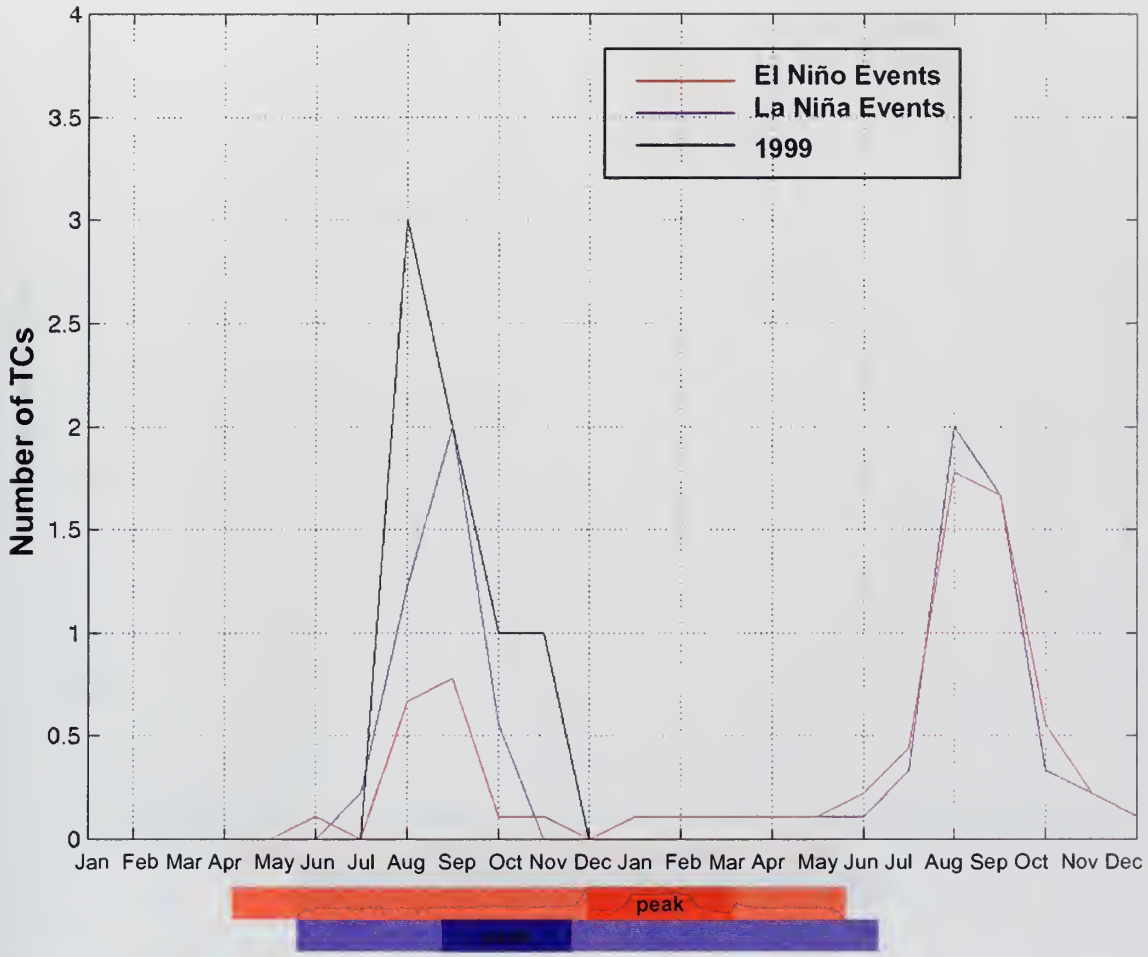

Figure 37. The average number of strong (>80 knot (41 ms^{-1}) maximum intensity) Atlantic TCs per month for composite El Niño and La Niña events, *based on nine strong events and for 1999*. Red and blue bars at bottom of figure indicate the duration of composite El Niño and La Niña events, with event peaks indicated in darker colors. The TC season in this region extends from April to December. This study focuses on the first season shown in this figure, the season that occurs during and immediately before the event peaks (see Chapter 2 for rationale). See Chapter 2 for information on evolution of events and selection of event years.

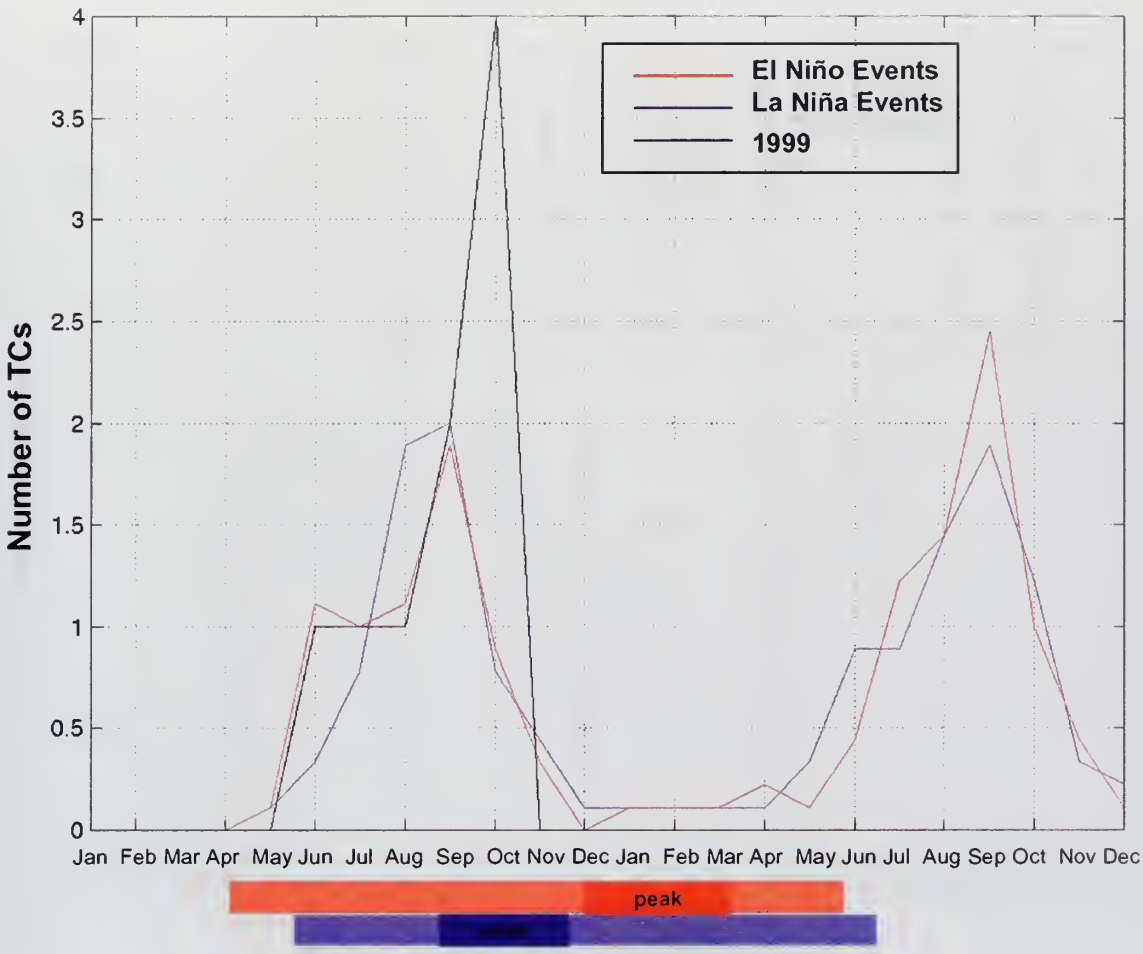

Figure 38. The average number of weak (<80 knot (41 ms^{-1}) maximum intensity) Atlantic TCs per month for composite El Niño and La Niña events, *based on nine strong events and for 1999*. Red and blue bars at bottom of figure indicate the duration of composite El Niño and La Niña events, with event peaks indicated in darker colors. The TC season in this region extends from April to December. This study focuses on the first season shown in this figure, the season that occurs during and immediately before the event peaks (see Chapter 2 for rationale). See Chapter 2 for information on evolution of events and selection of event years.

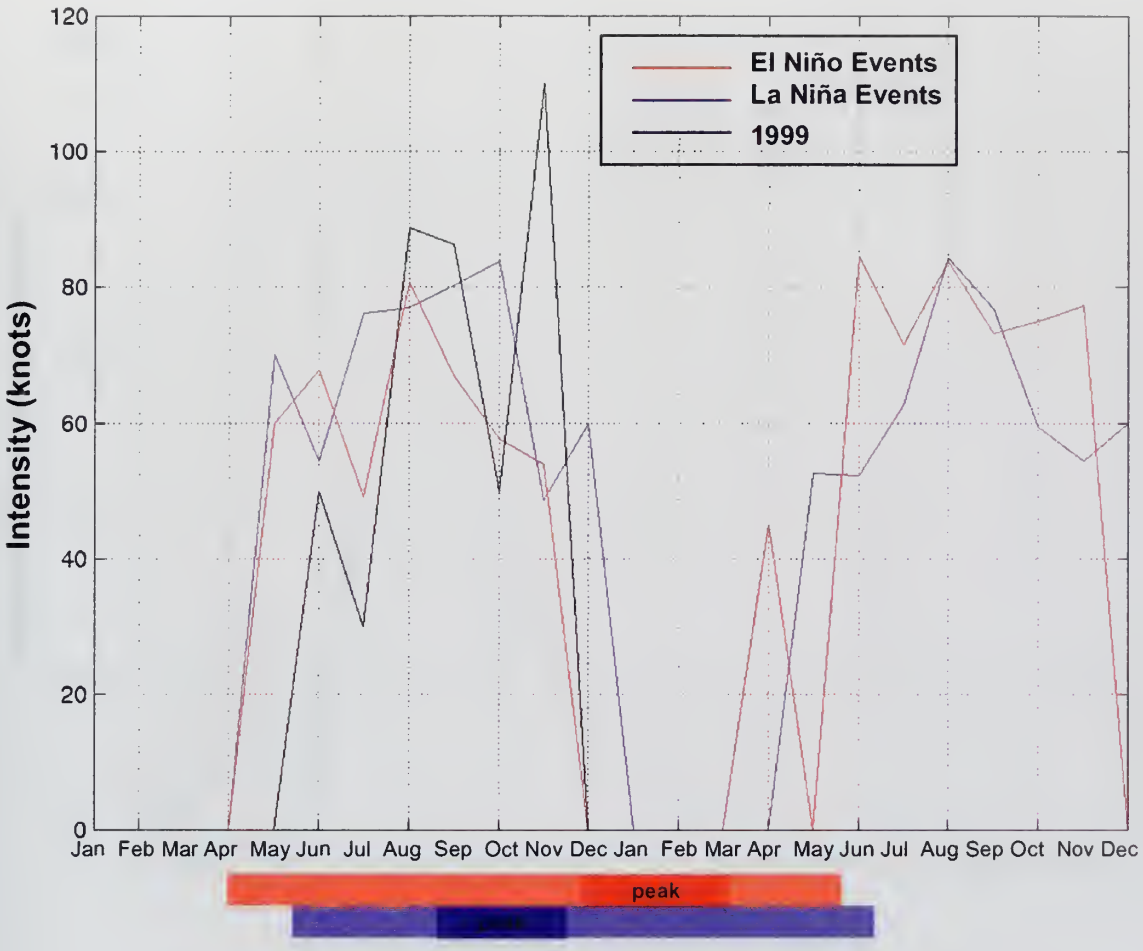

Figure 39. The average maximum intensity of Atlantic TCs per month for composite El Niño and La Niña events, *based on nine strong events and for 1999*. Red and blue bars at bottom of figure indicate the duration of composite El Niño and La Niña events, with event peaks indicated in darker colors. The TC season in this region extends from April to December. This study focuses on the first season shown in this figure, the season that occurs during and immediately before the event peaks (see Chapter 2 for rationale). See Chapter 2 for information on evolution of events and selection of event years.

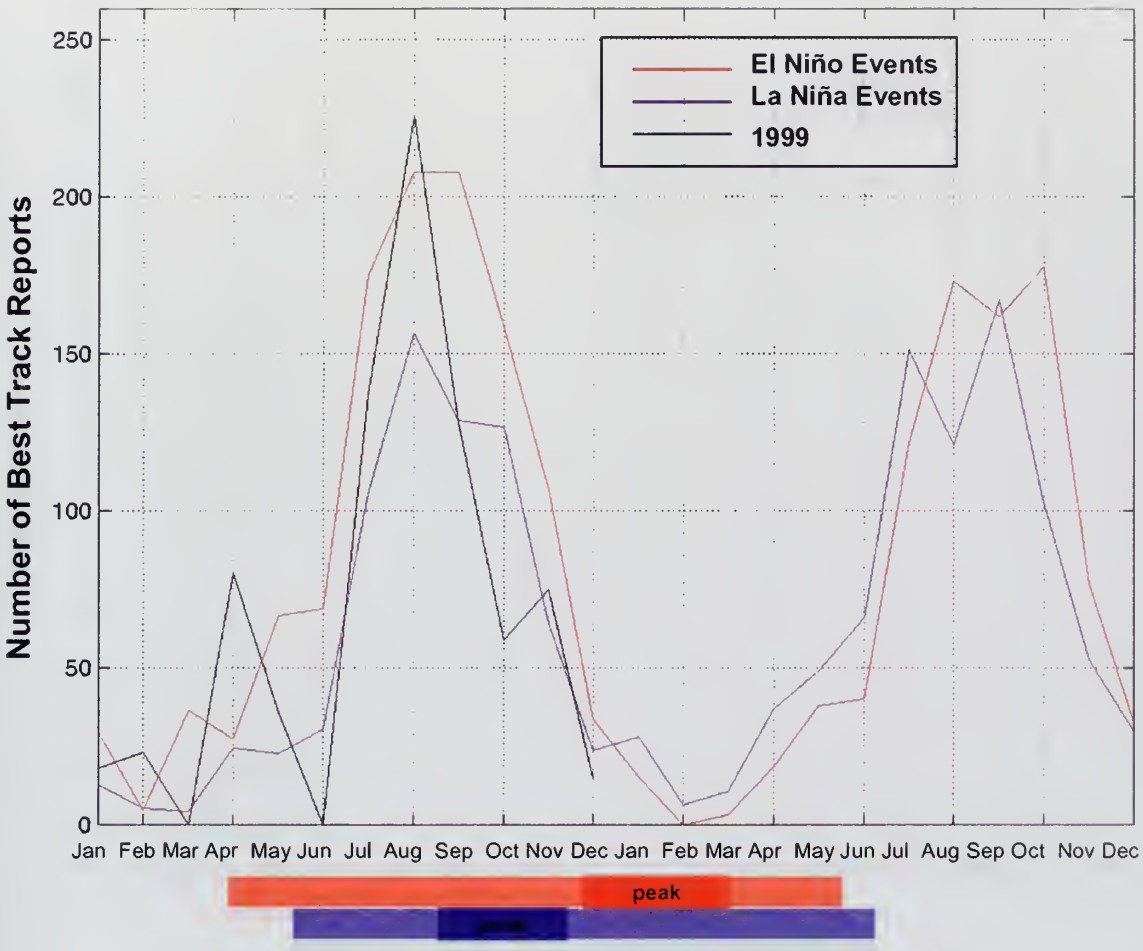

Figure 40. The average number of best track reports for western Pacific TCs per month for the nine strongest composite El Niño and La Niña events, *based on nine strong events and for 1999*. Red and blue bars at bottom of figure indicate the duration of composite El Niño and La Niña events, with event peaks indicated in darker colors. The TC season in this region extends from April to December. This study focuses on the first season shown in this figure, the season that occurs during and immediately before the event peaks (see Chapter 2 for rationale). See Chapter 2 for information on evolution of events and selection of event years.

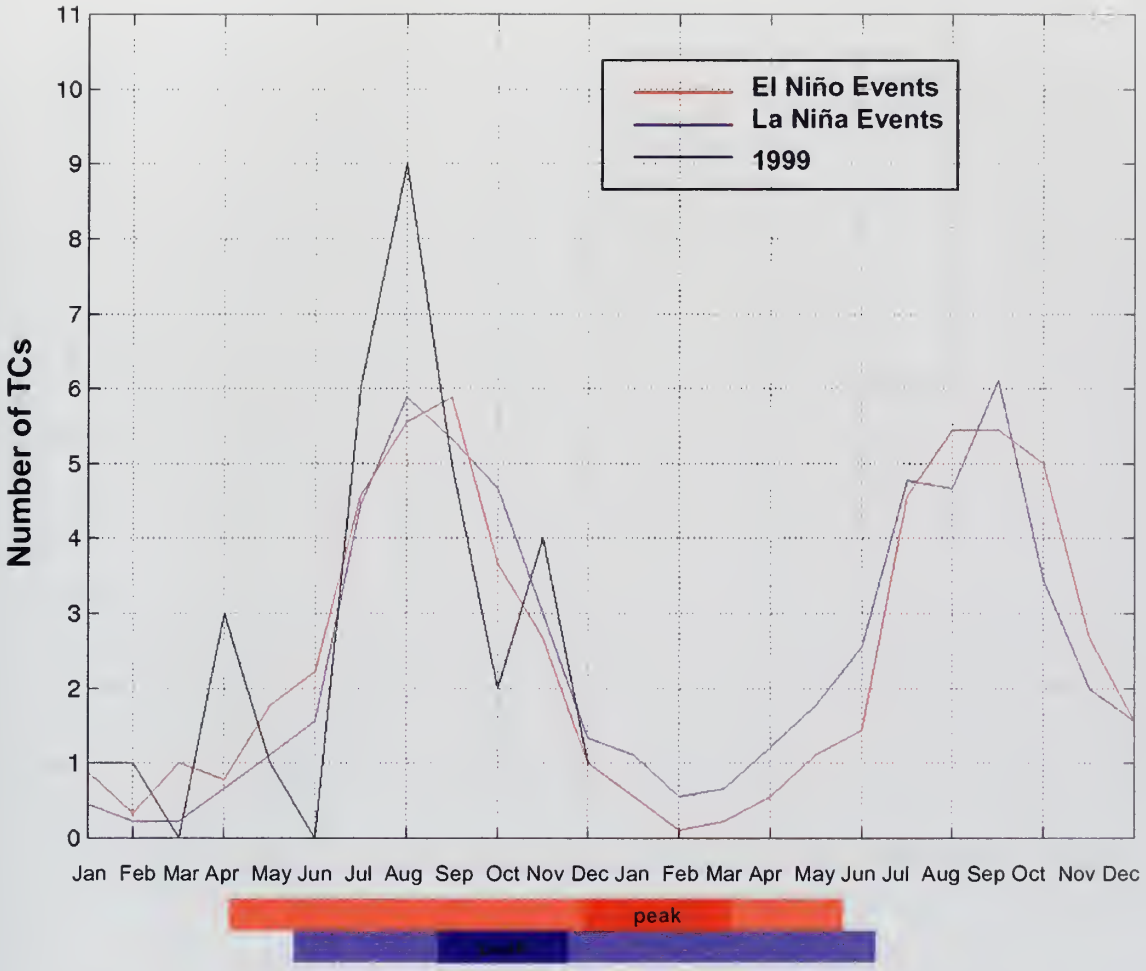

Figure 41. The average number of western Pacific TCs per month for composite El Niño and La Niña events, *based on nine strong events and for 1999*. Red and blue bars at bottom of figure indicate the duration of composite El Niño and La Niña events, with event peaks indicated in darker colors. The TC season in this region extends from April to December. This study focuses on the first season shown in this figure, the season that occurs during and immediately before the event peaks (see Chapter 2 for rationale). See Chapter 2 for information on evolution of events and selection of event years.

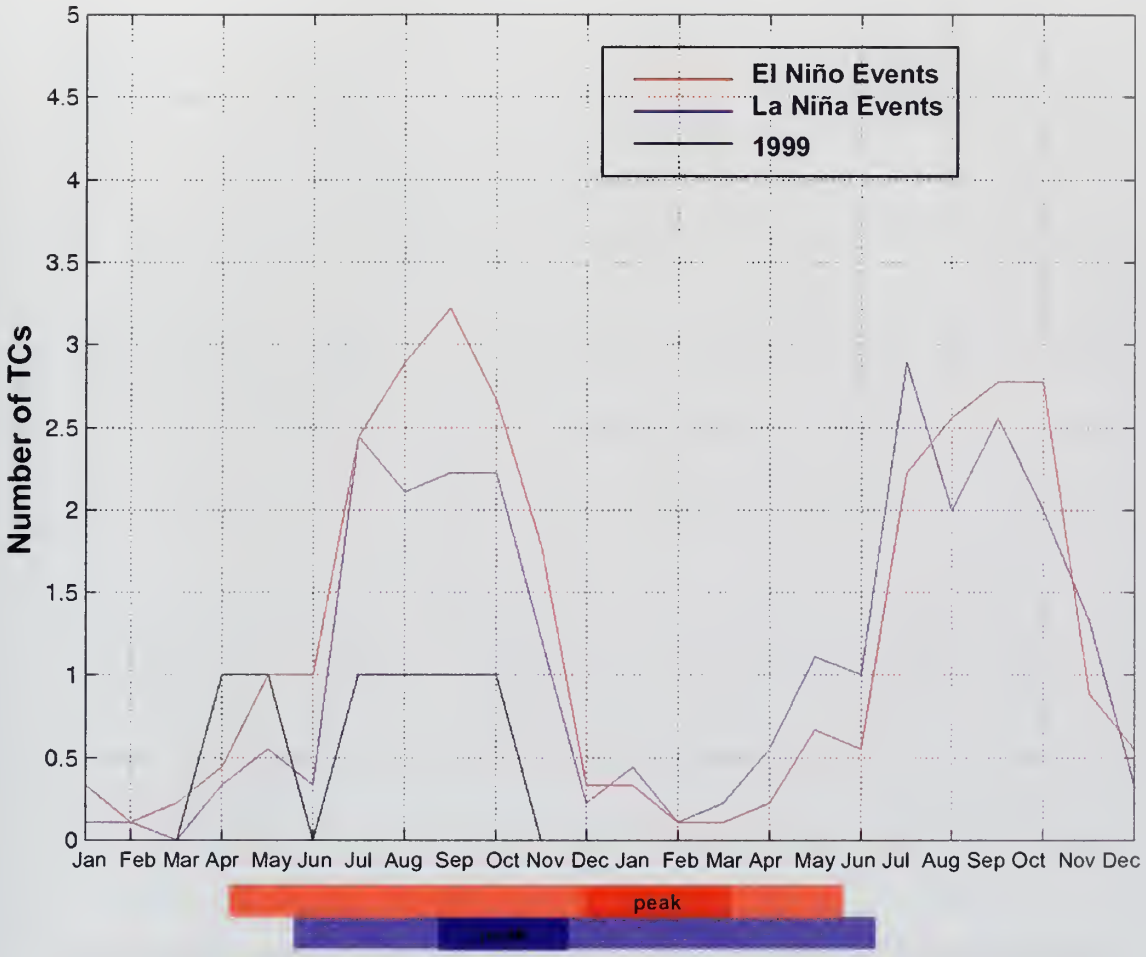

Figure 42. The average number of strong (>80 knot (41 ms^{-1}) maximum intensity) western Pacific TCs per month for composite El Niño and La Niña events, *based on nine strong events and for 1999*. Red and blue bars at bottom of figure indicate the duration of composite El Niño and La Niña events, with event peaks indicated in darker colors. The TC season in this region extends from April to December. This study focuses on the first season shown in this figure, the season that occurs during and immediately before the event peaks (see Chapter 2 for rationale). See Chapter 2 for information on evolution of events and selection of event years.

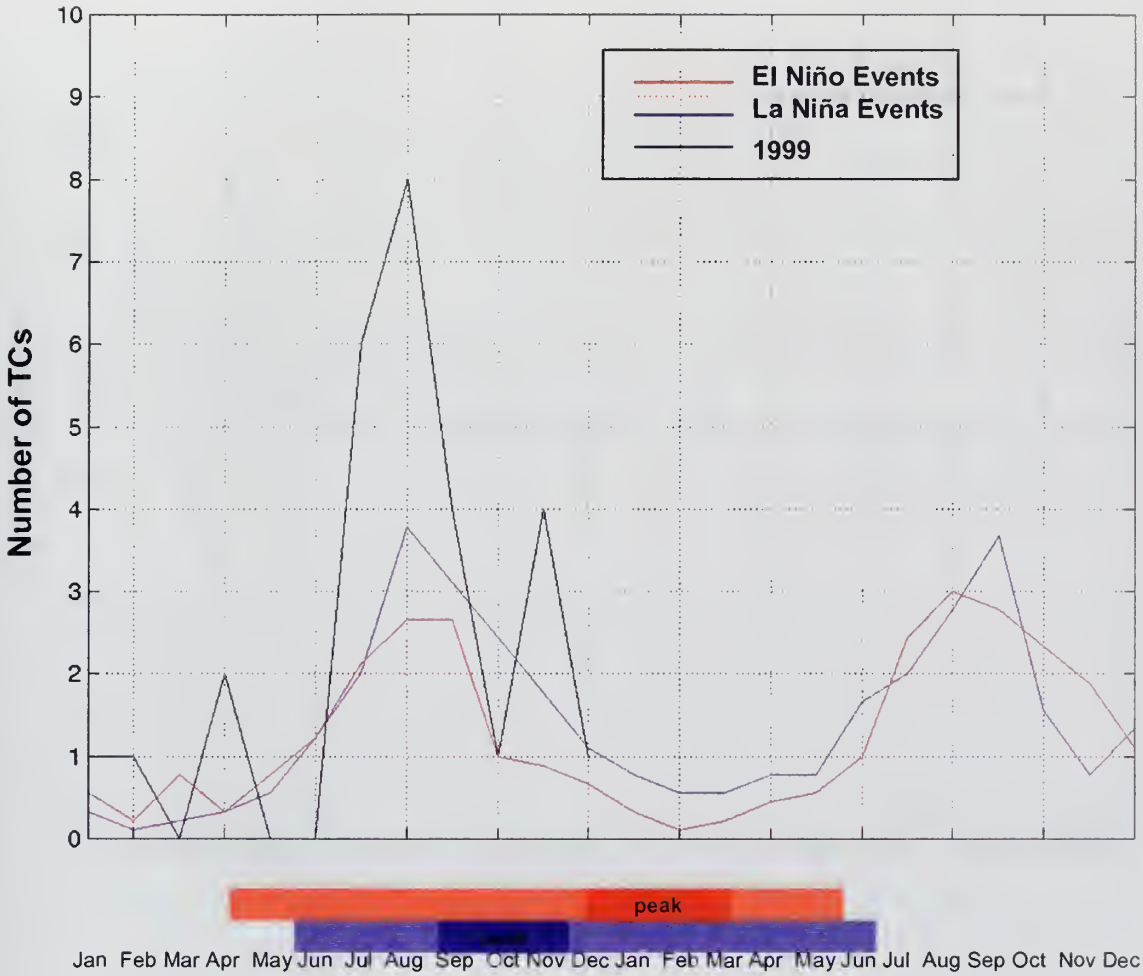

Figure 43. The average number of weak (<80 knot (41 ms^{-1}) maximum intensity) western Pacific TCs per month for composite El Niño and La Niña events, *based on nine strong events and for 1999*. Red and blue bars at bottom of figure indicate the duration of composite El Niño and La Niña events, with event peaks indicated in darker colors. The TC season in this region extends from April to December. This study focuses on the first season shown in this figure, the season that occurs during and immediately before the event peaks (see Chapter 2 for rationale). See Chapter 2 for information on evolution of events and selection of event years.

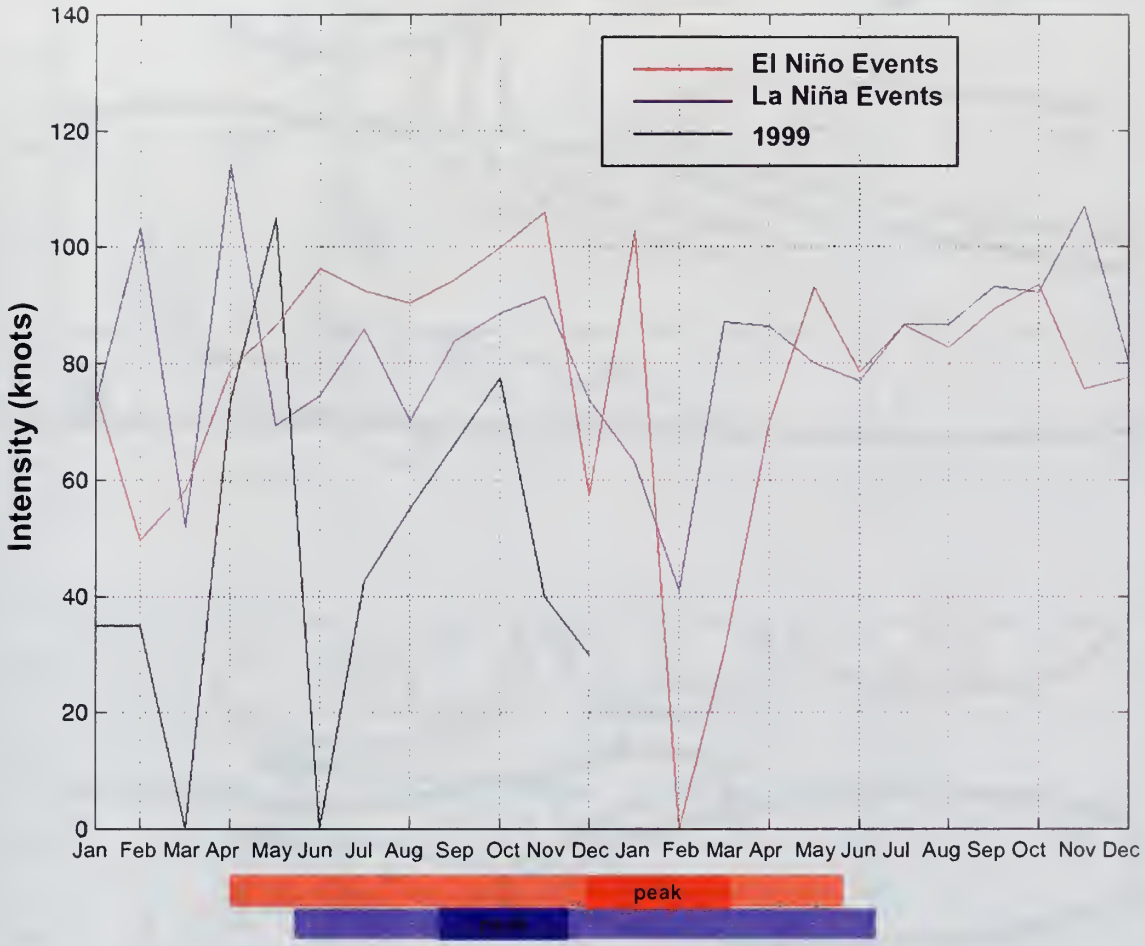

Figure 44. The average maximum intensity of western Pacific TCs per month for composite El Niño and La Niña events, *based on nine strong events and for 1999*. Red and blue bars at bottom of figure indicate the duration of composite El Niño and La Niña events, with event peaks indicated in darker colors. The TC season in this region extends from April to December. This study focuses on the first season shown in this figure, the season that occurs during and immediately before the event peaks (see Chapter 2 for rationale). See Chapter 2 for information on evolution of events and selection of event years.

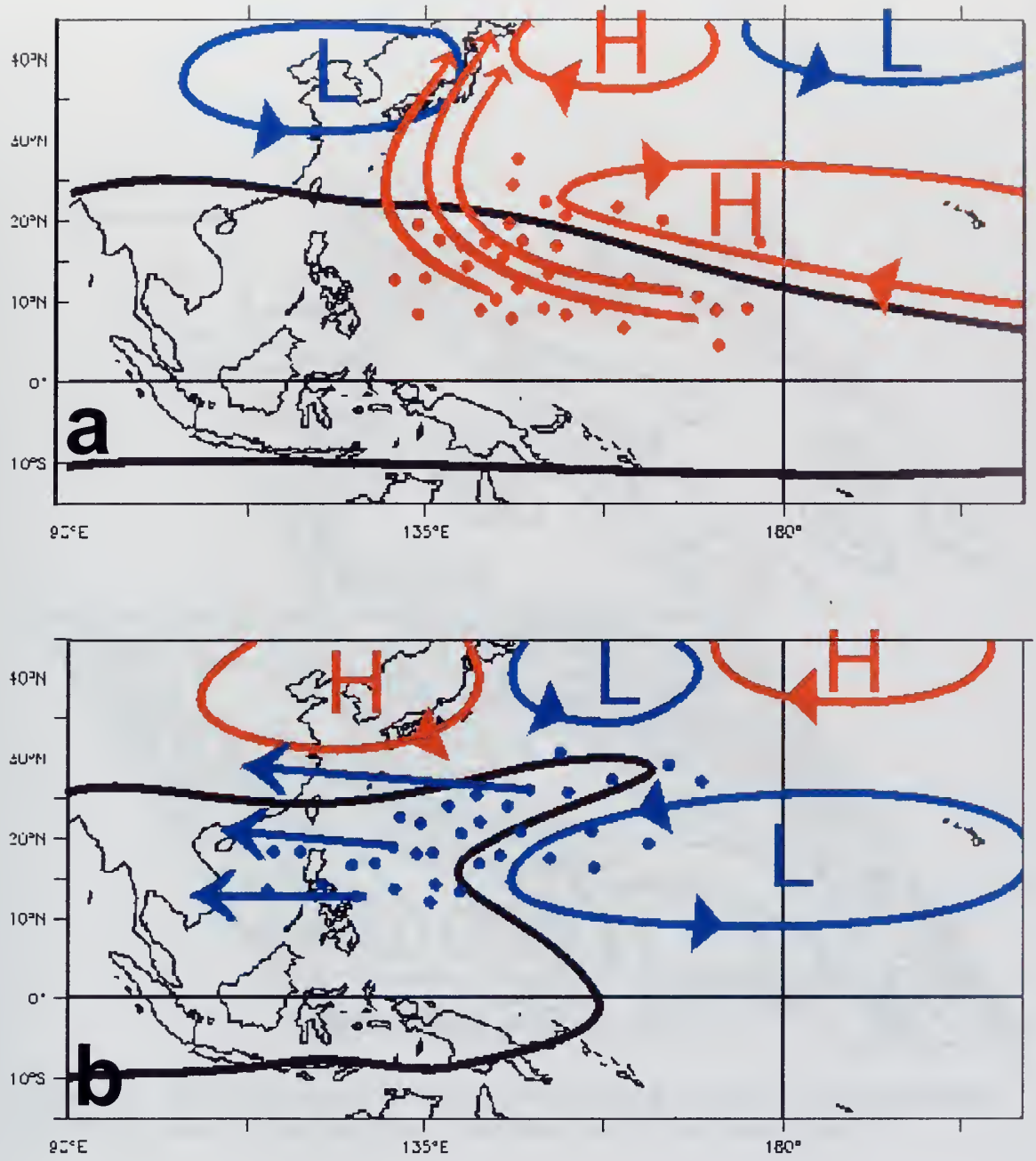

Figure 45. Schematic representation 200 hPa anomalous heights, the shear zero line, TC formation sites and preferred tracks from August-November during (a) El Niño events, and (b) La Niña events.

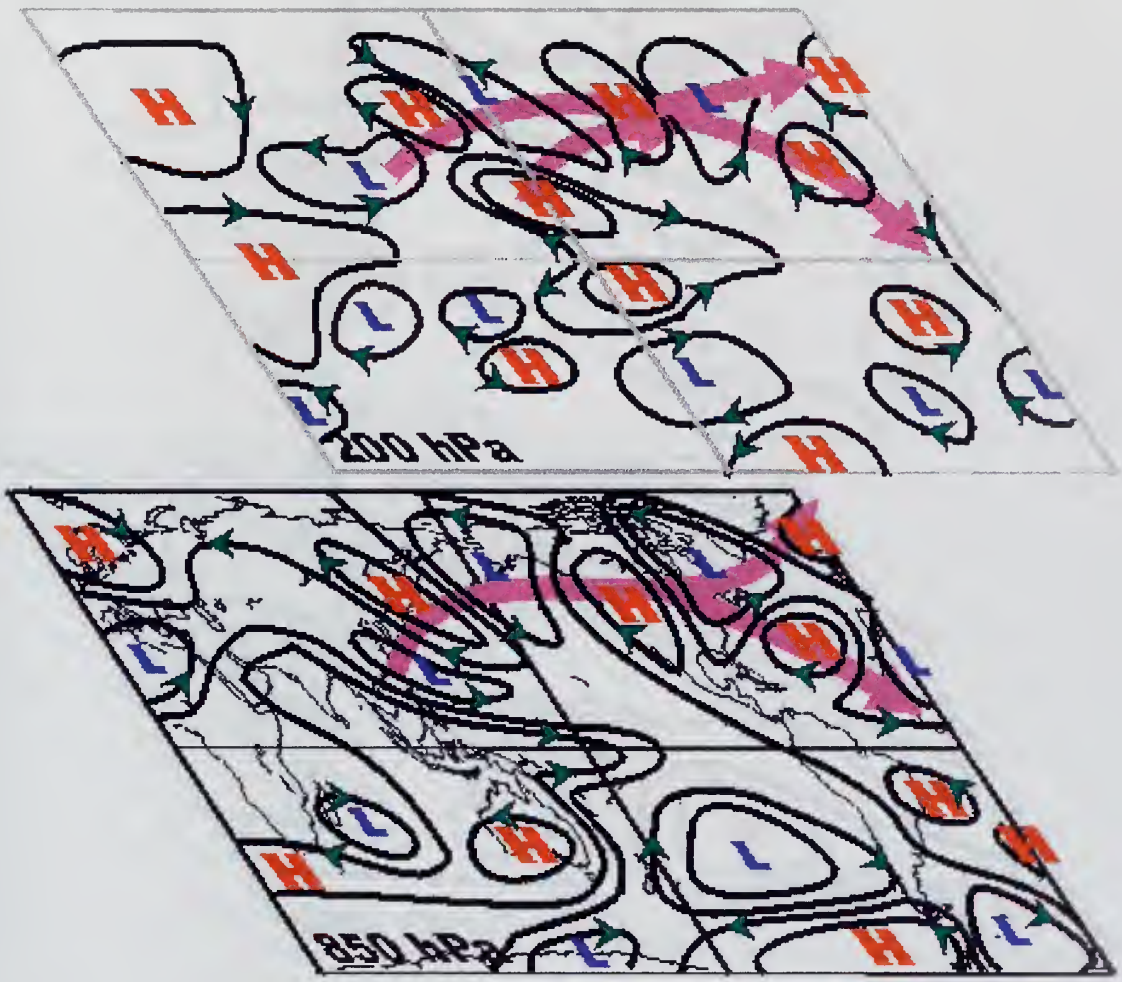

Figure 46. Schematic representation of anomalous circulation brought about by El Niño events during August-November prior to the event peak.

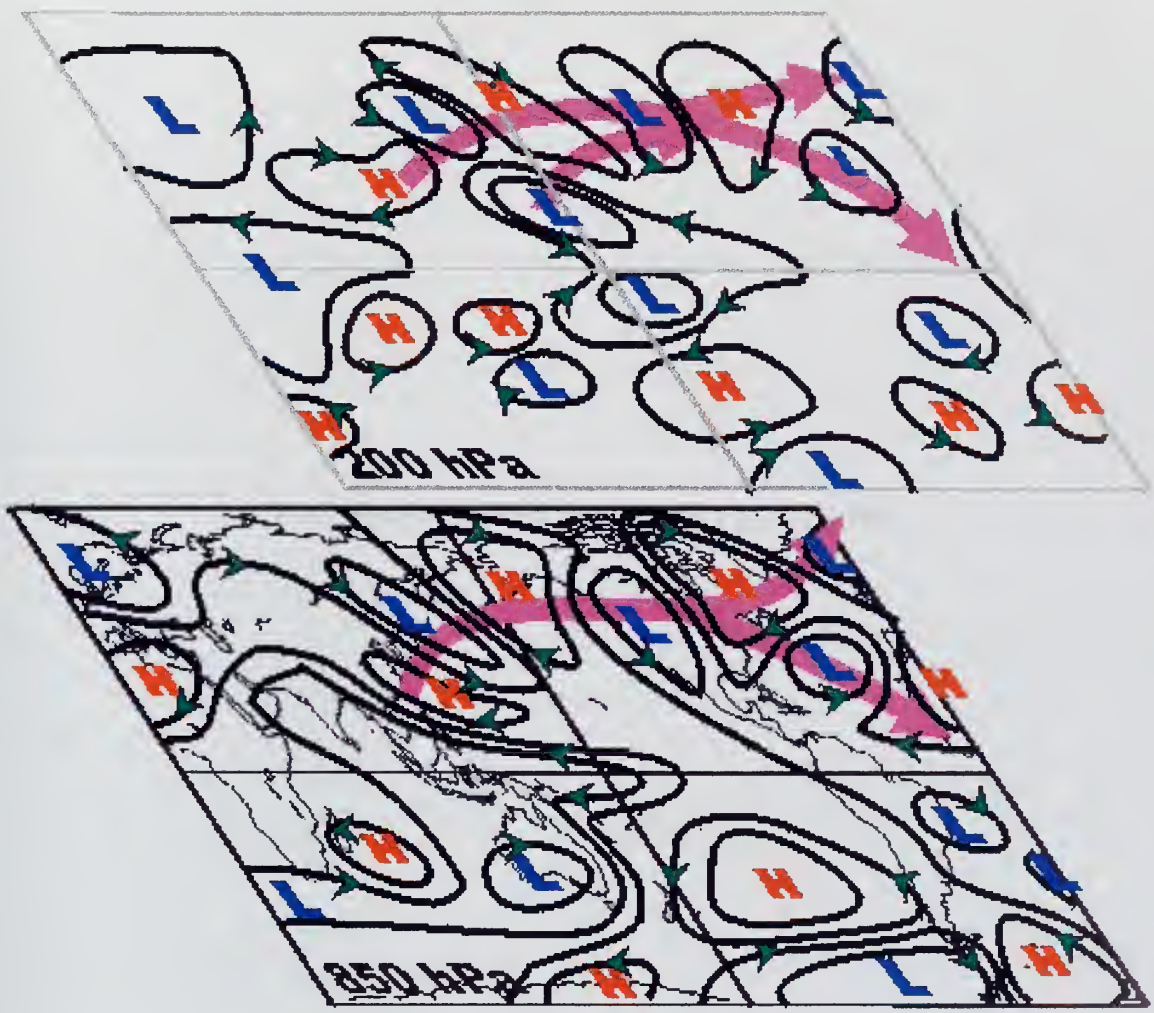

Figure 47. Schematic representation of anomalous circulation brought about by La Niña events during August-November to the event peak.

THIS PAGE INTENTIONALLY LEFT BLANK

LIST OF REFERENCES

Bjerknes, J., 1966: A possible response of the atmospheric Hadley circulation to equatorial anomalies of ocean temperature. *Tellus*, **18**, 820-829.

--------, 1969: Atmospheric teleconnections from the equatorial Pacific. *Mon. Wea. Rev.*, **97**, 163-172.

--------, 1972: Large-scale atmospheric response to the 1964-65 Pacific equatorial warming. *J. Phys. Oceanogr.*, **2**, 212-217.

Bradley, R.,H. Diaz, G. Kiladis, and J. Eischeid, 1987: ENSO signal in continental temperature and precipitation and zonal structure. *J. Atmos. Sci.*, **40**, 1689-1708.

Branstator, G., 1983: Horizontal energy propagation in a Barotrophic atmosphere with meridional and zonal structure. *J. Atmos Sci.* **40**, 1689-1708.

Carr, 1999: Personal communication.

--------, R.L. Elsberry, and M.A. Boothe, 1997: Condensed and updated version of the systematic approach meteorological knowledge base western North Pacific. Tech. Rep. NPS-MR-98-002, Naval Postgraduate School, Monterey, CA 93943-5114

Chan, J., 1985: Tropical cyclone activity in the northwest Pacific in relation to the El Niño/Southern Oscillation phenomenon. *Mon.Wea.Rev.*, **113**, 599-606.

Chen, T.,S. Weng, N. Yamazaki, S. Kiehne, 1998: Interannual variation in the tropical cyclone formation over the western North Pacific. *Mon. Wea. Rev.*, **126**, 1080-1090.

Chu, P., and J. Wang, 1997: Tropical cyclone occurances in the vicinity of Hawaii: are the differences between El Niño and non El Niño years significant? *J. Climate*, **10**, 2683-2689.

Gill, A.E., 1980: Some simple solutions for heat induced tropical circulation. *Quarterly Journal of the Royal Meteorology Society*, **106**, 447-462.

--------, 1982. Atmosphere-Ocean Dynamics. Academic Press, 662 pp.

Goldenberg, S., and L. Shapiro, 1996: Physical mechanisms for the association of El Niño and West African rainfall with Atlantic major hurricane activity. *J. Climate*, **9**, 1169-1187.

Gray, W.M., 1984: Atlantic seasonal hurricane frequency. Part 1: El Niño and 30 mb Quasi-Biennial Oscillation influences. *Mon. Wea. Rev.*, **112**, 1649-1668.

-------, C.W. Landsea, P.W. Mielke Jr., and K.J. Berry, 1993: Predicting Atlantic basin seasonal tropical cyclone activity by 1 August. *Wea. Forecasting*, **8**, 73-86.

-------, 1979. Hurricanes: Their formation, structure, and likely role in the tropical circulation. *Meteorology Over the Tropical Oceans.* D. B. Shaw,(Ed.), Roy. Met. Soc., James Glaisher House, Grenville Place, Bracknell, Berkshire, RG12 1BX,, 155-218.

Horel, J.D. and J.M Wallace, 1981: Planetary-scale atmospheric phenomena associated with the Southern Oscillation. *Mon. Wea. Rev.*, **109**, 813-829.

Hoskins, B., and D. Karoly, 1981: The steady linear response of a spherical atmosphere to thermal and orographic forcing. *J. Atmos Sci.*, **38**, 1179-1196.

Jakus, C.E., 1995: *The Remote Impacts of a Western Pacific Tropical Cyclone.* Master's Thesis, Naval Postgraduate School, Monterey, California, September 1995.

Kalnay, E. and Coauthors, 1996: The NCEP/NCAR Reanalysis 40-year Project. *Bull Amer. Meteor. Soc.*, **77**, 437-471.

Lander, M.A., 1994: An exploratory analysis of the relationships between tropical storm formation in the western North Pacific and ENSO. *Mon. Wea. Rev.*, **112**, 636-651.

-------, and C.P. Guard, 1999: A look at global tropical cyclone activity: Basin intercomparisons and relationships with ENSO, QBO and other large-scale climate features. *23rd Conference on Hurricanes and Tropical Meteorology*, I, 510-513.

Lau, N.-C., and H. Lim, 1984: On the dynamics of equatorial forcing of climate teleconnections. *J. Atmos. Sci.*, **41**, 161-176.

Liebmann, Brant and Catherine A. Smith, 1996: Description of a Complete (interpolated) Outgoing Longwave Radiation Dataset. *Bull Amer. Meteor. Soc.*, **77**, 1275-1277.

Malsick, M.E., 1995: *The Dynamics of Teleconnections Induced by Short Term Tropical Forcing.* Master's Thesis, Naval Postgraduate School, Monterey, California, September 1995.

Matsuno, T., 1996: Quasi-geostrophic motions in the equatorial area. *J. Meteor. Soc. Japan*, **44**, 25-42.

Meehl, Geral A., 1993: A coupled air-ocean biennial mechanism in the tropical Indian and Pacific regions: role of the ocean. *J.Climate*, **6**, 31-41.

McBride, J.L., 1995: Tropical cyclone formation. *Global Perspectives on Tropical Cyclones.* WMO/TD-No. 693, World Meteorological Organization, 63-105.

Murphree, T., and C. Reynolds, 1995: El Niño and La Niña effects on the northeast Pacific: the 1991-1993 and 1988-1989 events. *Cal Coop. Ocean. Fish. Rpt.*, **36**, 45-56.

Nitta, T., 1987: Convective activities in the tropical western Pacific and their impact on the northern hemisphere summer circulation. *J. Meteor. Soc. Japan*, **65**, 373-390.

Philander, G.S., 1990: *El Niño, La Niña, and the Southern Oscillation.* Academic Press, San Diego.

Rasmusson, E.G., and T.H. Carpenter, 1982: Variations in tropical sea surface temperature and surface wind fields associated with the Southern Oscillation/El Niño. *Mon. Wea. Rev.*, **110**, 354-384

Reynolds, C., R. Gelero, and T. Murphree, 1996: Observed and simulated northern hemisphere Intraseasonal circulation anomalies and the influence of model bias. *Mon. Wea. Rev.*, **124**, 1100-1118.

Sardeshmukh, P., and B. Hoskins, 1998: The generation of global rotational flow by idealized tropical divergence. *J. Atmos. Sci.*, **45**, 1228-1251.

Schwing, F., T. Murphree, and P. Green, 2000: A climate index for the northeast Pacific. Submitted to *Progress in Oceanography.*

Shapiro, L., 1887: Month-to-month variability of the Atlantic tropical circulation and its relationship to tropical storm formation. *Mon. Wea. Rev.*, **115**, 2598-2614.

Simmons, A.J.,J.M. Wallace, and G. Branstator, 1983: Barotrophic propagation and instability, and atmospheric teleconnections patterns. *J. Atmos. Sci.,* **40**, 1363-1392.

Springer, Cory A., 1994: *Short Term Teleconnections Associated with Western Pacific Tropical Cyclones*. Master's Thesis, Naval Postgraduate School, Monterey, California, June 1994.

Walker, G., 1924: Correlation in seasonal variations of weather IX: A further study of world weather. *Memoirs of the Royal Meteorological Society*, **24**, 275-322.

------, and E. Bliss, 1932: World Weather V. *Memoirs of the Royal Meteorological Society*, **4**, 53-84.

Weare, B., 1986: An extension of an El Niño index. *Mon. Wea. Rev.*, **114**, 644-647.

Woll, S., 1993: Short Term Teleconnections Associated with an Individual Tropical Cyclone. Master's Thesis, Naval Postgraduate School, Monterey, California, December 1993.

Wolter, K., and M.S. Timlin, 1993: Monitoring ENSO in COADS with a seasonally adjusted principal component index. *Proc. of the 17th Climate Diagnostics Workshop*, Norman OK, NOAA/N MC/ CAC, NSSL, Oklahoma Clim. Survey, CIMMS and the School of Meter., Univ. of Oklahoma, 52-57

INITIAL DISTRIBUTION LIST

No. Copies

1. Defense Technical Information Center.....2
   Cameron Station
   Alexandria, VA 22304-6145

2. Librarian, Code 52.....2
   Naval Postgraduate School
   411 Dyer Road, Room 104
   Monterey, CA 93943-5101

3. Oceanography Department.....1
   Code OC/CO
   Naval Postgraduate School
   833 Dyer Road, Room 331
   Monterey, CA 93943-5122

4. Meteorology Department 1
   Code MR/HY
   Naval Postgraduate School
   833 Dyer Road, Room 252
   Monterey, CA 93943-5122

5. Dr. Tom Murphree 1
   Code MR/ME
   Naval Postgraduate School
   833 Dyer Road, Room 267
   Monterey, CA 93943-5122

6. LT Bruce W. Ford 1
   215 Staysail St.
   Pensacola, FL 32507

7. Dr. Patrick Harr 1
   Code MR/HR
   Naval Postgraduate School
   833 Dyer Road, Room 244
   Monterey, CA 93943-5122

8. Director, Joint Typhoon Warning Center.....1
   Naval Pacific Meteorology and Oceanography Center, Pearl Harbor
   425 Luapele Road
   Pearl Harbor HI 96860-3103

9. Commanding Officer 1
Naval Training Meteorology and Oceanography Facility
280 Skyhawk Drive, Ste. C, Naval Air Station
Pensacola, Florida 32508-5514